



Universiteit
Leiden
The Netherlands

Magnetic resonance imaging of atherosclerosis : studies in visceral obesity

Alizadeh Dehnavi, R.

Citation

Alizadeh Dehnavi, R. (2009, October 6). *Magnetic resonance imaging of atherosclerosis : studies in visceral obesity*. Retrieved from <https://hdl.handle.net/1887/14046>

Version: Corrected Publisher's Version

License: [Licence agreement concerning inclusion of doctoral thesis in the Institutional Repository of the University of Leiden](#)

Downloaded from: <https://hdl.handle.net/1887/14046>

Note: To cite this publication please use the final published version (if applicable).

MAGNETIC RESONANCE IMAGING OF ATHEROSCLEROSIS

Studies in Visceral Obesity

Reza Alizadeh Dehnavi

Printed by: Optima Grafische Communicatie, Rotterdam

ISBN: 978-90-8559-566-3

© 2009 R. Alizadeh Dehnavi, Leiden, The Netherlands. All rights reserved. No part of this thesis may be reproduced or transmitted in any form, by any means, without prior written permission of the author.

MAGNETIC RESONANCE IMAGING OF ATHEROSCLEROSIS

Studies in Visceral Obesity

PROEFSCHRIFT

ter verkrijging van
de graad van Doctor aan de Universiteit Leiden,
op gezag van Rector Magnificus prof. mr. P.F. van der Heijden,
volgens besluit van het College voor Promoties
te verdedigen op dinsdag 6 oktober 2009

klokke 16.15 uur

door

Reza Alizadeh Dehnavi
geboren te Tehran
In 1976

PROMOTIECOMMISSIE

Promotores

Prof. Dr. J.A. Romijn

Prof. A. de Roos

Prof. J.W. Jukema

Co-Promotor

Dr. J.T. Tamsma

Referent

Prof. Dr. Y.M. Smulders, VU medisch Centrum, Amsterdam

Overige commissieleden

Prof. Dr. J.H. Bolk

Dr. M.V. Huisman

Financial support by the Netherlands Heart Foundation and J.E. Jurriaanse Foundation for the publication of this thesis is gratefully acknowledged.

Additional financial support was provided by: Novartis Pharma BV, Sanofi-Aventis BV, AstraZeneca BV, Genzyme BV, GlaxoSmithKline BV, Merck Sharp & Dohme BV, Menarini Farma BV, Pfizer BV.

CONTENTS

Chapter 1	Introduction	7
 PART I 3T MAGNETIC RESONANCE BLACK BLOOD VESSEL WALL IMAGING		
Chapter 2	Assessment of the Carotid Artery at 3T MR Imaging: a Study on Reproducibility. JMRI 2007;25:1035-43	21
Chapter 3	Assessment of carotid artery dimensions by MRI at 3-Tesla in patients at intermediate to high cardiovascular risk with reference to ultrasonography. Submitted	37
 PART II PHENOTYPING OF VISCERAL OBESITY		
Chapter 4	Carotid artery vessel wall imaging by 3T MRI in visceral obese subjects with and without the metabolic syndrome compared to STEMI patients: not all obese are equal. Submitted	51
Chapter 5	Elevated CRP levels are associated with increased carotid atherosclerosis independent of visceral obesity. Atherosclerosis 2008;200:417-23	61
Chapter 6	Apolipoprotein CI levels are associated with atherosclerosis in men with the metabolic syndrome and systemic inflammation. Atherosclerosis 2009;203:355-7	79
 PART III VISCERAL OBESITY AND SYSTEMIC INFLAMMATION AS THERAPEUTIC TARGETS IN ATHEROSCLEROSIS		
Chapter 7	Effect of Rosiglitazone plus Lifestyle Therapy on the Prevention of Progression of Atherosclerosis in Men with Visceral Obesity and Elevated C-reactive Protein. Submitted	89
Chapter 8	Rosiglitazone plus lifestyle therapy increases CD34+ cells in men with visceral obesity and elevated C-reactive protein. Submitted	105
Chapter 9	Summary and Conclusions	117
	<i>Samenvatting en Conclusies</i>	123
	<i>List of Publications</i>	129
	<i>Acknowledgments</i>	131
	<i>Curriculum Vitae</i>	133

CHAPTER

1

Introduction

INTRODUCTION

The aim of this thesis was to explore the relation between visceral obesity and the accompanying metabolic disturbances, systemic inflammation and the atherosclerotic process. For this purpose, a newly developed magnetic resonance vessel wall imaging technique was implemented in phenotyping patients and as a therapeutic endpoint in a randomised controlled setting. This introductory chapter gives an overview of the background of the studies contained within this thesis.

CARDIOVASCULAR DISEASE AND ATHEROSCLEROSIS

Cardiovascular disease is the leading cause of morbidity and mortality worldwide with atherosclerosis as the primary underlying pathophysiological process.^{1, 2} Atherosclerosis is a progressive disease characterized by the accumulation of lipids and fibrous elements in large arteries. The early stages of atherosclerosis is characterised by the accumulation of lipid-engorged macrophages beneath the endothelium.^{3, 4} These early atherosclerotic lesions also known as fatty streaks are not clinically relevant and can be seen in various vascular beds from an early age.⁵ Fatty streaks may progress into more advanced lesions known as atherosclerotic plaques, which are characterized by the accumulation of lipid-rich necrotic debris and smooth muscle cells.⁶ Although advanced plaques can grow sufficiently large to disrupt blood flow, the current evidence suggests that the main cause of cardiovascular events is a sudden expansion of the atheromatous plaque as a result of thrombosis in response to the physical disruption of the plaque integrity.^{7, 8} Three types of physical disruption may occur resulting into the instability of the plaque namely: ulceration at the luminal surface⁹, haemorrhage from the small vessels that grow into the lesion from the media of the blood vessel¹⁰, and finally the most common mechanism of plaque disruption, a fracture of the plaque's fibrous cap.¹¹ Epidemiological studies have revealed numerous risk factors for the development and progression of atherosclerosis.¹²⁻¹⁵ These can be grouped into factors with an important genetic component (gender, hypertension, diabetes and obesity, and familial dyslipidemias), and those that are largely environmental such as smoking, high-fat diet and lack of exercise. These traditional risk factors are used in the clinical setting to estimate the risk of future cardiovascular disease. This clinical use of the risk factors is however complicated by the presence of interactions between risk factors. As a result, the risk factors are not simply additive, and their effect might considerably be modified by the presence or absence of other risk factors.

The recent increase in cardiovascular morbidity and mortality is thought to be related to the epidemiologic increase in obesity.^{2, 16, 17} Significant proportions of western populations now suffer from overweight or obesity.¹⁸⁻²⁰ Obese subjects are at increased risk of developing

cardiovascular disease and type 2 diabetes mellitus (DM2).^{21, 22} Viscerally obese subjects in particular, are considered to have metabolic abnormalities that contribute to the increased risk of future cardiovascular events.²³⁻²⁵ The amount of visceral adipose tissue correlates with metabolic cardiovascular risk factors.²⁶⁻²⁹ Visceral obesity, quantified by waist circumference, has been identified as an independent risk factor for insulin resistance, cardiovascular disease, hypertension and stroke.³⁰⁻³³ In large epidemiological studies, waist circumference was shown to be a predictor of future cardiovascular events and cardiovascular mortality.^{17, 34} Based on these observations, visceral obesity has been applied as a tool for the identification of subjects at risk of developing cardiovascular disease.^{35, 36}

Over the past decade, the prominent role of inflammation has received increasing attention in the pathogenesis of atherosclerotic cardiovascular disease.^{37, 38} The infiltration and accumulation of lipoproteins in the arterial lamina intima initiates a local inflammatory response^{4, 39} resulting in the activation of endothelial cells.³⁹ This activation of endothelial cells, through the expression of adhesion molecules, facilitates the transmigration of blood-derived inflammatory cells, particularly monocytes, across the endothelial monolayer into the intima.⁴⁰⁻⁴³ Once in the intima, monocytes proliferate and differentiate into macrophages and take up lipoproteins, forming foam cells.⁴⁴ In time, foam cell necrosis increases the lipid core of the atherosclerotic plaque. In some plaques, the local immune response results in the accumulation of smooth muscle cells which migrate from the medial layer.³⁸ In parallel with these observations, the important role of inflammation has also been observed in clinical studies. Elevated C-reactive protein (CRP) levels have been demonstrated in individuals with manifest cardiovascular disease and in subjects at risk for developing cardiovascular disease.³⁸ CRP is known to be associated with cardiovascular risk factors⁴⁵ and atherosclerotic disease burden.⁴⁶⁻⁴⁸ Furthermore, CRP can predict future cardiovascular events.⁴⁹ Elevated CRP levels are now used frequently as a marker of systemic inflammation. Evidence has been provided demonstrating a strong association between inflammation and plaque instability.⁵⁰ The better understanding of the pathogenesis of atherosclerosis has resulted in viewing the process as a “response to injury” with lipoproteins or other risk factors as the injurious agents.^{44, 51}

IMAGING OF ATHEROSCLEROSIS

The increasing world wide mortality of atherosclerotic cardiovascular disease is thought to be related to the widespread under-recognition and under-treatment of individuals at risk of developing cardiovascular disease.⁵² Traditionally, evaluation of atherosclerosis was only possible at advanced clinical stages of the disease by either revealing arterial luminal narrowing, or by assessing the effect of arterial stenosis on organ perfusion. Advances in imaging techniques have resulted in the development of new imaging modalities for the assessment of

atherosclerosis in earlier stages of the disease, which allow accurate evaluation of the arterial vascular structure and the possible changes in time. These imaging parameters do not only reflect present disease burden, but can also be used to predict future events.⁵³⁻⁵⁷ Carotid intima media thickness (IMT) measured by ultrasound and vessel wall characteristics assessed by magnetic resonance imaging (MRI) are parameters of special interest in the primary prevention setting due to their non-invasive nature and the absence of radiation exposure. IMT is an established measure of atherosclerotic disease burden which has been widely used and extensively validated both with cardiovascular risk factors, coronary atherosclerosis and outcome data.⁵⁴⁻⁶⁴ MRI, on the other hand, is a relatively new imaging modality, which has been used in the assessment of atherosclerosis.⁶⁵⁻⁶⁷ Promising results have been demonstrated regarding the accuracy and reproducibility of the technique at the field strength of 1.5 tesla.^{66,68-72} Extending the MR vascular imaging to higher field strength of 3 Tesla could further improve the accuracy of the technique in detecting differences in atherosclerotic disease burden. In addition, vascular MRI has not yet been validated extensively, because of its relative recent introduction. A first step in this regard could be the evaluation of magnetic resonance carotid artery imaging with intima media thickness measurements using ultrasonography.

TREATMENT OF EARLY ATHEROSCLEROSIS

The treatment strategy to prevent the progression of atherosclerosis has been focused on influencing the known risk factors for the development of cardiovascular disease. Changes in life style, by restricting caloric intake and increasing physical activity, are effective in improving cardiovascular risk factors and decreasing events.⁷³ Lifestyle intervention is frequently complemented by drug therapy. In general, the focus of drug therapy has been to improve traditional risk factors such as LDL-cholesterol levels and blood pressure. In particular, statin treatment lowers levels of atherogenic lipoproteins, affects the progression of atherosclerosis and decreases clinical events and mortality from atherosclerotic cardiovascular disease.⁷⁴⁻⁷⁶ Nevertheless, heart disease and stroke have remained the most common causes of death in the developed countries. New treatment approaches affecting the atherosclerotic mechanism may prove effective in retarding the atherosclerotic process, especially when combined with intensive life style treatment. With respect to insuline resistance, thiazolidinediones could be of interest. Thiazolidinediones, such as rosiglitazone, target the peroxisome-proliferator-activated receptor γ (PPAR γ).⁷⁷ PPAR γ is a nuclear transcription factor that modulates metabolic and inflammatory gene repertoires. The complex biologic effects of rosiglitazone result from transactivation of metabolic and transrepression of inflammatory target genes.⁷⁸ Rosiglitazone improves insulin resistance, alters fat distribution from visceral to subcutaneous fat stores, and increases plasma HDL-c levels.^{79,80} Clinically, rosiglitazone has been shown to improve insulin sensitivity and hyperglycaemia, and decreases plasma CRP levels.^{79,81} Taken together, these

characteristics including its anti-inflammatory effects suggest a possible anti-atherosclerotic potential for rosiglitazone. The effect of rosiglitazone on atherosclerosis has been studied using IMT. In DM2 patients, a beneficial effect was observed on the progression of IMT after rosiglitazone treatment.^{82, 83} The effect of rosiglitazone in addition to lifestyle treatment on the progression of atherosclerosis has not yet been studied in viscerally obese subjects with systemic inflammation but without diabetes and overt cardiovascular disease. The influence of rosiglitazone on inflammation, adipose tissue distribution, insulin resistance and atherosclerosis as measured by 3 Tesla magnetic resonance vessel wall imaging are described in this thesis.

AIMS AND OUTLINE OF THE THESIS

The aim of this thesis was to explore the relation between visceral obesity and the accompanying metabolic disturbances, systemic inflammation and the atherosclerotic process. A newly developed magnetic resonance vessel wall imaging technique was implemented in phenotyping patients and as a therapeutic endpoint in a randomised controlled setting. For this purpose, we pursued a three step approach. First, the magnetic resonance black blood vessel wall imaging technique at the magnetic field strength of 3 Tesla was developed and validated. Secondly, the technique was used in the phenotyping of viscerally obese subjects with special focus on the role of systemic inflammation. Finally, the impact of reducing visceral obesity and systemic inflammation on the progression of atherosclerosis was assessed using lifestyle therapy and rosiglitazone or placebo treatment in a randomised controlled clinical trial that was named “A 52 week double-blind randomized controlled trial comparing the effect of Rosiglitazone versus placebo on the prevention of progression of atherosclerosis in high risk patients without diabetes (RUBENS) trial”

Part I: 3T magnetic resonance black blood vessel wall imaging

Carotid magnetic resonance black blood vessel wall imaging at the magnetic field strength of 3 Tesla was developed for the assessment of atherosclerotic disease burden and possible changes in time. After development and optimisation, this technique was validated and its accuracy in measuring vascular structural characteristics was evaluated. The scanning procedure and the reproducibility of the MRI measurements are described in **Chapter 2**. The carotid MRI measurements were further assessed with regard to the relation with cardiovascular risk factors and ultrasound measured IMT, a well validated intermediate endpoint in assessing atherosclerotic disease burden, in **Chapter 3**.

Part II: Phenotyping of visceral obesity

After establishing the 3T vascular MRI, this technique was applied in the phenotyping of viscerally obese subjects. In **Chapter 4** MRI was used in vascular phenotyping of patients with

varying cardiovascular risk profiles. Vessel wall characteristics of visceral obese subjects with and without the Metabolic Syndrome were evaluated in comparison to patients who recently suffered from a ST-segment elevation myocardial infarction. In **chapter 5**, the relation between elevated CRP levels and carotid atherosclerotic disease burden was assessed in subjects with visceral obesity. An association between visceral obesity, metabolic disturbances and systemic inflammation has long been established. To further explore the interrelation between these variables, we studied the concentrations of apolipoprotein CI (ApoCI) in relation with systemic inflammation and carotid atherosclerosis in viscerally obese subjects. ApoCI influences many proteins involved in the remodelling of lipoproteins in plasma and has been shown to possess modulating effects on the systemic inflammatory response. **Chapter 6** describes the influence of ApoCI concentrations in the presence of systemic inflammation on carotid atherosclerotic disease burden.

Part III: Visceral obesity and systemic inflammation as therapeutic targets in atherosclerosis

In these chapters, we evaluated the impact of the manipulation of visceral obesity and systemic inflammation on the progression of atherosclerosis in the setting of a randomised clinical trial. **Chapter 7** describes the results of a randomised controlled intervention study evaluating the effect of rosiglitazone treatment in addition to intensive lifestyle therapy on the progression of carotid atherosclerosis in viscerally obese non-diabetic subjects with elevated CRP levels. Another endpoint of the study was the evaluation of the influence of rosiglitazone treatment in addition to lifestyle intervention on circulating endothelial progenitor cells and haematopoietic stem cells (**chapter 8**).

REFERENCE LIST

1. Fuster V, Voute J. MDGs: chronic diseases are not on the agenda. *Lancet* 2005 October 29;366(9496):1512-4.
2. Murray CJ, Lopez AD. Global mortality, disability, and the contribution of risk factors: Global Burden of Disease Study. *Lancet* 1997 May 17;349(9063):1436-42.
3. Stary HC, Chandler AB, Glagov S et al. A definition of initial, fatty streak, and intermediate lesions of atherosclerosis. A report from the Committee on Vascular Lesions of the Council on Arteriosclerosis, American Heart Association. *Circulation* 1994 May;89(5):2462-78.
4. Skalen K, Gustafsson M, Rydberg EK et al. Subendothelial retention of atherogenic lipoproteins in early atherosclerosis. *Nature* 2002 June 13;417(6890):750-4.
5. Napoli C, D'Armiento FP, Mancini FP et al. Fatty streak formation occurs in human fetal aortas and is greatly enhanced by maternal hypercholesterolemia. Intimal accumulation of low density lipoprotein and its oxidation precede monocyte recruitment into early atherosclerotic lesions. *J Clin Invest* 1997 December 1;100(11):2680-90.
6. Stary HC, Chandler AB, Dinsmore RE et al. A definition of advanced types of atherosclerotic lesions and a histological classification of atherosclerosis. A report from the Committee on Vascular Lesions of the Council on Arteriosclerosis, American Heart Association. *Circulation* 1995 September 1;92(5):1355-74.
7. Hackett D, Davies G, Maseri A. Pre-existing coronary stenoses in patients with first myocardial infarction are not necessarily severe. *Eur Heart J* 1988 December;9(12):1317-23.
8. Davies MJ. Stability and instability: two faces of coronary atherosclerosis. The Paul Dudley White Lecture 1995. *Circulation* 1996 October 15;94(8):2013-20.
9. Faggiotto A, Ross R, Harker L. Studies of hypercholesterolemia in the nonhuman primate. I. Changes that lead to fatty streak formation. *Arteriosclerosis* 1984 July;4(4):323-40.
10. de Boer OJ, van der Wal AC, Teeling P, Becker AE. Leucocyte recruitment in rupture prone regions of lipid-rich plaques: a prominent role for neovascularization? *Cardiovasc Res* 1999 February;41(2):443-9.
11. Falk E, Shah PK, Fuster V. Coronary plaque disruption. *Circulation* 1995 August 1;92(3):657-71.
12. Nathan L, Chaudhuri G. Estrogens and atherosclerosis. *Annu Rev Pharmacol Toxicol* 1997;37:477-515.
13. Assmann G, Cullen P, Jossa F, Lewis B, Mancini M. Coronary heart disease: reducing the risk: the scientific background to primary and secondary prevention of coronary heart disease. A worldwide view. International Task force for the Prevention of Coronary Heart disease. *Arterioscler Thromb Vasc Biol* 1999 August;19(8):1819-24.
14. Gordon DJ, Rifkind BM. High-density lipoprotein--the clinical implications of recent studies. *N Engl J Med* 1989 November 9;321(19):1311-6.
15. Luft FC. Molecular genetics of human hypertension. *J Hypertens* 1998 December;16(12 Pt 2):1871-8.
16. Calle EE, Thun MJ, Petrelli JM, Rodriguez C, Heath CW, Jr. Body-mass index and mortality in a prospective cohort of U.S. adults. *N Engl J Med* 1999 October 7;341(15):1097-105.
17. Yusuf S, Hawken S, Ounpuu S et al. Obesity and the risk of myocardial infarction in 27,000 participants from 52 countries: a case-control study. *Lancet* 2005 November 5;366(9497):1640-9.
18. Mokdad AH, Bowman BA, Ford ES, Vinicor F, Marks JS, Koplan JP. The continuing epidemics of obesity and diabetes in the United States. *JAMA* 2001 September 12;286(10):1195-200.
19. Mokdad AH, Ford ES, Bowman BA et al. Diabetes trends in the U.S.: 1990-1998. *Diabetes Care* 2000 September;23(9):1278-83.
20. Mokdad AH, Serdula MK, Dietz WH, Bowman BA, Marks JS, Koplan JP. The spread of the obesity epidemic in the United States, 1991-1998. *JAMA* 1999 October 27;282(16):1519-22.
21. Adams KF, Schatzkin A, Harris TB et al. Overweight, obesity, and mortality in a large prospective cohort of persons 50 to 71 years old. *N Engl J Med* 2006 August 24;355(8):763-78.
22. Jee SH, Sull JW, Park J et al. Body-mass index and mortality in Korean men and women. *N Engl J Med* 2006 August 24;355(8):779-87.

23. Despres JP, Lemieux I, Prud'homme D. Treatment of obesity: need to focus on high risk abdominally obese patients. *BMJ* 2001 March 24;322(7288):716-20.
24. Van Gaal LF, Vansant GA, De L, I. Upper body adiposity and the risk for atherosclerosis. *J Am Coll Nutr* 1989 December;8(6):504-14.
25. Wong S, Janssen I, Ross R. Abdominal adipose tissue distribution and metabolic risk. *Sports Med* 2003;33(10):709-26.
26. Pascot A, Lemieux I, Prud'homme D et al. Reduced HDL particle size as an additional feature of the atherogenic dyslipidemia of abdominal obesity. *J Lipid Res* 2001 December;42(12):2007-14.
27. Pouliot MC, Despres JP, Nadeau A et al. Visceral obesity in men. Associations with glucose tolerance, plasma insulin, and lipoprotein levels. *Diabetes* 1992 July;41(7):826-34.
28. Lemieux I, Pascot A, Prud'homme D et al. Elevated C-reactive protein: another component of the atherothrombotic profile of abdominal obesity. *Arterioscler Thromb Vasc Biol* 2001 June;21(6):961-7.
29. Tchernof A, Lamarche B, Prud'homme D et al. The dense LDL phenotype. Association with plasma lipoprotein levels, visceral obesity, and hyperinsulinemia in men. *Diabetes Care* 1996 June;19(6):629-37.
30. Banerji MA, Lebowitz J, Chaiken RL, Gordon D, Kral JG, Lebovitz HE. Relationship of visceral adipose tissue and glucose disposal is independent of sex in black NIDDM subjects. *Am J Physiol* 1997 August;273(2 Pt 1):E425-E432.
31. Pouliot MC, Despres JP, Lemieux S et al. Waist circumference and abdominal sagittal diameter: best simple anthropometric indexes of abdominal visceral adipose tissue accumulation and related cardiovascular risk in men and women. *Am J Cardiol* 1994 March 1;73(7):460-8.
32. Kuo CS, Hwu CM, Chiang SC et al. Waist circumference predicts insulin resistance in offspring of diabetic patients. *Diabetes Nutr Metab* 2002 April;15(2):101-8.
33. Poirier P, Lemieux I, Mauriege P et al. Impact of waist circumference on the relationship between blood pressure and insulin: the Quebec Health Survey. *Hypertension* 2005 March;45(3):363-7.
34. Pischon T, Boeing H, Hoffmann K et al. General and abdominal adiposity and risk of death in Europe. *N Engl J Med* 2008 November 13;359(20):2105-20.
35. Alberti KG, Zimmet P, Shaw J. Metabolic syndrome--a new world-wide definition. A Consensus Statement from the International Diabetes Federation. *Diabet Med* 2006 May;23(5):469-80.
36. Grundy SM, Cleeman JJ, Daniels SR et al. Diagnosis and management of the metabolic syndrome: an American Heart Association/National Heart, Lung, and Blood Institute Scientific Statement. *Circulation* 2005 October 25;112(17):2735-52.
37. Libby P, Ridker PM, Maseri A. Inflammation and atherosclerosis. *Circulation* 2002 March 5;105(9):1135-43.
38. Libby P. Inflammation in atherosclerosis. *Nature* 2002 December 19;420(6917):868-74.
39. Leitinger N. Oxidized phospholipids as modulators of inflammation in atherosclerosis. *Curr Opin Lipidol* 2003 October;14(5):421-30.
40. POOLE JC, FLOREY HW. Changes in the endothelium of the aorta and the behaviour of macrophages in experimental atheroma of rabbits. *J Pathol Bacteriol* 1958 April;75(2):245-51.
41. Eriksson EE, Xie X, Werr J, Thoren P, Lindbom L. Importance of primary capture and L-selectin-dependent secondary capture in leukocyte accumulation in inflammation and atherosclerosis in vivo. *J Exp Med* 2001 July 16;194(2):205-18.
42. Cybulsky MI, Gimbrone MA, Jr. Endothelial expression of a mononuclear leukocyte adhesion molecule during atherogenesis. *Science* 1991 February 15;251(4995):788-91.
43. Smith JD, Trogan E, Ginsberg M, Grigaux C, Tian J, Miyata M. Decreased atherosclerosis in mice deficient in both macrophage colony-stimulating factor (op) and apolipoprotein E. *Proc Natl Acad Sci U S A* 1995 August 29;92(18):8264-8.

44. Ross R. The pathogenesis of atherosclerosis: a perspective for the 1990s. *Nature* 1993 April 29;362(6423):801-9.
45. Festa A, D'Agostino R, Jr., Howard G, Mykkanen L, Tracy RP, Haffner SM. Chronic subclinical inflammation as part of the insulin resistance syndrome: the Insulin Resistance Atherosclerosis Study (IRAS). *Circulation* 2000 July 4;102(1):42-7.
46. Hak AE, Stehouwer CD, Bots ML et al. Associations of C-reactive protein with measures of obesity, insulin resistance, and subclinical atherosclerosis in healthy, middle-aged women. *Arterioscler Thromb Vasc Biol* 1999 August;19(8):1986-91.
47. Jarvisalo MJ, Harmoinen A, Hakanen M et al. Elevated serum C-reactive protein levels and early arterial changes in healthy children. *Arterioscler Thromb Vasc Biol* 2002 August 1;22(8):1323-8.
48. Blackburn R, Giral P, Bruckert E et al. Elevated C-reactive protein constitutes an independent predictor of advanced carotid plaques in dyslipidemic subjects. *Arterioscler Thromb Vasc Biol* 2001 December;21(12):1962-8.
49. Ridker PM. Clinical application of C-reactive protein for cardiovascular disease detection and prevention. *Circulation* 2003 January 28;107(3):363-9.
50. Redgrave JN, Lovett JK, Gallagher PJ, Rothwell PM. Histological assessment of 526 symptomatic carotid plaques in relation to the nature and timing of ischemic symptoms: the Oxford plaque study. *Circulation* 2006 May 16;113(19):2320-8.
51. Libby P. Changing concepts of atherogenesis. *J Intern Med* 2000 March;247(3):349-58.
52. Bhatt DL, Steg PG, Ohman EM et al. International prevalence, recognition, and treatment of cardiovascular risk factors in outpatients with atherothrombosis. *JAMA* 2006 January 11;295(2):180-9.
53. Lorenz MW, Markus HS, Bots ML, Rosvall M, Sitzer M. Prediction of clinical cardiovascular events with carotid intima-media thickness: a systematic review and meta-analysis. *Circulation* 2007 January 30;115(4):459-67.
54. Bots ML, Hoes AW, Koudstaal PJ, Hofman A, Grobbee DE. Common carotid intima-media thickness and risk of stroke and myocardial infarction: the Rotterdam Study. *Circulation* 1997 September 2;96(5):1432-7.
55. Johnsen SH, Mathiesen EB, Joakimsen O et al. Carotid atherosclerosis is a stronger predictor of myocardial infarction in women than in men: a 6-year follow-up study of 6226 persons: the Tromso Study. *Stroke* 2007 November;38(11):2873-80.
56. Murakami S, Otsuka K, Hotta N et al. Common carotid intima-media thickness is predictive of all-cause and cardiovascular mortality in elderly community-dwelling people: Longitudinal Investigation for the Longevity and Aging in Hokkaido County (LILAC) study. *Biomed Pharmacother* 2005 October;59 Suppl 1:S49-S53.
57. O'Leary DH, Polak JF, Kronmal RA, Manolio TA, Burke GL, Wolfson SK, Jr. Carotid-artery intima and media thickness as a risk factor for myocardial infarction and stroke in older adults. Cardiovascular Health Study Collaborative Research Group. *N Engl J Med* 1999 January 7;340(1):14-22.
58. Baldassarre D, Amato M, Bondioli A, Sirtori CR, Tremoli E. Carotid artery intima-media thickness measured by ultrasonography in normal clinical practice correlates well with atherosclerosis risk factors. *Stroke* 2000 October;31(10):2426-30.
59. Chambless LE, Heiss G, Folsom AR et al. Association of coronary heart disease incidence with carotid arterial wall thickness and major risk factors: the Atherosclerosis Risk in Communities (ARIC) Study, 1987-1993. *Am J Epidemiol* 1997 September 15;146(6):483-94.
60. Ebrahim S, Papacosta O, Whincup P et al. Carotid plaque, intima media thickness, cardiovascular risk factors, and prevalent cardiovascular disease in men and women: the British Regional Heart Study. *Stroke* 1999 April;30(4):841-50.
61. Lekakis JP, Papamichael CM, Cimponeriu AT et al. Atherosclerotic changes of extracoronary arteries are associated with the extent of coronary atherosclerosis. *Am J Cardiol* 2000 April 15;85(8):949-52.
62. MackWJ, LaBree L, Liu C, Selzer RH, Hodis HN. Correlations between measures of atherosclerosis change using carotid ultrasonography and coronary angiography. *Atherosclerosis* 2000 June;150(2):371-9.

63. Vasankari T, Ahotupa M, Toikka J et al. Oxidized LDL and thickness of carotid intima-media are associated with coronary atherosclerosis in middle-aged men: lower levels of oxidized LDL with statin therapy. *Atherosclerosis* 2001 April;155(2):403-12.
64. Amato M, Montorsi P, Ravani A et al. Carotid intima-media thickness by B-mode ultrasound as surrogate of coronary atherosclerosis: correlation with quantitative coronary angiography and coronary intravascular ultrasound findings. *Eur Heart J* 2007 September;28(17):2094-101.
65. Adams GJ, Greene J, Vick GW, III et al. Tracking regression and progression of atherosclerosis in human carotid arteries using high-resolution magnetic resonance imaging. *Magn Reson Imaging* 2004 November;22(9):1249-58.
66. Shinnar M, Fallon JT, Wehrli S et al. The diagnostic accuracy of ex vivo MRI for human atherosclerotic plaque characterization. *Arterioscler Thromb Vasc Biol* 1999 November;19(11):2756-61.
67. Yuan C, Beach KW, Smith LH, Jr., Hatsukami TS. Measurement of atherosclerotic carotid plaque size in vivo using high resolution magnetic resonance imaging. *Circulation* 1998 December 15;98(24):2666-71.
68. Corti R, Fayad ZA, Fuster V et al. Effects of lipid-lowering by simvastatin on human atherosclerotic lesions: a longitudinal study by high-resolution, noninvasive magnetic resonance imaging. *Circulation* 2001 July 17;104(3):249-52.
69. Kang X, Polissar NL, Han C, Lin E, Yuan C. Analysis of the measurement precision of arterial lumen and wall areas using high-resolution MRI. *Magn Reson Med* 2000 December;44(6):968-72.
70. Chan SK, Jaffer FA, Botnar RM et al. Scan reproducibility of magnetic resonance imaging assessment of aortic atherosclerosis burden. *J Cardiovasc Magn Reson* 2001;3(4):331-8.
71. Varghese A, Crowe LA, Mohiaddin RH et al. Inter-study reproducibility of 3D volume selective fast spin echo sequence for quantifying carotid artery wall volume in asymptomatic subjects. *Atherosclerosis* 2005 December;183(2):361-6.
72. Varghese A, Crowe LA, Mohiaddin RH et al. Interstudy reproducibility of three-dimensional volume-selective fast spin echo magnetic resonance for quantifying carotid artery wall volume. *J Magn Reson Imaging* 2005 February;21(2):187-91.
73. Chiuve SE, McCullough ML, Sacks FM, Rimm EB. Healthy lifestyle factors in the primary prevention of coronary heart disease among men: benefits among users and nonusers of lipid-lowering and antihypertensive medications. *Circulation* 2006 July 11;114(2):160-7.
74. de GE, Jukema JW, Montauban van Swijndregt AD et al. B-mode ultrasound assessment of pravastatin treatment effect on carotid and femoral artery walls and its correlations with coronary arteriographic findings: a report of the Regression Growth Evaluation Statin Study (REGRESS). *J Am Coll Cardiol* 1998 June;31(7):1561-7.
75. Hodis HN, Mack WJ, LaBree L et al. Reduction in carotid arterial wall thickness using lovastatin and dietary therapy: a randomized controlled clinical trial. *Ann Intern Med* 1996 March 15;124(6):548-56.
76. Randomised trial of cholesterol lowering in 4444 patients with coronary heart disease: the Scandinavian Simvastatin Survival Study (4S). *Lancet* 1994 November 19;344(8934):1383-9.
77. Lehmann JM, Moore LB, Smith-Oliver TA, Wilkison WO, Willson TM, Kliewer SA. An antidiabetic thiazolidinedione is a high affinity ligand for peroxisome proliferator-activated receptor gamma (PPAR gamma). *J Biol Chem* 1995 June 2;270(22):12953-6.
78. Yki-Jarvinen H. Thiazolidinediones. *N Engl J Med* 2004 September 9;351(11):1106-18.
79. Lebovitz HE, Dole JF, Patwardhan R, Rappaport EB, Freed MI. Rosiglitazone monotherapy is effective in patients with type 2 diabetes. *J Clin Endocrinol Metab* 2001 January;86(1):280-8.
80. Viljanen AP, Virtanen KA, Jarvisalo MJ et al. Rosiglitazone treatment increases subcutaneous adipose tissue glucose uptake in parallel with perfusion in patients with type 2 diabetes: a double-blind, randomized study with metformin. *J Clin Endocrinol Metab* 2005 December;90(12):6523-8.
81. Mohanty P, Aljada A, Ghanim H et al. Evidence for a potent antiinflammatory effect of rosiglitazone. *J Clin Endocrinol Metab* 2004 June;89(6):2728-35.

82. Hedblad B, Zambanini A, Nilsson P, Janzon L, Berglund G. Rosiglitazone and carotid IMT progression rate in a mixed cohort of patients with type 2 diabetes and the insulin resistance syndrome: main results from the Rosiglitazone Atherosclerosis Study. *J Intern Med* 2007 March;261(3):293-305.
83. Stocker DJ, Taylor AJ, Langley RW, Jezior MR, Vigersky RA. A randomized trial of the effects of rosiglitazone and metformin on inflammation and subclinical atherosclerosis in patients with type 2 diabetes. *Am Heart J* 2007 March;153(3):445-6.

PART I

3T Magnetic resonance black blood vessel wall imaging

CHAPTER

2

Assessment of the Carotid Artery at 3T MR Imaging: a Study on Reproducibility

Reza Alizadeh Dehnavi MD¹, Joost Doornbos PhD², Jouke T. Tamsma MD¹, Matthias Stuber PhD³, Hein Putter PhD⁴, Rob J. van der Geest MS⁵, Hildo J. Lamb MD², Albert de Roos MD²

¹Vascular Medicine, Department of General Internal Medicine and Endocrinology, Leiden University Medical Center, Leiden, The Netherlands

²Department of Radiology, Leiden University Medical Center, Leiden, The Netherlands

³Department of Radiology, Division of MRI Research, Johns Hopkins University Medical School, Baltimore, Maryland, USA

⁴Department of Medical Statistics and Bio-Informatics, Leiden University Medical Center, Leiden, The Netherlands

⁵Image Processing, Department of Radiology, Leiden University Medical Center, Leiden, The Netherlands

J Magn Reson Imaging 2007 May;25(5):1035-43

ABSTRACT

Purpose

To examine the reproducibility of carotid artery dimension measurements using 3T MRI.

Materials and Methods

Ten healthy volunteers underwent three scans on two occasions for assessment of total vessel wall area (TVWA), total luminal area (TLA), and minimum (MinT) and maximum (MaxT) vessel wall thickness. A double inversion-recovery (IR) fast gradient-echo (FGRE) sequence was used on a commercial 3T system. During the first visit the subjects were scanned twice. The third scan was performed at least four days later. One observer traced all scans, and a second observer retraced the first scan series.

Results

For TVWA an interclass correlation (ICC) of 0.994 was calculated with all three scans taken into account. The interobserver ICC was 0.984. The agreement between the scans for TLA showed an ICC of 0.982 with an interobserver ICC of 0.998. For MinT and MaxT an ICC of 0.843 and 0.935 were calculated, with interobserver ICCs of 0.860 and 0.726, respectively.

Conclusion

With the use of a commercial 3T MR system, TVWA, TLA, and wall thickness measurements of the carotid artery can be assessed with good reproducibility.

INTRODUCTION

Cardiovascular disease is the leading cause of morbidity and mortality in the western world, and atherosclerosis is the primary underlying pathophysiological process. Atherosclerosis is regarded as a chronic inflammatory disease that can start at an early age¹ and progress throughout life, causing structural changes in the arterial wall.² This process is modulated by known risk factors such as dyslipidemia, diabetes, and hypertension, and can result in more prominent arterial wall structural changes in subjects who are at risk for developing cardiovascular disease.³ The relevance of arterial vascular structural changes for both clinical and research settings has been demonstrated in several studies.⁴⁻⁹

The carotid intima media thickness (IMT) as measured by high-resolution B-mode ultrasound imaging has been shown to correlate both with clinical cardiovascular disease and the level of risk factors present.⁵⁻⁸ Both the absolute IMT and its increase have been demonstrated to be predictive of future coronary events in subjects with prior coronary heart disease.⁹ The predictive power of the IMT has been shown to be independent of other risk factors.⁴⁻⁹ Furthermore, the importance of tomographic assessments of the arterial wall has been illustrated in studies in which, after a pharmacological intervention, a reduction in either the event rate or the vessel wall area was observed disproportionately to or in the absence of luminal changes.¹⁰⁻¹² Accurate assessments of the arterial vascular structure and possible changes in that structure over time are therefore of great importance because they both reflect the current disease burden and are predictive of future events. Magnetic resonance imaging (MRI) has emerged in recent years as a promising noninvasive imaging modality for the serial assessment of atherosclerosis.¹³⁻¹⁵ Its ability to quantify total plaque volume and disease burden has been demonstrated.¹⁶⁻¹⁸ The accuracy of the technique for assessing the atherosclerotic plaques was validated in comparison with histopathology in an ex vivo study.¹⁹ MRI has also been shown to be able to characterize plaque composition in vivo.²⁰

The introduction of whole-body 3.0T field-strength magnets has created new opportunities to further develop MRI. Improved signal-to-noise ratio (SNR), contrast-to-noise ratio (CNR), and image quality of the carotid artery images at 3T in comparison to 1.5T field strength have been demonstrated.²¹ However, to our knowledge, no reproducibility studies have been conducted to date. Accordingly, the aim of the present study was to test the reproducibility of the carotid artery lumen and wall dimension measurements on images obtained on a 3T system.

MATERIALS AND METHODS

Ten healthy adult subjects (seven males and three females, 25-79 years old, mean age = 57 years) underwent three MRI scans on two different occasions. During the first visit and after the first scan (SC1), the subjects were removed from the scanner, the coils were removed, and the subjects were repositioned. After this procedure a second scan (SC2) was performed. The third scan (SC3) was performed at least four days after the first visit. The local medical ethics committee approved the study, and all volunteers gave informed consent.

MRI

MRI was performed using a 3T scanner (Achieva; Philips, Best, The Netherlands) using a standard phased-array coil with two flexible elements of 14×17 cm. The subjects were scanned in the supine position with the neck positioned at the isocenter of the magnet. A special cushion was used to fix the position of the neck and head to reproduce a stable flexion angle. We avoided left-right rotation by positioning the patient's nose in the midsagittal plane. Figure 1 demonstrates the scanning setup. In all subjects the left carotid artery was examined. Three survey scans were performed: the first used a fast gradient-echo (FGRE) sequence and resulted in 20 contiguous transverse slices (acquired pixel size = $1 \text{ mm} \times 1.23 \text{ mm} \times 5.0 \text{ mm}$, field of view (FOV) = 300 mm, echo time (TE) =

Figure 1. The scanning setup.

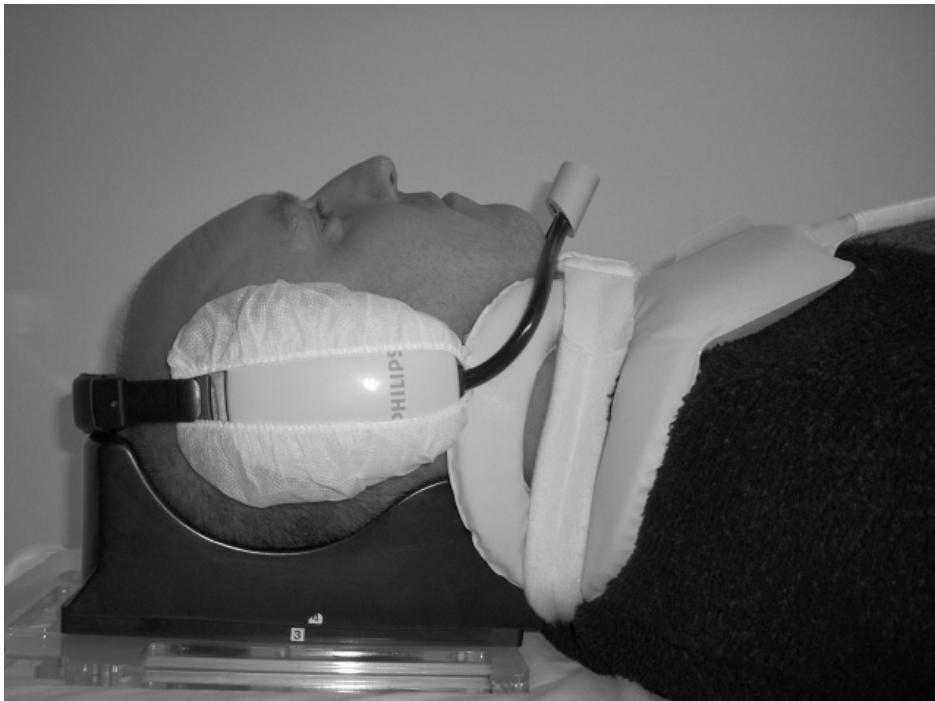
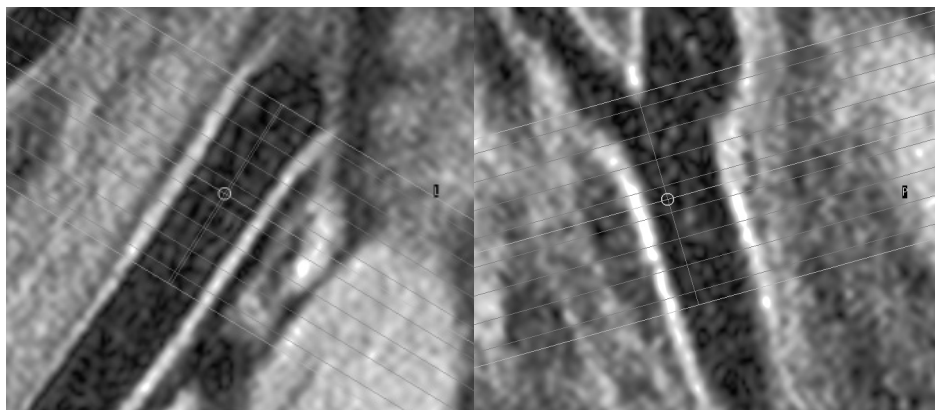


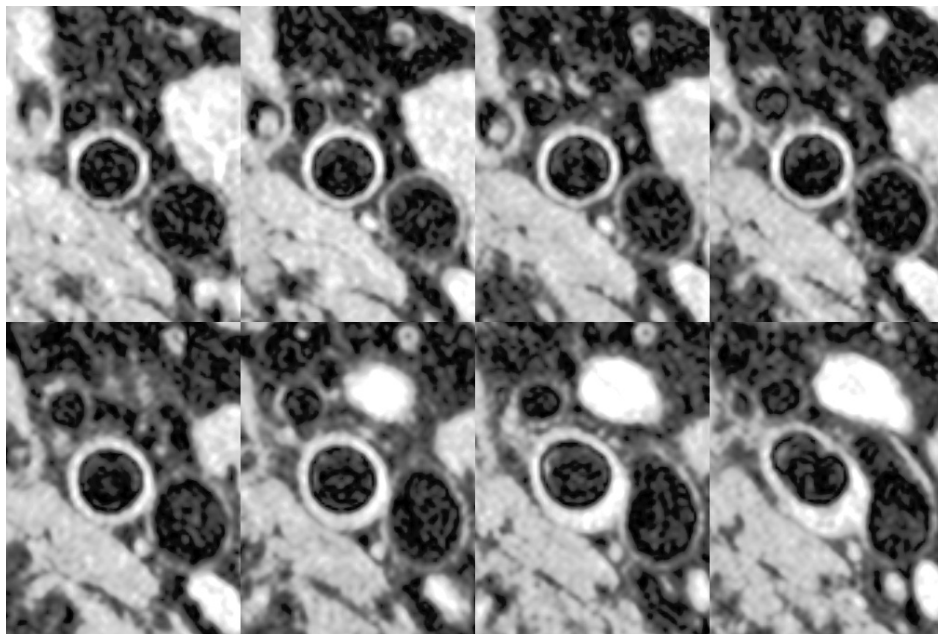
Figure 2. Oblique sagittal view of the carotid bifurcation, and oblique coronal plane of the common carotid artery. The yellow lines indicate beginning, end and the middle of the stack. Red lines indicate the middle of slices. Note that the slices are planned perpendicular to the course of the common carotid artery starting at the level of the flow divider.



3.8 msec, repetition time (TR) = 7.7 msec, and flip angle = 20°). We planned the second scout view by defining three points (three-point planscan tool) in the center of the common, internal, and external carotid arteries, which resulted in an oblique sagittal view of the carotid bifurcation (Fig. 2). The third survey was planned in an oblique sagittal plane, following the course of the common carotid artery, to obtain an oblique coronal plane (Fig. 2). For the second and third surveys, an FGRE sequence was used with dual inversion recovery (IR) and ECG triggering (FOV = 140 mm, matrix = 304×304 pixels reconstructed to 512×512 pixels. Acquired slice thickness = 2.5 mm, thickness of the reinverted slice = 3 mm, flip angle = 20° , TR = 11.8 msec, and TE = 3.6 msec). A standardized series of oblique axial slices were planned on the sagittal and coronal planes, perpendicular to the course of the common carotid artery in both views (Fig. 2). A total of eight contiguous transverse slices with 2-mm thickness were then acquired for the analysis starting from the flow divider in the proximal (caudal) direction covering 1.6 cm of the carotid bulb and the common carotid artery (Fig. 3). The flow divider on the oblique sagittal scouts was used as a landmark to ensure that the acquisition was planned at the same location for all three scans. A dual IR (black-blood), spoiled segmented k -space FGRE sequence with spectral selective fat suppression was used to maximize contrast between the carotid wall and the lumen blood pool. Images were acquired at each RR interval (TE = 3.6 msec, TR = 12 msec, flip angle = 45° , and two signal averages). ECG triggering was used for data acquisition at the end-diastole. A reinversion slice thickness of 3 mm was used. The FOV was 140 mm. With a matrix size of 306, a voxel size of $0.46 \text{ mm} \times 0.46 \text{ mm} \times 2 \text{ mm}$ was obtained. Each MR study took approximately 30 minutes depending on the cardiac frequency.

A GRE technique may be more prone to residual blood-pool signal than fast spin-echo (FSE) imaging. We performed an optimization procedure to avoid this possibility by optimally nulling the signal from blood utilizing a heart-rate-dependent inversion time (TI) according to the

Figure 3. Transverse slices acquired starting from the flow-divider in the proximal (caudal) direction covering 1.6 cm of the carotid bulb and the common carotid artery.



formula proposed by Fleckenstein et al.²² Furthermore, to maximize the likelihood for flow exchange (and therefore signal attenuation in the blood pool) in the imaged slice, the slice thickness of the reinverted slice was only 1 mm thicker than that of the imaged slice. During the developmental phase of the protocol, the radiofrequency (RF) excitation angle, the number of *k*-space segments, and the trigger delay were carefully optimized for image quality. During that process we tried to maximize the conspicuity of the inner and outer borders of the vessel wall.

Image analysis

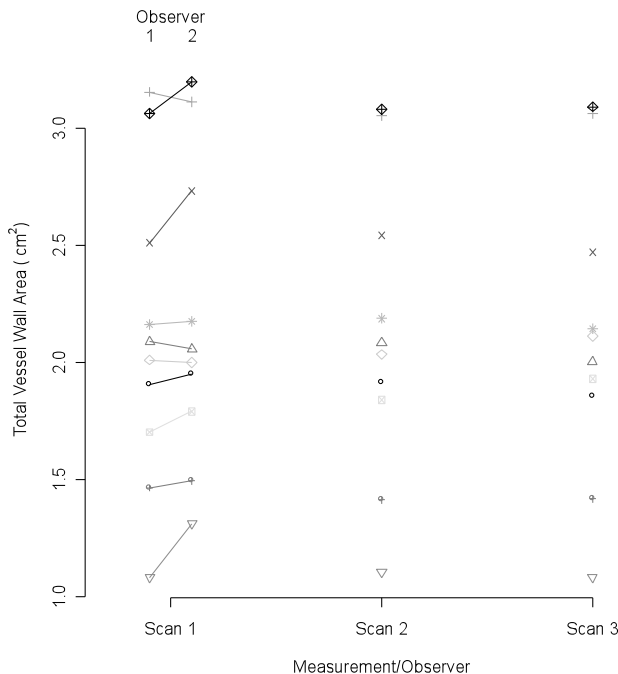
We analyzed all of the images using the VesselMASS software package developed at our institution.²³ This software package allows the semiautomated detection of the luminal and outer wall boundaries of the vessel wall from MR images, and the subsequent derivation of various quantitative parameters describing the vessel wall. All three scan series were traced by one observer. The first scan series was also traced by a second observer. The observers were blinded to each other's results. We calculated the vessel wall area by subtracting the luminal area from the outer contour area. We calculated the total vessel wall area (TVWA) by adding the vessel wall area from all eight slices, and the total luminal area (TLA) by adding the luminal area in all eight slices. We also calculated a vascular wall area-luminal area (W/L) index by dividing the TVWA by the TLA. Minimum vessel wall thickness (MinT) and maximum vessel wall thickness (MaxT) measurements were obtained from the slice at a distance of 1.8 cm from the flow divider in each scan series. We automatically divided the contour of the vessel wall on this slice into six, 10, 20, and 100 segments

using the centerline method as previously described.²⁴ An average thickness was automatically calculated per segment, and the MinT and MaxT values per segmentation group were used for the analysis. We evaluated these segmentation groups to determine the best analysis method for obtaining reproducible thickness measurements.

Statistical analysis

Interclass correlations (ICCs) were calculated to quantify the agreement between the measurements obtained at various time points and analyzed by different observers. Per endpoint, the ICC was calculated for the following measurements: SC1 vs. 2, SC1 vs. 3, and SC2 vs. 3, all three scans at the same time, and finally observer 1 vs. observer 2 (for SC1 only). Bland-Altman plots for the above pair wise comparisons were also made.²⁵ For all endpoints of the study, both intra- and interobserver mean relative errors (MREs) were calculated. For this calculation, first the absolute difference between the measurements was calculated per volunteer for the respective endpoint. The absolute difference was then divided by the average of the measurements to yield the relative error. We then calculated the mean absolute difference (MAD) and the mean relative error (MRE) for all endpoints by averaging the absolute difference and relative error calculated for all individual volunteers, respectively. It should be noted that for the

Figure 4. Scatter plot of the measurements of total vessel wall area (cm^2). Note the large inter-volunteer variation (range) and the good inter-scan agreement (See table 2).



intraobserver calculation of the absolute difference and the mean, all three analyses of the first observer were used.

RESULTS

A total of four analyses per volunteer were available (Table 1). Figure 4 demonstrates a scatter plot of all TVWA measurements per volunteer. The agreement between the different measurements was calculated using the ICCs. An overview of the calculated ICCs for the TVWA, TLA, and W/L index is provided in Table 2. The calculated agreement between the measurements remained very similar per endpoint irrespectively of the measurement combination used. For TVWA an ICC of 0.994 was calculated when all three measurements were taken into account. The observers had an ICC of 0.984 for this endpoint. The Bland-Altman plots, including limits of

Table 1. Measurements of TVWA and TLA obtained at different time points and analysed by the two observers.

Volunteer	TVWA (cm ²) Observer 1 SC 1	TVWA (cm ²) Observer 1 SC 2	TVWA (cm ²) Observer 1 SC 3	TVWA (cm ²) Observer 2 SC 1	TLA (cm ²) Observer 1 SC 1	TLA (cm ²) Observer 1 SC 2	TLA (cm ²) Observer 1 SC 3	TLA (cm ²) Observer 2 SC 1
1	1.907	1.9164	1.8580	1.9522	2.9250	2.8175	2.7750	2.8835
2	2.0887	2.0834	2.0019	2.0579	2.6795	2.8450	2.7595	2.6025
3	3.1526	3.0523	3.0597	3.1108	5.5465	5.2595	5.0945	5.5765
4	2.5088	2.5408	2.4691	2.7321	4.1110	4.3755	4.2120	4.0085
5	2.0109	2.0345	2.1135	1.9997	4.3570	4.4125	4.3405	4.2105
6	1.0835	1.1082	1.0856	1.3138	3.3180	3.2005	2.9380	3.2815
7	1.7038	1.8402	1.9313	1.7919	2.6215	2.4760	2.8530	2.5620
8	2.1620	2.1883	2.1443	2.1749	3.5720	3.6295	3.3425	3.4940
9	3.0612	3.0798	3.0894	3.1954	5.5695	5.8275	5.7155	5.5300
10	1.4655	1.4150	1.4193	1.4950	4.0350	3.8610	3.8455	3.9580

TVWA: Total vessel wall area

TLA: Total luminal area

SC 1;2;3: Scan 1;2;3

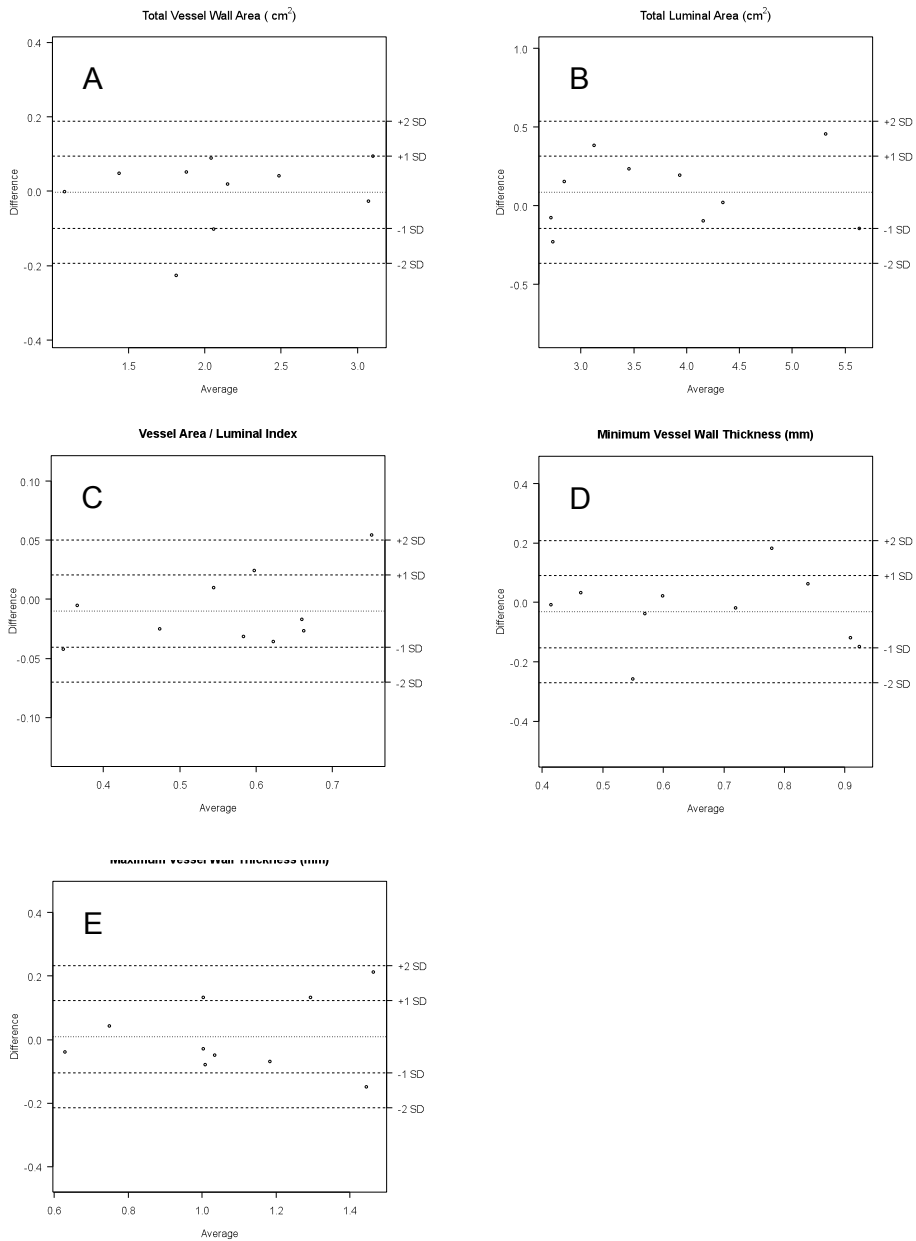
Table 2. Interclass correlations between the different scan series for TVWA, TLA and W/L index.

	Scan 1 vs 2	Scan 1 vs 3	Scan 2 vs 3	All three scans	Inter-observer
TVWA	0.996	0.990	0.996	0.994	0.984
TLA	0.986	0.975	0.984	0.982	0.998
W/L index	0.965	0.973	0.978	0.971	0.960

TVWA: Total vessel wall area

TLA: Total luminal area

W/L index: Vascular wall area/luminal area index

Figure 5.

A: Bland-Altman plot for Total Vessel Wall Area (cm^2), SC1 versus SC3.

B: Bland-Altman plot for TLA (cm^2), SC1 versus SC3.

C: Bland-Altman plot for vessel wall area/luminal area index, SC1 versus SC3.

D: Bland-Altman plot for Minimum vessel wall thickness, SC1 versus SC3.

E: Bland-Altman plot for Maximum vessel wall thickness, SC1 versus SC3.

Table 3. Interclass correlations between the different scan series minimum and maximum vessel wall thickness on the slice with 1.8 cm distance from the flow-divider.

	Scan 1 vs 2	Scan 1 vs 3	Scan 2 vs 3	All three scans	Inter-observer
Minimum vessel wall thickness					
6 Segments	0.873	0.923	0.740	0.843	0.860
10 Segments	0.699	0.920	0.694	0.781	0.807
20 Segments	0.632	0.910	0.697	0.761	0.840
100 Segments	0.602	0.881	0.654	0.732	0.809
Maximum vessel wall thickness					
6 Segments	0.923	0.925	0.958	0.935	0.726
10 Segments	0.919	0.871	0.930	0.907	0.718
20 Segments	0.895	0.862	0.924	0.894	0.717
100 Segments	0.903	0.901	0.931	0.912	0.800

agreement for SC1 vs. SC3, are shown in Fig. 5 for TVWA, TLA, W/L index, MinT, and MaxT when six segments were used to assess the vascular thickness. No dependence of the difference vs. the mean was observed. When all three scans were considered, the agreement between the analyses for TLA resulted in an ICC of 0.982, with an interobserver ICC of 0.998. For the W/L index the ICC calculated was 0.971, with an interobserver ICC of 0.960. Dividing the slice into six segments resulted in optimal agreement between the measurements for both MinT and MaxT (see Table 3). When the analysis was performed based on all three scans, ICCs of 0.843 and 0.935 were calculated for MinT and MaxT, respectively (six-segment method). The interobserver agreement for this segmentation method for MinT and MaxT resulted in ICC = 0.860 and 0.726, respectively. Furthermore, both intra- and interobserver MREs were calculated for all endpoints (see Table 4). The intraobserver MRE was calculated to be 2.6% for TVWA, and the interobserver MRE was 4.5%.

DISCUSSION

This study shows a high agreement between the repeated measurements of the TVWA, TLA, and W/L index of the carotid arteries as assessed using dual-inversion black-blood segmented *k*-space GRE imaging at 3T. Excellent image quality with high vessel wall-lumen contrast was obtained in all subjects, and a good reproducibility of the MinT and MaxT measurements at a predefined position in the common carotid artery relative to the flow divider was demonstrated.

The reliability of MRI measurements at 1.5T was previously demonstrated in a population with pre-existing atherosclerotic plaques.¹⁶ Errors in the vessel wall area of 2.6% and 3.5% were

Table 4. Means, standard deviations, intra- and interobserver MAD and MRE for all endpoints

	Observer1 SC 1 Mean (SD) (cm ²)	Observer1 SC 2 Mean (SD) (cm ²)	Observer1 SC 3 Mean (SD) (cm ²)	Observer1 Overall Mean (SD) (cm ²)	Intraobserver MAD (cm ²)	Intraobserver MRE (%)	Observer 2 SC1 Mean (SD) (cm ²)	Interobserver MAD (cm ²)	Interobserver MRE (%)
TVWA	2.114 (0.653)	2.126 (0.634)	2.117 (0.635)	2.119 (0.639)	0.053	2.6	2.182 (0.639)	0.085	4.5
TLA	3.874 (1.069)	3.870 (1.102)	3.788 (1.043)	3.844 (1.065)	0.173	4.8	3.811 (1.083)	0.069	1.9
W/L index	0.557 (0.138)	0.562 (0.139)	0.567 (0.125)	0.562 (0.133)	0.025	4.3	0.586 (0.135)	0.031	6.0
MinT	0.662 (0.191)	0.673 (0.147)	0.693 (0.195)	0.676 (0.162)	0.087	12.2	0.690 (0.161)	0.086	13.0
6 segments									
MinT	0.614 (0.183)	0.642 (0.149)	0.657 (0.175)	0.638 (0.153)	0.088	13.4	0.648 (0.155)	0.088	15.2
10 segments									
MinT	0.581 (0.183)	0.600 (0.148)	0.613 (0.180)	0.598 (0.153)	0.090	14.8	0.618 (0.152)	0.089	16.4
20 segments									
MinT	0.530 (0.180)	0.562 (0.149)	0.581 (0.184)	0.558 (0.153)	0.088	15.3	0.563 (0.148)	0.091	18.9
100 segments									
MaxT	1.087 (0.289)	1.047 (0.291)	1.078 (0.268)	1.071 (0.274)	0.093	8.2	1.079 (0.273)	0.120	10.2
6 segments									
MaxT	1.153 (0.299)	1.127 (0.337)	1.137 (0.273)	1.139 (0.292)	0.106	8.9	1.126 (0.293)	0.119	9.9
10 segments									
MaxT	1.190 (0.283)	1.165 (0.344)	1.196 (0.286)	1.184 (0.289)	0.137	11.6	1.172 (0.313)	0.140	11.1
20 segments									
MaxT	1.232 (0.275)	1.210 (0.346)	1.247 (0.289)	1.230 (0.287)	0.145	12.0	1.210 (0.315)	0.126	9.6
100 segme									

TVWA: Total vessel wall area
TLA: Total luminal area
W/L index: Vascular wall area/luminal area index

MinT: Minimum vessel wall thickness
MaxT: Maximum vessel wall thickness
SD: Standard deviation

MAD: Mean absolute difference
MRE: Mean relative error
SC 1;2;3: Scan 1;2;3

reported for the aortic and carotid plaques, respectively. Errors in wall volume measurements in hypercholesterolemic subjects were shown in another study (also performed at 1.5T) to range from 3% to 6%.¹⁷ The mean relative error of 2.6% obtained in the present study at 3T for vessel wall area measurements in healthy adult subjects with a wide age range further confirms these previous observations. However, it is difficult to determine whether the field strength of 3T is superior to 1.5T, as far as the reproducibility of the vessel wall measurements is concerned, by comparing the above-mentioned results. The present data was obtained from a heterogeneous population without occlusive carotid plaques; however, most previous studies of reproducibility were performed in more homogeneous populations with pre-existing carotid atherosclerotic disease, which affects the statistical outcome in terms of reproducibility and relative error. Real evidence can only be obtained by scanning one group of volunteers at both field strengths and comparing the data.

We observed a high level of agreement for TVWA between the different analyses of the scans as evaluated by one observer (ICC = 0.994). The interobserver agreement for this endpoint was slightly lower (ICC = 0.984). The agreement between measurements for the MaxT (ICC = 0.935), when using six segments, was lower than that of TVWA. A further decrease in agreement was seen when six segments were used for the assessment of the MinT (ICC = 0.843). The precision of such measurements decreases when smaller structures are measured (i.e., the total quantity of wall area and wall thickness). Wall thickness measurements are obtained using 100 centerlines. One can obtain these measurements of wall thickness from all 100 centerlines individually or by grouping the centerlines into a predefined number of segments, and then calculating the average per segment (e.g., 5 centerlines \times 20 segments). Table 3 illustrates that the ICC for MinT decreases when the number of wall segments increases (thereby decreasing the number of centerlines per segment). A decrease in the number of centerlines per segment is expected to result in a relative lower calculated average MinT, which will in turn result in a decreased precision. On the other hand, this effect is not observed when all 100 centerlines are used individually to estimate the MaxT. The precision for MaxT measurements does not decrease when 100 centerlines are used individually, due to the relatively larger wall thickness. One would expect higher reproducibility of thickness measurements in patients with pre-existing atherosclerotic plaques or elevated disease burden using this method. This effect on the precision of the total measured quantity may also contribute to the observed agreement between the different analyses of TLA. Compared to TVWA, a lower ICC of 0.982 was calculated for the TLA measurements. The differences between the different measurements were in this case less prominent due to the greater total quantity assessed. TLA ranged from 2.48 to 5.83 cm² (mean = 3.84 cm²), whereas TVWA ranged from 1.08 to 3.20 cm² (mean = 2.13 cm²). The agreement between the measurements for the W/L index was very good (ICC = 0.971), although slightly lower than its components. This index could be important when the technique is used to assess the long-term effects of an intervention, since both of its components have been

shown to change after an intervention. Earlier reports have shown a reduction in either the event rate or the vessel wall area after a pharmacological intervention disproportionately to or in the absence of luminal changes.¹⁰⁻¹² In a follow-up study of patients on statin therapy, no luminal changes were observed in the thoracic aorta by MRI after a short treatment period of six months, but plaque volume and area decreased significantly.¹² Prolonged treatment has been shown to significantly increase the luminal area with a range of 4% to 6% in both the aorta and the carotid artery, along with a regression in the vessel wall thickness and area of up to 20%.¹¹ The W/L index together with the TLA could also provide information about the early stages of the atherosclerotic process, during which outward remodeling can occur. This process is defined by an increase in the vessel wall disease burden (plaque) in the absence of luminal changes.²⁶ Since the index contains the two components that could possibly be affected by the atherosclerotic process or an intervention, it has the potential to detect changes more sensitively.

Technical requirements for high-resolution carotid vessel imaging include high spatial resolution, high contrast between the vessel wall and blood pool without flow artifacts, high contrast between the vessel wall and surrounding fat, and suppression of motion artifacts. FSE sequences with multiple contrast weightings are commonly used to meet these requirements, and some reports have shown reliable results with GRE sequences.²⁷ Recent studies have shown the reproducibility of a 3D volume-selective FSE sequence in both patients with known atherosclerotic disease²⁸ and asymptomatic patients.²⁹ While most prior work on carotid vessel wall imaging was performed at 1.5T using FSE techniques, the present study was conducted at 3T using a spoiled GRE (SPGRE) imaging sequence. During the developmental phase of our protocol, we initially focused on the use of dual-inversion FSE imaging as well. However, based on our prior experience with black-blood imaging of the coronary vessel wall at 1.5T and 3T^{30, 31}, we decided to simultaneously work on the development of a dual-inversion SPGRE technique. We found that both the visual sharpness and contrast of the carotid vessel wall were superior on the SPGRE images as compared to those obtained with the more conventional FSE approach. Since our goal was to optimize black-blood carotid vessel wall image quality at 3T, we decided to move forward with the SPGRE imaging technique. However, based on prior and extensive experience with FSE imaging at 1.5T, the use of FSE imaging at 3T may have to be revisited, and specific 3T issues, including the specific absorption rate (SAR), prolonged T1, and increased B1 inhomogeneity, may have to be addressed to further optimize FSE imaging of the carotids. Here, in one of the first studies to assess the measurement capabilities of MRI in the carotid artery at 3T, we demonstrated the high reproducibility of vessel wall area measurements using a dual-inversion segmented *k*-space GRE imaging technique.

Black-blood techniques are commonly used to achieve flow suppression, even though they require a relatively long acquisition duration.³² The technique uses a nonselective inversion RF

pulse that inverts the longitudinal magnetization of the entire volume in the transmit coil. This is immediately followed by a slice-selective RF pulse that reinverts the longitudinal magnetization at the anatomical level of interest. By placing the double IR prepulse before a period of rapid flow and acquiring data during the slow flow, one can maximize the flow suppression of intraluminal signal.³³ In a study using the black-blood technique²⁹, residual blood signal was observed in asymptomatic subjects. This is thought to be the result of recirculation in the bulb region, which can be influenced by several factors.³⁴ Two such factors are the blood flow velocity (which is influenced by, e.g., the extent of possible stenoses) and the distensibility of the carotid artery (which can vary with age and the risk profile). Our experience suggests that one can minimize flow artifacts caused by the residual blood signal by planning the transverse slices perpendicular to the flow direction. Motion artifacts can be reduced by cardiac triggering, and perivascular fat signal suppression can be achieved with the use of fat-saturation prepulses. The field strength at which images are acquired is another factor that can influence the precision of the measurements. In a recent study³⁵ a considerable increase in SNR was observed when the field strength was increased from 1.5T to 3T. This increase could be traded for a better in-plane resolution, which in turn could improve the accuracy of the measurements. This is reflected by the improved detection of complex atherosclerotic plaque at 3T, as validated by histology³⁶, and the increased SNR, CNR, and improved image quality of the carotid images at 3T²¹ as compared to 1.5T. In the current study we evaluated a GRE sequence with 0.46 mm × 0.46 mm × 2 mm spatial resolution, which is comparable to that employed in recent studies at 1.5T.^{28, 29}

We observed good reproducibility of the vessel wall thickness measurements at a fixed position in the carotid artery (see Table 3). Different segmentation methods were used to evaluate the optimum method of analysis for the reproducible thickness measurements. Averages calculated per segment when the vessel contour was divided into six segments were most reproducible for MinT and MaxT. The interobserver agreement for MinT was also optimal using this segmentation method. For the MaxT, the highest agreement between the observers was seen when the analysis was performed using 100 segments.

In conclusion, the TVWA, TLA, and W/L index of the carotid artery can be assessed with high reproducibility at a field strength of 3T. Thickness measurements of the carotid vessel wall at a fixed position can be evaluated with good reproducibility in subjects without occlusive atherosclerotic plaques.

REFERENCE LIST

1. Napoli C, D'Armiento FP, Mancini FP et al. Fatty streak formation occurs in human fetal aortas and is greatly enhanced by maternal hypercholesterolemia. Intimal accumulation of low density lipoprotein and its oxidation precede monocyte recruitment into early atherosclerotic lesions. *J Clin Invest* 1997 December 1;100(11):2680-90.
2. Lusis AJ. Atherosclerosis. *Nature* 2000 September 14;407(6801):233-41.
3. Lavrencic A, Kosmina B, Keber I, Videcnik V, Keber D. Carotid intima-media thickness in young patients with familial hypercholesterolaemia. *Heart* 1996 October;76(4):321-5.
4. Furberg CD, Adams HP, Jr., Applegate WB et al. Effect of lovastatin on early carotid atherosclerosis and cardiovascular events. Asymptomatic Carotid Artery Progression Study (ACAPS) Research Group. *Circulation* 1994 October;90(4):1679-87.
5. Chambless LE, Heiss G, Folsom AR et al. Association of coronary heart disease incidence with carotid arterial wall thickness and major risk factors: the Atherosclerosis Risk in Communities (ARIC) Study, 1987-1993. *Am J Epidemiol* 1997 September 15;146(6):483-94.
6. Chambless LE, Folsom AR, Clegg LX et al. Carotid wall thickness is predictive of incident clinical stroke: the Atherosclerosis Risk in Communities (ARIC) study. *Am J Epidemiol* 2000 March 1;151(5):478-87.
7. O'Leary DH, Polak JF, Kronmal RA, Manolio TA, Burke GL, Wolfson SK, Jr. Carotid-artery intima and media thickness as a risk factor for myocardial infarction and stroke in older adults. Cardiovascular Health Study Collaborative Research Group. *N Engl J Med* 1999 January 7;340(1):14-22.
8. Bots ML, Hoes AW, Koudstaal PJ, Hofman A, Grobbee DE. Common carotid intima-media thickness and risk of stroke and myocardial infarction: the Rotterdam Study. *Circulation* 1997 September 2;96(5):1432-7.
9. Hodis HN, Mack WJ, LaBree L et al. The role of carotid arterial intima-media thickness in predicting clinical coronary events. *Ann Intern Med* 1998 February 15;128(4):262-9.
10. Brown G, Albers JJ, Fisher LD et al. Regression of coronary artery disease as a result of intensive lipid-lowering therapy in men with high levels of apolipoprotein B. *N Engl J Med* 1990 November 8;323(19):1289-98.
11. Corti R, Fuster V, Fayad ZA et al. Lipid lowering by simvastatin induces regression of human atherosclerotic lesions: two years' follow-up by high-resolution noninvasive magnetic resonance imaging. *Circulation* 2002 December 3;106(23):2884-7.
12. Lima JA, Desai MY, Steen H, Warren WP, Gautam S, Lai S. Statin-induced cholesterol lowering and plaque regression after 6 months of magnetic resonance imaging-monitored therapy. *Circulation* 2004 October 19;110(16):2336-41.
13. Fayad ZA, Fuster V. The human high-risk plaque and its detection by magnetic resonance imaging. *Am J Cardiol* 2001 July 19;88(2A):42E-5E.
14. Choudhury RP, Fuster V, Badimon JJ, Fisher EA, Fayad ZA. MRI and characterization of atherosclerotic plaque: emerging applications and molecular imaging. *Arterioscler Thromb Vasc Biol* 2002 July 1;22(7):1065-74.
15. Fayad ZA, Fuster V, Nikolaou K, Becker C. Computed tomography and magnetic resonance imaging for noninvasive coronary angiography and plaque imaging: current and potential future concepts. *Circulation* 2002 October 8;106(15):2026-34.
16. Corti R, Fayad ZA, Fuster V et al. Effects of lipid-lowering by simvastatin on human atherosclerotic lesions: a longitudinal study by high-resolution, noninvasive magnetic resonance imaging. *Circulation* 2001 July 17;104(3):249-52.
17. Kang X, Polissar NL, Han C, Lin E, Yuan C. Analysis of the measurement precision of arterial lumen and wall areas using high-resolution MRI. *Magn Reson Med* 2000 December;44(6):968-72.
18. Chan SK, Jaffer FA, Botnar RM et al. Scan reproducibility of magnetic resonance imaging assessment of aortic atherosclerosis burden. *J Cardiovasc Magn Reson* 2001;3(4):331-8.

19. Shinnar M, Fallon JT, Wehrli S et al. The diagnostic accuracy of ex vivo MRI for human atherosclerotic plaque characterization. *Arterioscler Thromb Vasc Biol* 1999 November;19(11):2756-61.
20. Toussaint JF, LaMuraglia GM, Southern JF, Fuster V, Kantor HL. Magnetic resonance images lipid, fibrous, calcified, hemorrhagic, and thrombotic components of human atherosclerosis in vivo. *Circulation* 1996 September 1;94(5):932-8.
21. Yarnykh VL, Terashima M, Hayes CE et al. Multicontrast black-blood MRI of carotid arteries: comparison between 1.5 and 3 tesla magnetic field strengths. *J Magn Reson Imaging* 2006 May;23(5):691-8.
22. Fleckenstein JL, Archer BT, Barker BA, Vaughan JT, Parkey RW, Peshock RM. Fast short-tau inversion-recovery MR imaging. *Radiology* 1991 May;179(2):499-504.
23. Adame IM, van der Geest RJ, Wasserman BA, Mohamed MA, Reiber JH, Lelieveldt BP. Automatic segmentation and plaque characterization in atherosclerotic carotid artery MR images. *MAGMA* 2004 April;16(5):227-34.
24. van der Geest RJ, Reiber JH. Quantification in cardiac MRI. *J Magn Reson Imaging* 1999 November;10(5):602-8.
25. Bland JM, Altman DG. Statistical methods for assessing agreement between two methods of clinical measurement. *Lancet* 1986 February 8;1(8476):307-10.
26. Glagov S, Weisenberg E, Zarins CK, Stankunavicius R, Kolettis GJ. Compensatory enlargement of human atherosclerotic coronary arteries. *N Engl J Med* 1987 May 28;316(22):1371-5.
27. Leiner T, Gerretsen S, Botnar R et al. Magnetic resonance imaging of atherosclerosis. *Eur Radiol* 2005 June;15(6):1087-99.
28. Varghese A, Crowe LA, Mohiaddin RH et al. Interstudy reproducibility of three-dimensional volume-selective fast spin echo magnetic resonance for quantifying carotid artery wall volume. *J Magn Reson Imaging* 2005 February;21(2):187-91.
29. Varghese A, Crowe LA, Mohiaddin RH et al. Inter-study reproducibility of 3D volume selective fast spin echo sequence for quantifying carotid artery wall volume in asymptomatic subjects. *Atherosclerosis* 2005 December;183(2):361-6.
30. Botnar RM, Stuber M, Kissinger KV, Kim WY, Spuentrup E, Manning WJ. Noninvasive coronary vessel wall and plaque imaging with magnetic resonance imaging. *Circulation* 2000 November 21;102(21):2582-7.
31. Botnar RM, Stuber M, Lamerichs R et al. Initial experiences with in vivo right coronary artery human MR vessel wall imaging at 3 tesla. *J Cardiovasc Magn Reson* 2003;5(4):589-94.
32. Edelman RR, Chien D, Kim D. Fast selective black blood MR imaging. *Radiology* 1991 December;181(3):655-60.
33. Fayad ZA, Fuster V. Atherothrombotic plaques and the need for imaging. *Neuroimaging Clin N Am* 2002 August;12(3):351-64.
34. Box FM, van der Geest RJ, Rutten MC, Reiber JH. The influence of flow, vessel diameter, and non-newtonian blood viscosity on the wall shear stress in a carotid bifurcation model for unsteady flow. *Invest Radiol* 2005 May;40(5):277-94.
35. Anumula S, Song HK, Wright AC, Wehrli FW. High-resolution black-blood MRI of the carotid vessel wall using phased-array coils at 1.5 and 3 Tesla. *Acad Radiol* 2005 December;12(12):1521-6.
36. Cury RC, Houser SL, Furie KL et al. Vulnerable plaque detection by 3.0 tesla magnetic resonance imaging. *Invest Radiol* 2006 February;41(2):112-5.

CHAPTER

3

Assessment of carotid artery dimensions by MRI at 3-Tesla in patients at intermediate to high cardiovascular risk with reference to ultrasonography

Arghya Ray, MD¹; Reza Alizadeh Dehnavi, MD¹; Rob J van der Geest²; Menno V Huisman, MD¹; Mark A van Buchem, MD²; Albert de Roos, MD²; Jouke T Tamsma, MD¹

¹Vascular Medicine Unit, Department of Endocrinology and General Internal Medicine, Leiden University Medical Center, Leiden, The Netherlands

²Department of Radiology, Leiden University Medical Center, Leiden, The Netherlands

Submitted

ABSTRACT

Objectives

To assess carotid artery vessel wall dimensions in patients at intermediate-to-high cardiovascular (CV) risk compared to healthy young control subjects with 3 Tesla MRI. As a second objective the MRI measurements were compared with those values obtained by ultrasonography.

Materials and Methods

Patients in Group 1 (n=28; age 61.8 ± 4.64 yrs) had intermediate-to-high CV-risk, whereas group 2 (n=11; age 24.7 ± 3.74 yrs) consisted of healthy subjects. Mean wall thickness (MWT), wall area and lumen diameter, were measured in the left carotid artery using a black blood fast gradient MRI pulse sequence at 3 Tesla. Intima-media thickness (IMT) and lumen diameter were also measured by ultrasound in the same vessel segment.

Results

Group 1 subjects had significantly higher MWT and wall area as compared to group 2 (1.40 ± 0.30 mm vs 0.87 ± 0.07 mm; $p < 0.001$ and 1.90 ± 0.61 mm vs 0.96 ± 0.11 mm; $p < 0.001$). MRI assessment of lumen diameters showed high agreement with US (intraclass correlation coefficient 0.882). Furthermore, significant correlations were found between IMT and both MWT and wall area ($r = 0.84$, $p < 0.001$; 0.78 , $p < 0.001$, respectively).

Conclusion

MRI successfully discriminated vessel wall characteristics in intermediate and high risk patients from those in young healthy control subjects. MRI showed high dimensional precision with US as reference and significantly correlated with IMT.

INTRODUCTION

Vessel wall assessment is increasingly used to improve cardiovascular risk stratification. Ultrasonographic (US) evaluation of the carotid artery has been developed and yields a measure of the vascular intima-media complex. Intima media thickness (IMT) is an established marker of atherosclerosis. IMT is related to cardiovascular risk factors (1;2), coronary atherosclerosis (3-5), and future cardiovascular events (6;7). Therefore, IMT is frequently used as an intermediate end-point in clinical trials and is approved by the Food and Drug Administration for this purpose.

Magnetic resonance imaging (MRI) is now emerging as an imaging modality for the assessment of carotid artery atherosclerosis. Several studies have addressed the potential of 1.5 Tesla MRI to assess carotid artery vessel wall characteristics (8-11). Recently, MRI at 3T has been validated as a reproducible technique to assess the carotid artery vessel wall (11). However, the use of MRI at 3T to discriminate between the vessel wall dimensions of patients at intermediate-to-high cardiovascular risk from normal subjects has not been extensively studied.

Accordingly, the purpose of this study was to assess carotid artery vessel wall area characteristics in patients at intermediate-to-high cardiovascular risk versus those in healthy young subjects using 3 Tesla MRI. In addition, the MRI measurements of the vessel wall area and diameter were compared to those obtained by ultrasonography.

METHODS

Study Design & Subjects

The study was prospectively performed over a 1 year period. The study population was formed by 30 older male subjects attending our outpatient ward (group 1). These patients were treated in a primary prevention setting and had an intermediate to high cardiovascular risk as assessed using Framingham risk scores. The subjects of group 1 were contrasted to 11 young healthy volunteers (group 2). The US and MRI scans were performed by fully trained single observers, blinded for the results of the scan with the other imaging modality. Both observers were physicians with at least 4 years of experience using the carotid artery scanning protocol. The time between ultrasound (US) and MRI examination was never more than 2 months. In 2 cases the MRI was not interpretable due to insufficient quality resulting in 39 subjects for analysis. Informed consent was obtained and the study protocol was approved by the hospital ethics committee.

Magnetic Resonance Imaging Protocol

Magnetic resonance imaging was performed on a 3-Tesla scanner (Philips, Achieva, Best, The Netherlands). The reproducibility of this technique has been previously reported (11). In brief, a standard

Philips SENSE-flex-M surface coil was used for imaging. The left carotid artery was examined in all subjects. Three fast gradient echo sequence surveys were performed to localize the course of the common carotid artery. Subsequently, five contiguous transverse slices with 2mm slice thickness were acquired, starting from 1cm proximal to the flow divider, thereby covering the most distal 1 cm of the common carotid artery. A dual inversion recovery (black-blood), spoiled segmented k-space fast gradient echo sequence with spectral selective fat suppression was used for the acquisition of transverse slices. Images were acquired in cardiac end-diastole at each RR interval using ECG triggering. The following imaging parameters were used: echo time 3.6ms, repetition time (TR) 12ms, flip angle 45 degrees, and 2 signal averages were performed. A re-inversion slice thickness of 3mm was used. The field of view was 140mm. When using a matrix size of 306 the resulting voxel size was 0.46mm x 0.46mm x 2mm. Each MRI study took approximately 30 minutes depending on the cardiac frequency. All images were analyzed by a single observer with 4 years experience, using the VesselMASS software package, allowing manual tracing of vessel boundaries and automated quantification of lumen diameter, wall area and mean wall thickness (12). Mean wall thickness (MWT) was calculated by averaging the mean thickness at all 5 slices of the common carotid artery. Vessel wall area (VWA) was quantified by extracting the luminal area from the detected outer vascular boundary at each slice. The sum of these 5 area values was used as the outcome parameter VWA. Figure 1 shows a representative example of an MRI scan of the carotid artery.

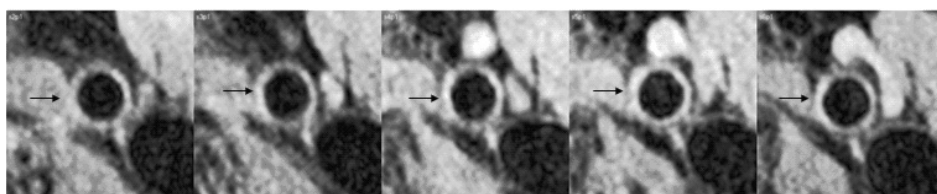


Figure 1. Representative example of 3-Tesla MRI image of the carotid artery of a 62-year old male subject. Black arrows indicate the carotid artery. Five contiguous transverse slices of 2mm, covering the most distal 1cm of the common carotid artery are shown.

Ultrasound protocol

IMT measurement was performed using an Acuson Sequoia 512 (Siemens Medical Solutions, CA, USA) high-resolution ultrasound machine with an 8MHz linear transducer. One IMT-certified sonographer (4 years of experience) performed all the ultrasounds. First, a transverse scan was performed for orientation, starting at the clavicle and moving cranially up to the mandible, hereby locating the height of the carotid bifurcation. Subsequently, longitudinal images were obtained. This technique allows visualization of two echogenic lines, separated by an anechoic space. It has previously been established that these lines indicate the blood-intima and the media-adventitia interfaces, and that the distance between the lines represents a reliable measure for IMT (13). The scan included visualization of the near and far walls of the left common carotid artery, at four angles of insonation (anterior, two antero-lateral projections and lateral). The caudal tip of the flow divider

was used as the anatomical landmark to localize the most distal 1 cm of the common carotid artery. Overall gain settings were kept at 0 dB when possible. The sonographer was free to adjust the gain levels if necessary, within the limits of -7 dB to 7 dB. The scan was recorded on sVHS video cassettes and digitalized for off-line analysis. IMT values were quantified using computer aided automatic boundary detection where possible and manual adjustment where necessary. Analyses were done by a trained analyst, using the ASM II software package version 1.1364. IMT was defined as the average of the mean values of the common carotid artery, at all four angles. Lumen diameter was also determined at four angles and defined as the distance between the intima-lumen interface of the near wall and the lumen-intima interface of the far wall. Quantification of all parameters was timed to coincide with cardiac end-diastole using an on-screen 3-lead ECG.

Statistical analysis

All data followed normal distribution, calculated by levels of skewness and kurtosis. All data are expressed as means \pm SD. Comparisons between the groups were performed with independent samples *t* tests. Correlations between US and MRI were calculated using Pearson's correlation coefficients. Bland-Altman analyses (14) and intraclass correlations coefficients (ICC) were calculated and used to assess agreement of the two imaging modalities. Linear regression between IMT and MRI wall thickness were plotted to approach the MRI value corresponding to an IMT of 0.9 mm, considered the clinically relevant cut-off value (6). *P*-values of <0.05 were designated as statistically significant.

Table 1: Subject characteristics and main outcome parameters

Variable	Group 1	Group 2
N	28	11
age (yrs)	61.8 [± 4.64]	24.7 [± 3.74]*
Framingham CHD risk score (%/10yrs)	15.8 [± 4.76]	-
MWT; MRI (mm)	1.40 [± 0.30]	0.87 [± 0.07]*
VWA; MRI (cm²)	1.90 [± 0.61]	0.96 [± 0.11]*
mean IMT; US (mm)	0.86 [± 1.60]	0.50 [± 0.03]*
lumen diameter; MRI (mm)	7.00 [± 0.80]	6.00 [± 0.43]
lumen diameter; US (mm)	7.00 [± 0.86]	5.96 [± 0.34]

Values are expressed in means (\pm SD). group 1=older subset; group 2=young healthy volunteers. Data show the expected differences between the younger and the older group in vessel wall parameters. No difference was observed between MRI and US in measurement of lumen diameter, confirming dimensional compatibility between the techniques. Asterisk (*) indicates statistically significant difference between group 1 and 2 ($p < 0.001$).

CHD: coronary heart disease

IMT: intima-media thickness

MWT: mean wall thickness

VWA: common carotid vessel wall area

Table 2: Bivariate correlations between main outcomes by MRI and US

Variable	Pearson coefficient (r)	P-value
MWT vs. IMT	0.84	<0.001
VWA vs. IMT	0.78	<0.001
lumen diameter (MRI vs. US)	0.88	<0.001

The high correlations with IMT validate the use of these MRI parameters as surrogate markers for atherosclerosis

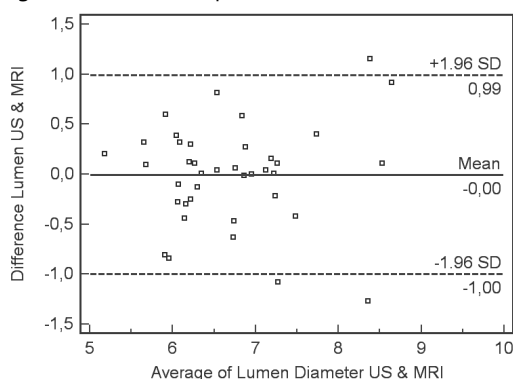
IMT: intima media thickness

MWT: mean wall thickness

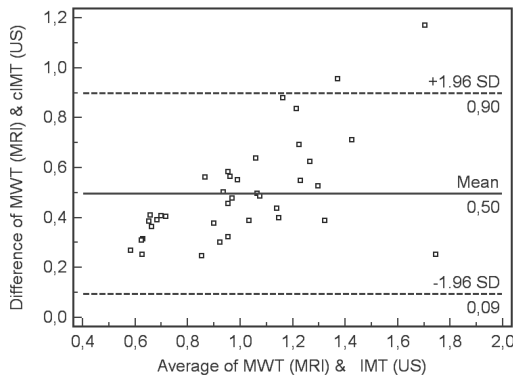
VWA: vessel wall area

RESULTS

A summary of the results is given in Table 1. The Framingham risk scores of group 1 subjects ranged from 6 to 29%/ 10 years. In young subjects the estimated cardiovascular risk is low to very low (<<5%/10 years) but difficult to estimate as age puts substantial weight in the algorithms. MWT and VWA were significantly higher in group 1 compared to group 2. IMT values were also significantly higher in group 1 compared to group 2. MWT and VWA correlated strongly with IMT. A highly significant correlation was observed for assessment of lumen diameters measured using the two modalities (Table 2). A Bland-Altman plot (figure 2) showed no significant difference of US and MRI in measured lumen diameters. An acceptable variation around the mean (within 1.96 standard deviations) was observed without upward or downward bias. US and MRI assessment of mean lumen diameters showed high intraclass correlation for absolute

Figure 2. Bland-Altman plot of ultrasound and MRI values for lumen diameter.

Data indicate a very high agreement between the two imaging modalities, shown by the mean line coinciding exactly with 0.0 and acceptable distribution within a range of 1.96 standard deviations (SD). No trend is seen in the distribution around the mean.

Figure 3. Bland-Altman plot of ultrasound and MRI values for carotid vessel wall thickness.

Data indicates that MRI findings for MWT are systematically higher than US values of IMT, shown by the mean line coinciding with 0.50. A significant upward trend is seen in the distribution around the mean ($r=0.72$, $p<0.001$), implying the difference between US and MRI evaluation is more pronounced with increasing vessel wall thickness.

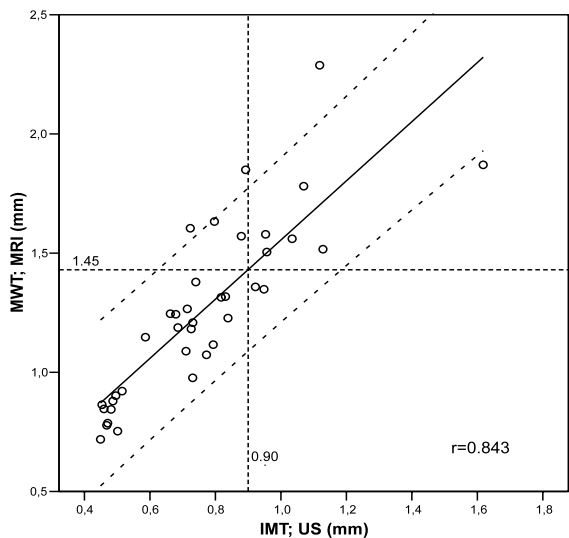
agreement (0.882, $p<0.001$). Bland Altman analysis of MWT versus IMT showed MWT was on average 0.50 mm higher than IMT. A systematic upward bias was observed of MWT compared to IMT (paired sample T-test $p<0.001$). Figure 3 illustrates this upward tendency with increasing IMT+MWT ($r=0.72$ ($p<0.001$)). Lastly, the regression analyses are given in figure 4 (MWT vs IMT) and 5 (VWA vs IMT). Based on these data, the IMT cut-off level of 0.9 mm is expected to correspond with a MWT value of 1.45 mm and a VWA value of 2.00 cm².

DISCUSSION

The main finding of the current study is that MRI can successfully discriminate between vessel wall characteristics of intermediate to high risk asymptomatic patients versus young healthy subjects. Furthermore, 3 Tesla MRI showed excellent dimensional agreement with US, and MRI measurements of wall thickness and wall area correlated well with IMT.

We compared intermediate and high cardiovascular risk patients to healthy control subjects regarding MRI measured vessel wall characteristics. Thus, our results extend the previous findings of Underhill et al (15) and Mani et al (16). Underhill studied the potential of MRI in 28 cases out of 43 patients with 16-79% carotid stenosis. Mani et al reported 17 patients with at calculated mean intermediate to high risk of 14% (range 6-31%). This risk may have been underestimated in this study as 30% of the patients had suffered from cardiovascular events. Taken together, these studies have now clearly shown the discriminative potential of MRI regarding vessel wall characteristics in intermediate to high risk patients either with carotid

Figure 4. Scatterplot of mean thickness; IMT (US) vs. MWT (MRI).



Data demonstrate strong correlation between these thickness parameters ($r=0.84$). The dotted extrapolation lines indicate that the clinically relevant cut-off value of 0.9mm for IMT corresponds with 1.45mm for MWT

IMT=intima media thickness

MWT=mean wall thickness

(—) indicates linear regression line

(---) indicates 95% confidence interval

(-----) indicates linear extrapolation lines

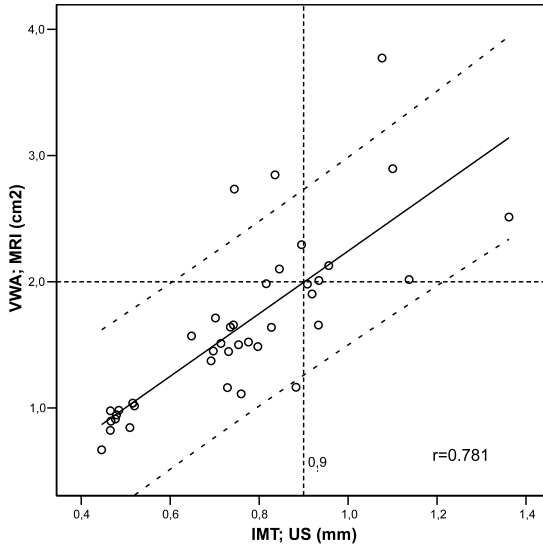
stenosis (15), within intermediate risk patients (16) or in comparison to healthy young control subjects as shown in our study. In addition, the current findings extend the results of the previous studies in 1.5T field strength to 3T MR imaging. Compared to the abovementioned studies, the technical success rate of our 3T imaging protocol was excellent with 39 of 41 total scans being interpretable (95.1%).

Our study showed a high dimensional agreement between MRI and US for lumen diameter. High reproducibility of our protocol has previously been demonstrated (11). The current data add high dimensional precision of 3T MRI when using US as reference. This dimensional precision is of relevance when interpreting the relation between IMT and MWT. As previously described, MWT significantly correlated with IMT but was found to be consistently higher than IMT. This is in line with previous observations (15-17). This finding may reflect the difference between the histopathological substrate of IMT (intima-media complex), and MWT (total vessel wall). Intriguingly, the degree of overestimation of MWT versus IMT (0.5 mm) we observed is reminiscent of the estimated thickness of the lamina adventitia. In patients with higher values

of MWT and IMT this overestimation was larger. It is noteworthy that very few published data are available on the exact thickness of the human carotid lamina adventitia *in vivo*. This points to the importance of the definition of cutoff values for MRI in relation to cardiovascular risk assessment. In our hands values corresponding to established IMT cut-off values could be approached using regression analysis (figure 4 and figure 5). However, we emphasize these are preliminary data and further studies are required to define threshold values for MRI in relation to clinical cardiovascular events.

Our study has limitations. We studied a limited number of young healthy control subjects. Extending this group would have increased the statistical power of the study. However, the level of significance obtained is compatible with a low chance of a type II error. The coverage of the common carotid artery was limited to 1 cm. Three-dimensional MRI acquisition schemes have recently been proposed that allow more extensive coverage (18). Furthermore, IMT was assessed in longitudinal - MRI in cross-sectional samples. Nevertheless, the images obtained are acquired in an optimal technical setting for both techniques as also pointed out by Underhill et al. (15).

Figure 5. Scatterplot of IMT (US) vs. VWA (MRI). Data demonstrate strong correlation between the parameters ($r=0.78$). The dotted extrapolation lines indicate that the clinically relevant cut-off value of 0.9mm for IMT corresponds with 2.00cm^2 for VWA.



IMT=intima media thickness

VWA=vessel wall area.

- (—) indicates linear regression line
- (- - -) indicates 95% confidence interval
- (.....) indicates linear extrapolation lines

In conclusion, MRI successfully discriminated vessel wall characteristics in intermediate and high risk patients from those in young healthy control subjects. MRI showed high dimensional precision with US as reference and significantly correlated with IMT. Adding these characteristics to its previously shown high reproducibility, the potential of 3T MRI in cardiovascular risk assessment and as clinical research tool is promising.

REFERENCE LIST

1. Bots, M. L., Hoes, A. W., Hofman, A., Witteman, J. C., et al. Cross-Sectionally Assessed Carotid Intima-Media Thickness Relates to Long-Term Risk of Stroke, Coronary Heart Disease and Death As Estimated by Available Risk Functions. *J.Intern.Med.* 1999;245(3):269-76.
2. Chambless, L. E., Heiss, G., Folsom, et al. Association of Coronary Heart Disease Incidence With Carotid Arterial Wall Thickness and Major Risk Factors: the Atherosclerosis Risk in Communities (ARIC) Study, 1987-1993. *Am.J.Epidemiol.* 15-9-1997;146(6):483-94.
3. Lekakis, J. P., Papamichael, C. M., Cimponeriu, et al. Atherosclerotic Changes of Extracoronary Arteries Are Associated With the Extent of Coronary Atherosclerosis. *Am.J.Cardiol.* 15-4-2000;85(8):949-52.
4. Mack, W. J., LaBree, L., Liu, C., et al. Correlations Between Measures of Atherosclerosis Change Using Carotid Ultrasonography and Coronary Angiography. *Atherosclerosis* 2000;150(2):371-9.
5. Vasankari, T., Ahotupa, M., Toikka, J., et al. Oxidized LDL and Thickness of Carotid Intima-Media Are Associated With Coronary Atherosclerosis in Middle-Aged Men: Lower Levels of Oxidized LDL With Statin Therapy. *Atherosclerosis* 2001;155(2):403-12.
6. Bots, M. L., Hoes, A. W., Koudstaal, P. J., Hofman, A., and Grobbee, D. E. Common Carotid Intima-Media Thickness and Risk of Stroke and Myocardial Infarction: the Rotterdam Study. *Circulation* 2-9-1997;96(5):1432-7.
7. O'Leary, D. H., Polak, J. F., Kronmal, et al. Carotid-Artery Intima and Media Thickness As a Risk Factor for Myocardial Infarction and Stroke in Older Adults. Cardiovascular Health Study Collaborative Research Group. *N.Engl.J.Med.* 7-1-1999;340(1):14-22.
8. Adams, G. J., Greene, J., Vick, G. W., III, et al. Tracking Regression and Progression of Atherosclerosis in Human Carotid Arteries Using High-Resolution Magnetic Resonance Imaging. *Magn Reson.Imaging* 2004;22(9):1249-58.
9. Shinnar, M., Fallon, J. T., Wehrli, S., et al. The Diagnostic Accuracy of Ex Vivo MRI for Human Atherosclerotic Plaque Characterization. *Arterioscler.Thromb.Vasc.Biol.* 1999;19(11):2756-61.
10. Yuan, C., Beach, K. W., Smith, L. H., Jr., et al. Measurement of Atherosclerotic Carotid Plaque Size in Vivo Using High Resolution Magnetic Resonance Imaging. *Circulation* 15-12-1998;98(24):2666-71.
11. Alizadeh, Dehnavi R., Doornbos, J., Tamsma, J. T., et al. Assessment of the Carotid Artery by MRI at 3T: a Study on Reproducibility. *J.Magn Reson.Imaging* 2007;25(5):1035-43.
12. Adame, I. M., van der Geest, R. J., Bluemke, D. A., et al. Automatic Vessel Wall Contour Detection and Quantification of Wall Thickness in in-Vivo MR Images of the Human Aorta. *J.Magn Reson.Imaging* 2006;24(3):595-602.
13. Pignoli, P., Tremoli, E., Poli, A., et al. Intimal Plus Medial Thickness of the Arterial Wall: a Direct Measurement With Ultrasound Imaging. *Circulation* 1986;74(6):1399-406.
14. Bland, J. M. and Altman, D. G. Statistical Methods for Assessing Agreement Between Two Methods of Clinical Measurement. *Lancet* 8-2-1986;1(8476):307-10.
15. Underhill, H. R., Kerwin, W. S., Hatsukami, T. S., et al. Automated Measurement of Mean Wall Thickness in the Common Carotid Artery by MRI: a Comparison to Intima-Media Thickness by B-Mode Ultrasound. *J.Magn Reson.Imaging* 2006;24(2):379-87.
16. Mani, V., Aguiar, S. H., Itskovich, V. V., et al. Carotid Black Blood MRI Burden of Atherosclerotic Disease Assessment Correlates With Ultrasound Intima-Media Thickness. *J.Cardiovasc.Magn Reson.* 2006;8(3):529-34.
17. Crowe, L. A., Ariff, B., Keegan, J., et al. Comparison Between Three-Dimensional Volume-Selective Turbo Spin-Echo Imaging and Two-Dimensional Ultrasound for Assessing Carotid Artery Structure and Function. *J.Magn Reson.Imaging* 2005;21(3):282-9.
18. Varghese, A., Crowe, L. A., Mohiaddin, R. H., et al. Inter-Study Reproducibility of 3D Volume Selective Fast Spin Echo Sequence for Quantifying Carotid Artery Wall Volume in Asymptomatic Subjects. *Atherosclerosis* 2005;183(2):361-6.

PART II

Phenotyping of Visceral Obesity

CHAPTER

4

Carotid artery vessel wall imaging by 3T MRI in visceral obese subjects with and without the metabolic syndrome compared to STEMI patients: not all obese are equal

Reza Alizadeh Dehnavi¹ MD, J. Wouter Jukema² MD PhD,
Rachel L.M. van der Ham¹ MD, Johannes A. Romijn¹ MD PhD,
Hildo J. Lamb³ MD PhD, Jolein van der Kraan¹, Raoul van der
Vleugel² MD, Albert de Roos³ MD PhD, Jouke T. Tamsma¹ MD
PhD

*¹Section of Vascular Medicine, Department of General Internal
Medicine & Endocrinology, Leiden University Medical Centre, Leiden,
The Netherlands*

*²Department of Cardiology, Leiden University Medical Centre, Leiden,
The Netherlands*

*³Department of Radiology, Leiden University Medical Centre, Leiden,
The Netherlands*

Submitted

ABSTRACT

Objective

To assess carotid artery vessel wall characteristics using three Tesla MRI in visceral obese male subjects with and without the Metabolic Syndrome (MS) compared to patients who recently suffered from a ST-segment elevation myocardial infarction (STEMI).

Methods

Black blood 3T MR vessel wall imaging was used to assess the carotid artery vessel wall characteristics in male subjects with visceral obesity with and without the Metabolic Syndrome (VO+MS and VO respectively). A group of male patients with proven clinical relevant atherosclerosis, having recently (<1 month) suffered from a STEMI, were chosen as comparator. In addition, a group of young healthy volunteers were assessed. As endpoints, carotid artery vessel wall area was used as a global marker of atherosclerotic disease burden and carotid artery maximum vessel wall thickness (MaxT) was used to address focal atherosclerotic vessel wall changes.

Results

Maximum vessel wall thickness (MaxT) of the carotid artery bulb was highest in STEMI patients followed by VO+MS and VO and the healthy volunteers (difference between the groups $P < 0.001$). MaxT in the carotid bulb of patients in VO+MS approached the level observed in STEMI patients and significantly differed from VO patients ($p \leq 0.01$). Total vessel wall area of patients with STEMI, VO+MS and VO were significantly increased compared to young healthy volunteers.

Conclusions

The presence of Metabolic Syndrome in visceraally obese subjects, without manifest cardiovascular disease or type 2 diabetes mellitus, is associated with increased maximum vessel wall thickness of the carotid bulb approaching the level observed in STEMI. Three Tesla MRI was successfully used in vascular phenotyping of visceral obese subjects.

INTRODUCTION

Significant proportions of western populations suffer from overweight or obesity.¹⁻³ Obese subjects are at increased risk of developing cardiovascular disease and type 2 diabetes mellitus.^{4,5} In large epidemiological studies, visceral obesity was shown to be a predictor of future cardiovascular events and cardiovascular mortality.^{6,7} Viscerally obese subjects in particular, are considered to have metabolic abnormalities that contribute to the increased risk of cardiovascular events.⁸⁻¹⁰ Visceral obesity, quantified by waist circumference (WCR), has been identified as an independent risk factor for insulin resistance, cardiovascular disease, hypertension and stroke.¹¹⁻¹⁴ However, not all individuals with an increased waist circumference have disturbed metabolic profiles.¹⁵ Obese patients have been reported without insulin resistance and the related metabolic changes.¹⁶ The influence of the presence of metabolic disturbances in visceral obese subjects has not previously been studied in relation to atherosclerotic disease burden as measured by MRI.

Magnetic resonance imaging (MRI) is a relatively new imaging modality used for the detection of atherosclerosis.¹⁷ MRI provides a circumferential view of the vessel of interest together with an accurate luminal dimensional characterization.¹⁸ MRI detected carotid artery vessel wall characteristics can be measured with good reproducibility.¹⁸⁻²¹ The validation of the technique requires further support, especially regarding the discrimination between subjects with different levels of cardiovascular risk and with respect to cardiovascular outcome.

Accordingly, we set out to assess carotid artery vessel wall characteristics using three Tesla MRI in visceral obese male subjects with and without the Metabolic Syndrome (MS) and compared these to the characteristics as observed in patients who recently suffered from ST-segment elevation myocardial infarction (STEMI).

METHODS

Study design & Subjects

Sixteen patients with visceral obesity (VO), and 25 patients with visceral obesity and the metabolic syndrome (VO+MS) were compared to a group of patients (n=12) who recently (<one month) suffered from a ST-segment elevation myocardial infarction (STEMI). An additional group of young healthy volunteers (HV, n=12) was also assessed. The international diabetes federation (IDF) criteria were used to define visceral obesity and the metabolic syndrome.²² Subjects in the VO and the VO+MS group were without manifest clinical cardiovascular disease or type 2 diabetes mellitus (fasting blood glucose level <7 mmol/L). The Framingham risk score was used to assess future cardiovascular risk. For HV, the Framingham risk score was calculated

by entering the lowest possible entry into the equation when the actual value of the variable was below the predefined minimum of the risk calculator. In all subjects, medical history, anthropometry and extensive laboratory assessments were performed within two weeks of MRI assessments. Statin use was defined as an exclusion criterion except in the STEMI group. In the STEMI group, MRI assessments were performed within 4 weeks after discharge to minimize the influence of statin use on the vessel wall characteristics. The study protocol was approved by the institutional review committee and all subjects gave informed consent.

3T Carotid Magnetic Resonance Imaging Protocol

Magnetic resonance imaging was performed on a 3T scanner (Philips, Achieva, Best, The Netherlands) using a standard Philips SENSE-flex-M surface coil as previously described and validated.¹⁸ In brief, the left carotid artery was examined in all subjects. After localization of the vessel using fast gradient echo sequence surveys, a total of ten contiguous transverse slices were acquired from the carotid bifurcation covering 2 cm of the carotid bulb and the common carotid artery from the flow-divider in the proximal (caudal) direction. A dual inversion recovery (black-blood), spoiled segmented k-space fast gradient echo sequence with spectral selective fat suppression was used for image acquisition using the following parameters: echo time 3.6 ms, repetition time (TR) 12 ms, pulse angle 45 degrees, and 2 signal averages were performed. A reinversion slice thickness of 3 mm was used. The field of view was 140 mm. With a matrix size of 306, a voxel size of 0.46mm x 0.46mm x 2mm was obtained. Each MR study took approximately 30 minutes depending on the cardiac frequency. All images were analysed using VesselMASS software package, allowing for a semi-automated quantification of various descriptive parameters of the vessel. After tracing all scan series, vessel wall area (VWA) was calculated by subtracting the luminal area from the outer contour area. Maximum vessel wall thickness (MaxT) was assessed for the carotid bulb region.

Statistical analysis

Continuous variables are presented as mean values \pm standard deviation or as medians and interquartile ranges if the assumption of normality was not met. Comparisons between groups were made by one-way ANOVA with post hoc least significant difference (LSD) testing. For parameters that were not normally distributed, Kruskal-Wallis tests were performed. If Kruskal-Wallis tests showed significant differences between the groups, differences between individual groups were tested by Mann-Whitney tests. These p values were multiplied by 3 to correct for multiple testing. Analyses were performed using SPSS version 16.0 (SPSS, Chicago, Illinois, USA). All analyses were two-sided, with a level of significance of $\alpha=0.05$.

Table 1. Patient characteristics

	HV (0) N=12	VO (1) N=16	VO+MS (2) N=25	STEMI (3) N=12
Age (y)	25.7 (6.1)	61.2 (4.6)	60.6 (5.5)	57.3 (4.9)
Family History †	1 (16.6%)	0 (0%) 3‡	2 (8%) 3‡	5 (41.7%) 1‡, 2†
Smoking †	1 (16.6%) 2†	0 (0%) 3†	0 (0%) 0†, 3‡	4 (33.3%) 1†, 2‡
Statin use	0 (0%)	0 (0%)	0 (0%)	12 (100%)
AHM	0 (0%)	1 (6.3%)	10 (41.7%)	12 (100%)
Length (cm)	172.5 (12.6)	178.6 (7.1)	178.4 (6.9)	180.2 (5.1)
Weight (kg) §	70.3 (8.3) 1‡, 2§, 3‡	90.5 (11.2) 0‡	84.1 (13.7) 0§	88.14 (10.6) 0‡
WCR (cm) §	83.8 (8.2) 1§, 2§, 3‡	105.9 (8.7) 0§	106.8 (9.3) 0§, 3†	99.7 (8.4) 1‡
RRS (mmHg) §	120.2 (6.2) 1‡, 2§	142.1 (17.3) 0‡	151.6 (17.8) 0§, 3‡	131.4 (11.6) 2‡
RRD (mmHg) §	76.0 (7.9) 1‡, 2‡	88.7 (8.7) 0‡, 3‡	90.2 (9.5) 0‡, 3§	77.1 (8.9) 1‡, 2§
TC (mmol/L) §	4.99 (0.82) 3‡	5.66 (0.88) 3§	5.40 (0.80) 3§	4.05 (0.77) 0†, 1§, 2§
TG (mmol/L)* ‡	0.89 (0.63-1.36) 2†	1.18 (0.76-1.56) 0†, 2†	1.70 (1.22-3.26) 0†, 1†	1.37 (1.14-1.80)
HDL-c (mmol/L) §	1.72 (0.46) 2§, 3§	1.75 (0.27) 2§, 3§	1.18 (0.22) 0§, 1§	1.09 (0.23) 0§, 1§
LDL-c (mmol/L) * §	3.05 (2.43-3.21)	3.49 (2.71-4.12) 3‡	3.25 (2.88-3.73) 3§	2.26 (1.85-2.49) 1‡, 2§
HbA1c (%) * †	4.7 (4.4-5.1) 3†	4.9 (4.7-5.3)	4.9 (4.6-5.3)	5.3 (5.0-5.4) 0†
Glucose (mmol/L)	4.67 (0.79)	4.74 (0.57)	5.15 (0.65)	5.17 (0.60)
Insulin (µU/ml) * §	5.5 (2.0-10.8)	6.5 (4.3-8.8)	8.0 (5.5-12.8)	8 (3.8-9.5)
hsCRP (mg/L) * §	0.93 (0.66-1.03)	1.09 (0.65-1.63)	0.98 (0.60-1.62)	1.94 (1.07-3.25)
Framingham * §	0 (0-1.3) 1§, 2§	8.5 (6-11.8) 0§, 2†	13 (8.5-17.5) 0§, 1†	NA

Data are means with SD (in case of normal distribution) or medians with inter quartile range (in case of skewed distribution, indicated by *). Statistical differences are shown by symbols (†=p<0.05, ‡=p<0.01, §=p<0.001), and accompanying numbers (0-3) refer to the group to which the data in the cell are significantly different. ANOVA, Kruskal-Wallis or Pearson Chi-square p values are given in the first column.||: patients on statins and treated intensively to reduce blood pressure.

AHM: Antihypertensive medication. HV: Young healthy volunteers. VO: Viscerally obese patients. VO+MS: Patients with visceral obesity and the metabolic syndrome. STEMI: Patients with a recent ST-segment elevation myocardial infarction. NA: not applicable. RRD: Diastolic blood pressure. RRS: Systolic blood pressure. TC: Total cholesterol. WCR: Waist circumference.

RESULTS

Patient characteristics

Clinical and laboratory characteristics of the study subjects are provided in Table 1. Mean (SD) waist circumference was not significantly different between VO and VO+MS patients, 105.0 (8.7) vs. 106.8 (9.3) respectively. Similarly no statistically significant differences were observed for systolic and diastolic blood pressure and total cholesterol levels between VO and VO+MS. The calculated cardiovascular risk (Framingham risk score) were significantly higher in VO+MS compared to VO. STEMI patients received intensive antihypertensive and lipid-lowering treatment since the onset of myocardial infarction. Framingham risk scores are not used for risk assessment in the secondary prevention setting and were therefore not calculated for STEMI patients.

MRI assessments (table2)

Both VWA and MaxT were significantly different between the groups ($p < 0.001$, see Table 2). MaxT of the carotid bulb region was highest in STEMI ($2.28 \pm 0.40\text{mm}$), followed by VO+MS, VO and HV. MaxT of VO+MS group ($2.20 \pm 0.55\text{mm}$) was significantly higher than MaxT in VO ($1.86 \pm 0.30\text{mm}$, $p \leq 0.05$). MaxT was significantly lower in HV compared to all groups. Figure 1

Table 2. MRI detected carotid atherosclerotic burden across the groups.

	HV (0) N=12	VO (1) N=16	VO+MS (2) N=25	STEMI (3) N=12
VWA (cm²) §	2.29 (0.57) 1§, 2§, 3§	4.34 (0.87) 0§	4.53 (1.09) 0§	4.51 (0.64) 0§
Bulbus MaxT (mm) §	1.27 (0.36) 1§, 2§, 3§	1.86 (0.30) 0§, 2†, 3†	2.20 (0.55) 0§, 1†	2.28 (0.40) 0§, 1†

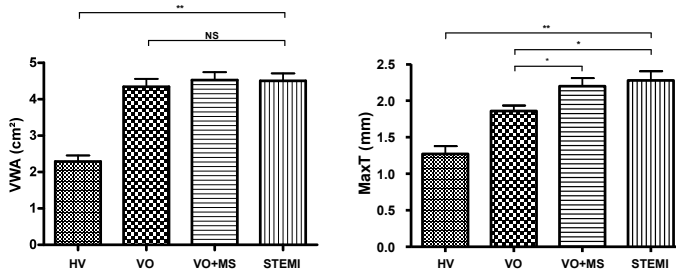
Data are means with SD. Statistical differences are shown by symbols (†= $p \leq 0.05$, ‡= $p \leq 0.01$, §= $p \leq 0.001$), and accompanying numbers (0-3) refer to the group to which the data in the cell are significantly different. ANOVA p values are given in the first column. HV: Young healthy volunteers. VO: Patients with visceral obesity. VO+MS: Patients with visceral obesity and the metabolic syndrome. STEMI: Patients with ST-segment elevation myocardial infarction. MaxT: maximal vessel wall thickness. VWA: vessel wall area.

illustrates MaxT and VWA values of the groups.

For VWA no significant differences were observed between STEMI, VO+MS and VO. VWA was significantly lower in HV compared to all other groups ($p < 0.001$ for all pair wise comparisons).

DISCUSSION

This study demonstrates that the presence of Metabolic Syndrome in viscerally obese subjects, without manifest clinical cardiovascular disease and type 2 diabetes mellitus, is associated with

Figure 1. Differences between groups in vessel wall area and bulbus maximum vessel wall thickness.

*: $p < 0.05$, **: $p < 0.001$, NS: not significant. VWA: vessel wall area. MaxT: maximal vessel wall thickness. HV: Young healthy volunteers. VO: Patients with visceral obesity. VO+MS: Patients with visceral obesity and metabolic syndrome. STEMI: Patients with ST-segment elevation myocardial infarction.

increased maximum vessel wall thickness of the carotid bulb approaching the level observed in recent onset STEMI patients. Furthermore, three Tesla vascular MRI was successfully used to phenotype visceral obese subjects with different metabolic profiles.

Visceral obesity increases the risk of cardiovascular morbidity and mortality.^{6, 7} Metabolic abnormalities contribute to the increased risk of future cardiovascular events in visceral obese subjects.⁸⁻¹⁰ In this study, we demonstrate that not all visceral obese patients are equal, as focal atherosclerosis is less outspoken in subjects with visceral obesity alone compared to subjects with visceral obesity and the metabolic syndrome. Several factors could contribute to the pathogenesis of the observed differences between the groups. Systolic (142.1 ± 17.3 mmHg vs. 151.6 ± 17.8 mmHg, $p > 0.05$) and diastolic blood pressure (88.7 ± 8.7 mmHg vs. 90.2 ± 9.5 mmHg, $p > 0.05$) were not statistically significantly different between the groups. However, from large studies it is known that every mmHg counts on endpoints and the mean difference of 9 mmHg may have a pathophysiological impact on vessel wall biology. As both groups (i.e. VO and VO+MS) had comparable values for waist circumference (105.9 ± 8.7 cm vs. 106 ± 9.3 cm, $p > 0.05$) a possible explanation from the viewpoint of central obesity to explain the increased MaxT in VO+MS could be a different pattern in adipose tissue distribution. Adipose tissue distribution has been causally related to metabolic disturbances²³ and patients with increased WCR due to expanded subcutaneous fat deposits have been reported with normal risk factor profiles.²⁴ Unfortunately, we are not informed about adipose tissue distribution in our study population. Another explanation for the observed difference in atherosclerotic disease burden could be differences between groups in atherogenic dyslipidemia. Significant differences were observed in triglyceride and HDL-cholesterol levels between the groups. VO+MS patients had significantly higher triglyceride levels and lower HDL-cholesterol levels compared to VO patients. The more outspoken atherogenic dyslipidemia may have had a pathophysiological role in the observed increased MaxT in VO+MS. This is inline with the well known cardiovascular risk associated with elevated triglycerides and low HDL-cholesterol levels.²⁵⁻²⁷

At present, intima media thickness (IMT) measured by ultrasound is the most used and best validated non-invasive imaging modality for the study of atherosclerosis in the carotid artery.²⁸⁻³¹ MRI has now emerged as an alternative technique to assess atherosclerosis. Vascular MRI has high reproducibility,¹⁸ and it significantly correlates with echographically measured IMT.^{32, 33} However, the validation of vascular MRI is ongoing and steps in this regard are to show that MRI can discriminate between subjects at different levels of cardiovascular risk, and to compare subjects at risk for atherosclerotic events with patients with established cardiovascular disease. Using 3T black blood MRI of the carotid artery, we were able to show that elevated serum C-reactive protein level was associated with increased measures of atherosclerosis.³⁴ Using the same technique, we now addressed the question whether MRI could discriminate between visceral obese subjects with and without the metabolic syndrome and compared them to patients who recently suffered a ST-segment elevation myocardial infarction. Three tesla MRI was able to discriminate vessel wall characteristics between these groups. Intriguingly, maximum vessel wall thickness of the carotid bulb was not significantly different between STEMI patients and VO+MS patients ($p>0.05$), and the absolute values of MaxT observed were very similar. If maximum vessel wall thickness reflects focal atherosclerotic changes of the vessel wall³⁴, this could imply that patients with VO+MS approach the level of atherosclerosis that associates with overt cardiovascular events whereas VO only patients have less pronounced atherosclerosis. This is in line with the observation that presence of atherosclerotic plaques predict cardiovascular events.³⁵

Our study has limitations. First, the possible limited power due to a relatively small sample size may have resulted in a type II error with regard to the less pronounced differences in atherosclerotic disease burden. Nonetheless, statistically significant differences were detected in MaxT of the carotid bulb between VO and VO+MS. The STEMI patients were all treated with statins and antihypertensive medication. This could have influenced the carotid artery vessel wall. However, we performed the MRI within 4 weeks of discharge, and none of these subjects were treated with these medications before STEMI-onset. Finally, the participants of this study were all males. These observations will have to be confirmed in female populations.

In conclusion, this study demonstrates that the presence of Metabolic Syndrome in visceraally obese subjects is associated with increased maximum vessel wall thickness of the carotid bulb approaching the level observed in recent onset STEMI patients. Finally, this study shows that 3T vascular MRI is able to discriminate vessel wall characteristics in patients with different clinical profiles.

REFERENCE LIST

1. Mokdad AH, Bowman BA, Ford ES, Vinicor F, Marks JS, Koplan JP. The continuing epidemics of obesity and diabetes in the United States. *JAMA* 2001 September 12;286(10):1195-200.
2. Mokdad AH, Ford ES, Bowman BA et al. Diabetes trends in the U.S.: 1990-1998. *Diabetes Care* 2000 September;23(9):1278-83.
3. Mokdad AH, Serdula MK, Dietz WH, Bowman BA, Marks JS, Koplan JP. The spread of the obesity epidemic in the United States, 1991-1998. *JAMA* 1999 October 27;282(16):1519-22.
4. Adams KF, Schatzkin A, Harris TB et al. Overweight, obesity, and mortality in a large prospective cohort of persons 50 to 71 years old. *N Engl J Med* 2006 August 24;355(8):763-78.
5. Jee SH, Sull JW, Park J et al. Body-mass index and mortality in Korean men and women. *N Engl J Med* 2006 August 24;355(8):779-87.
6. Yusuf S, Hawken S, Ounpuu S et al. Obesity and the risk of myocardial infarction in 27,000 participants from 52 countries: a case-control study. *Lancet* 2005 November 5;366(9497):1640-9.
7. Pischon T, Boeing H, Hoffmann K et al. General and abdominal adiposity and risk of death in Europe. *N Engl J Med* 2008 November 13;359(20):2105-20.
8. Despres JP, Lemieux I, Prud'homme D. Treatment of obesity: need to focus on high risk abdominally obese patients. *BMJ* 2001 March 24;322(7288):716-20.
9. Van Gaal LF, Vansant GA, De L, I. Upper body adiposity and the risk for atherosclerosis. *J Am Coll Nutr* 1989 December;8(6):504-14.
10. Wong S, Janssen I, Ross R. Abdominal adipose tissue distribution and metabolic risk. *Sports Med* 2003;33(10):709-26.
11. Banerji MA, Lebowitz J, Chaiken RL, Gordon D, Kral JG, Lebovitz HE. Relationship of visceral adipose tissue and glucose disposal is independent of sex in black NIDDM subjects. *Am J Physiol* 1997 August;273(2 Pt 1):E425-E432.
12. Pouliot MC, Despres JP, Lemieux S et al. Waist circumference and abdominal sagittal diameter: best simple anthropometric indexes of abdominal visceral adipose tissue accumulation and related cardiovascular risk in men and women. *Am J Cardiol* 1994 March 1;73(7):460-8.
13. Kuo CS, Hwu CM, Chiang SC et al. Waist circumference predicts insulin resistance in offspring of diabetic patients. *Diabetes Nutr Metab* 2002 April;15(2):101-8.
14. Poirier P, Lemieux I, Mauriege P et al. Impact of waist circumference on the relationship between blood pressure and insulin: the Quebec Health Survey. *Hypertension* 2005 March;45(3):363-7.
15. Reaven GM. The metabolic syndrome: is this diagnosis necessary? *Am J Clin Nutr* 2006 June;83(6):1237-47.
16. Abbasi F, Brown BW, Jr., Lamendola C, McLaughlin T, Reaven GM. Relationship between obesity, insulin resistance, and coronary heart disease risk. *J Am Coll Cardiol* 2002 September 4;40(5):937-43.
17. Fuster V, Kim RJ. Frontiers in cardiovascular magnetic resonance. *Circulation* 2005 July 5;112(1):135-44.
18. Alizadeh DR, Doornbos J, Tamsma JT et al. Assessment of the carotid artery by MRI at 3T: a study on reproducibility. *J Magn Reson Imaging* 2007 May;25(5):1035-43.
19. Corti R, Fayad ZA, Fuster V et al. Effects of lipid-lowering by simvastatin on human atherosclerotic lesions: a longitudinal study by high-resolution, noninvasive magnetic resonance imaging. *Circulation* 2001 July 17;104(3):249-52.
20. Varghese A, Crowe LA, Mohiaddin RH et al. Inter-study reproducibility of 3D volume selective fast spin echo sequence for quantifying carotid artery wall volume in asymptomatic subjects. *Atherosclerosis* 2005 December;183(2):361-6.
21. Varghese A, Crowe LA, Mohiaddin RH et al. Interstudy reproducibility of three-dimensional volume-selective fast spin echo magnetic resonance for quantifying carotid artery wall volume. *J Magn Reson Imaging* 2005 February;21(2):187-91.

22. Alberti KG, Zimmet P, Shaw J. Metabolic syndrome--a new world-wide definition. A Consensus Statement from the International Diabetes Federation. *Diabet Med* 2006 May;23(5):469-80.
23. Despres JP, Lemieux I. Abdominal obesity and metabolic syndrome. *Nature* 2006 December 14;444(7121):881-7.
24. Lemieux I, Drapeau V, Richard D et al. Waist girth does not predict metabolic complications in severely obese men. *Diabetes Care* 2006 June;29(6):1417-9.
25. Jeppesen J, Hein HO, Suadicani P, Gyntelberg F. Low triglycerides-high high-density lipoprotein cholesterol and risk of ischemic heart disease. *Arch Intern Med* 2001 February 12;161(3):361-6.
26. Sarwar N, Danesh J, Eiriksdottir G et al. Triglycerides and the risk of coronary heart disease: 10,158 incident cases among 262,525 participants in 29 Western prospective studies. *Circulation* 2007 January 30;115(4):450-8.
27. Miller M, Seidler A, Moalemi A, Pearson TA. Normal triglyceride levels and coronary artery disease events: the Baltimore Coronary Observational Long-Term Study. *J Am Coll Cardiol* 1998 May;31(6):1252.
28. Lekakis JP, Papamichael CM, Cimponeriu AT et al. Atherosclerotic changes of extracoronary arteries are associated with the extent of coronary atherosclerosis. *Am J Cardiol* 2000 April 15;85(8):949-52.
29. Bots ML, Hoes AW, Hofman A, Witteman JC, Grobbee DE. Cross-sectionally assessed carotid intima-media thickness relates to long-term risk of stroke, coronary heart disease and death as estimated by available risk functions. *J Intern Med* 1999 March;245(3):269-76.
30. Bots ML, Hoes AW, Koudstaal PJ, Hofman A, Grobbee DE. Common carotid intima-media thickness and risk of stroke and myocardial infarction: the Rotterdam Study. *Circulation* 1997 September 2;96(5):1432-7.
31. O'Leary DH, Polak JF, Kronmal RA, Manolio TA, Burke GL, Wolfson SK, Jr. Carotid-artery intima and media thickness as a risk factor for myocardial infarction and stroke in older adults. Cardiovascular Health Study Collaborative Research Group. *N Engl J Med* 1999 January 7;340(1):14-22.
32. Underhill HR, Kerwin WS, Hatsukami TS, Yuan C. Automated measurement of mean wall thickness in the common carotid artery by MRI: a comparison to intima-media thickness by B-mode ultrasound. *J Magn Reson Imaging* 2006 August;24(2):379-87.
33. Mani V, Aguiar SH, Itskovich VV et al. Carotid black blood MRI burden of atherosclerotic disease assessment correlates with ultrasound intima-media thickness. *J Cardiovasc Magn Reson* 2006;8(3):529-34.
34. Alizadeh DR, de RA, Rabelink TJ et al. Elevated CRP levels are associated with increased carotid atherosclerosis independent of visceral obesity. *Atherosclerosis* 2008 October;200(2):417-23.
35. Johnsen SH, Mathiesen EB, Joakimsen O et al. Carotid atherosclerosis is a stronger predictor of myocardial infarction in women than in men: a 6-year follow-up study of 6226 persons: the Tromso Study. *Stroke* 2007 November;38(11):2873-80.

CHAPTER

5

Elevated CRP levels are associated with increased carotid atherosclerosis independent of visceral obesity

Reza Alizadeh Dehnavi¹, Albert de Roos², Ton J. Rabelink³,
Johannes van Pelt⁴, Maarten J. Wensink¹, Johannes A. Romijn¹,
and Jouke T. Tamsma¹

*¹Vascular Medicine, Department of General Internal Medicine
& Endocrinology, Leiden University Medical Centre, Leiden, The
Netherlands*

*²Department of Radiology, Leiden University Medical Centre, Leiden,
The Netherlands*

*³Department of Nephrology & Einthoven Laboratory, Leiden University
Medical Centre, Leiden, The Netherlands*

*⁴Department of Clinical Chemistry, Leiden University Medical Centre,
Leiden, The Netherlands*

Atherosclerosis 2008 Oct;200(2):417-23

ABSTRACT

Background

Visceral obesity (VO) is associated with an increased risk of cardiovascular disease. Elevated C-reactive protein (CRP) levels are associated with VO and cardiovascular disease. After exploring the relation between CRP and VO, we aimed to evaluate the VO independent relation between CRP and carotid atherosclerosis.

Methods and results

The prevalence of inflammation was evaluated in 439 male subjects with VO without type 2 diabetes and manifest cardiovascular disease. Waist circumference significantly correlated with CRP ($r: 0.20, p < 0.001$). However, 18.2% of patients in the waist circumference group 94–102 had elevated CRP levels while 9.6% of patients in the waist circumference group >118 cm had low CRP levels. From the 439 subjects, 40 subjects were prospectively selected for MRI assessment of carotid atherosclerosis and visceral and subcutaneous adipose tissue distribution in a case–control setting matching for age and waist circumference. Twenty male subjects with age >50 years with CRP levels >2.5 mg/L (CRP+) were compared to 20 controls with CRP levels <1.8 mg/L (CRP–). Maximum vessel wall thickness in CRP+ was significantly higher both in the common carotid artery (15%, $p < 0.01$) and the bulb region (18%, $p < 0.01$). The distribution of fat in visceral and subcutaneous deposits was not significantly different between CRP+ and CRP–.

Conclusion

Elevated CRP levels are associated with significantly increased maximum vessel wall thickness independent of VO and of MRI measured adipose tissue distribution, both in the common carotid artery and the carotid bulb.

INTRODUCTION

Obesity is associated with increased risk of cardiovascular disease, type 2 diabetes mellitus and mortality. Viscerally obese subjects in particular, are considered to have metabolic abnormalities that contribute to the increased risk of future cardiovascular events.¹⁻³ The amount of visceral adipose tissue has been shown to correlate with metabolic cardiovascular risk factors.⁴⁻⁶ However, not all individuals with an increased waist circumference (WCR) have disturbed metabolic profiles.⁷ Obese patients have been reported without insulin resistance and the related metabolic changes.⁸

Plasma levels of C-reactive protein (CRP), a marker of the systemic inflammatory state, is associated with obesity and visceral obesity (VO).⁹⁻¹¹ The highest CRP levels were observed in obese patients with a selective excess of visceral adipose tissue.¹¹ Both CRP and VO have predictive potential regarding future cardiovascular events.^{12, 13} The extent of systemic inflammation may also vary considerably in obese subjects, similar to the variability in the metabolic profiles. Due to the association between VO and CRP levels, assessment of the independent contribution of CRP versus VO to cardiovascular disease and atherosclerosis is challenging. For instance, higher measures of intima media thickness (IMT) have been reported in association with elevated CRP levels¹⁴⁻¹⁶, but this effect was not independent of the influence of obesity.

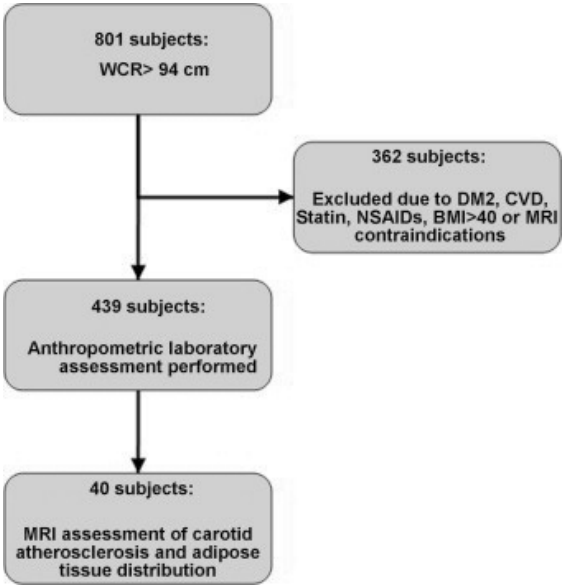
Therefore, in the present study, after exploring the relation between inflammation and VO, we aimed to evaluate the relation between CRP and carotid atherosclerosis independent of the influence of VO. We hypothesize that elevated CRP levels would associate with increased measures of atherosclerosis. Magnetic resonance imaging at the field strength of 3 T was used for the assessment of carotid atherosclerosis.

MATERIALS AND METHODS

Study design and subjects

A total of 801 men above 50 years of age were recruited through the local media. The inclusion criterion was a WCR above 94 cm. Exclusion criteria were type 2 diabetes mellitus, manifest cardiovascular disease, use of statins, non-steroidal anti-inflammatory drugs, severe obesity (BMI > 40 kg/m²), and contraindications for MRI. A group of 439 subjects met the criteria and were included in the study. Figure 1 demonstrates the flow diagram of the screening and selection process. Four different strata were defined for both CRP levels (CRP ≤ 1 mg/L, 1 < CRP < 1.8 mg/L, 1.8 ≤ CRP < 3 mg/L, and CRP ≥ 3 mg/L) and WCR (94–101 cm, 102–109 cm, 110–117 cm, and ≥118 cm). The distribution across these strata and the differences between the groups

Figure 1. Flow chart of the screening and selection process.



were addressed. The study protocol was approved by the institutional review committee and all subjects gave informed consent. The study had no external funding source.

CRP and the vessel wall

To evaluate the VO independent relation between CRP and atherosclerosis a case–control design was used in 40 subjects matched for age, WCR and gender. The subjects were prospectively retrieved from the total study population ($n = 439$). 20 male subjects with hsCRP > 2.5 mg/L (CRP+) were matched by age (maximum difference 1 year) and WCR (maximum difference 2 cm) to 20 male control subjects with hsCRP < 1.8 mg/L (CRP–). The subjects were evenly selected across the WCR-strata. In each WCR-stratum five subjects with high CRP levels were matched to five controls with low CRP levels. CRP was measured twice to exclude outliers. In addition to the exclusion criteria of the study, none of the subjects were current smokers or had a familial history of premature cardiovascular disease.

Anthropometric and laboratory assessments

Medical history and physical examination including anthropometry and blood sampling were performed on the same day. Blood pressure was assessed using an automatic blood pressure monitor (Omron 705IT, Hoofddorp, The Netherlands). Three measurements were averaged for use in the analysis. Blood samples were collected after a 12-h overnight fast for chemical and haematological laboratory assessments. The high-sensitive CRP assay was performed with the Tina Quant C-reactive protein (latex) high sensitive assay (Roche, Basel, Switzerland).

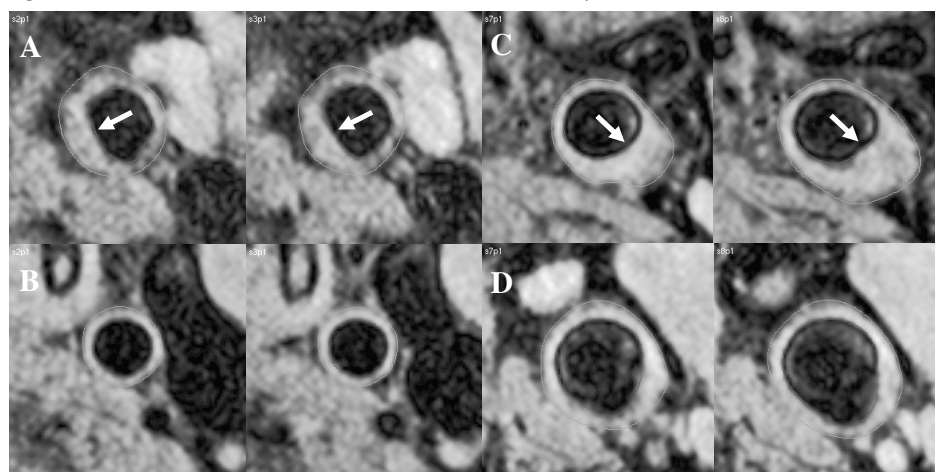
Participants with CRP levels above 15 mg/L were regarded as having an inter-current infection and were not included in the assessments. Insulin was determined in heparinised plasma using a solid-phase, two-site chemiluminescent immunometric assay carried out on an Immulite 2500 (DPC, Los Angeles, USA).

Magnetic resonance imaging protocol

Carotid imaging

Magnetic resonance imaging was performed on a 3 T scanner (Philips, Achieva, Best, The Netherlands) as previously described and validated.¹⁷ In all subjects, the left carotid artery was examined. After localization of the carotid artery, 10 contiguous transverse slices were acquired covering 2 cm of the carotid bulb and the common carotid artery. A dual inversion recovery (black-blood), spoiled segmented *k*-space fast gradient echo sequence with spectral selective fat suppression was used for image acquisition with the following parameters: echo time 3.6 ms, repetition time (TR) 12 ms, pulse angle 45°, and 2 signal averages were performed. ECG triggering was used for data acquisition at each RR interval at end diastole. Reinversion slice thickness was 3 mm. The field of view was 140 mm. With a matrix size of 306, a voxel size of 0.46 mm × 0.46 mm × 2 mm was obtained. Images were analysed, using the VesselMASS software package developed at our institution. Disease burden was assessed by the following derived parameters: Maximum vessel wall thickness in the common carotid artery (commonMVT) and the carotid bulb (bulbMVT). Vessel wall area in the common carotid artery (commonVWA),

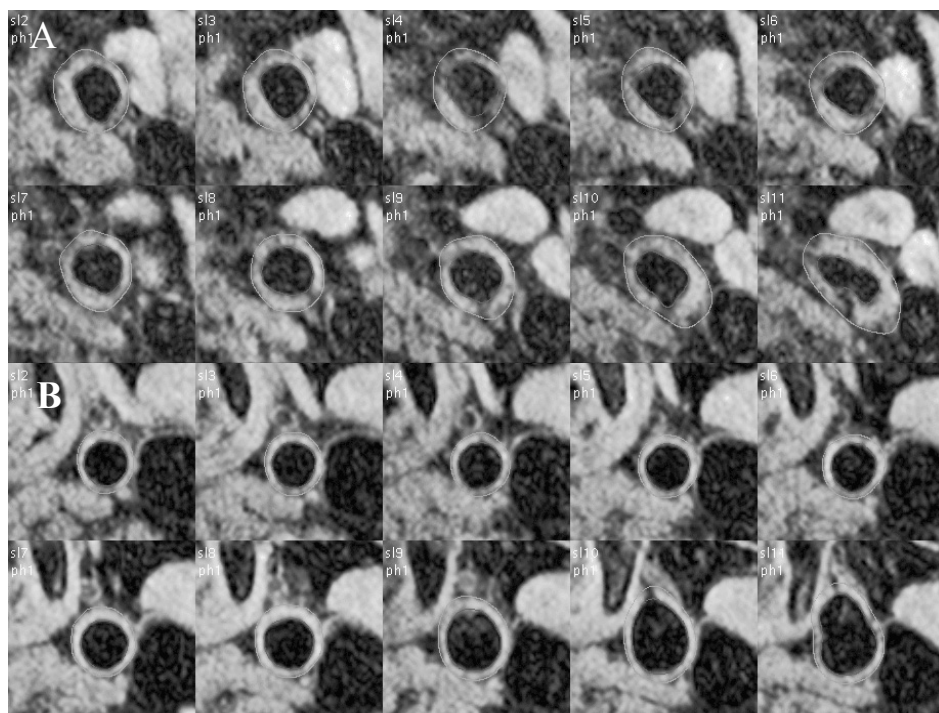
Figure 2. Maximum vessel thickness in the common carotid artery and the carotid bulb.



Maximum vessel thickness reflects the local formation of an atherosclerotic plaque both in the common carotid artery (A and B) and the carotid bulb (C and D). Elevated maximum vessel thickness measurements (A = 2.52 mm and C = 3.73 mm) are associated with atherosclerotic plaque formation in comparison to low thickness measurements (B = 1.22 mm and D = 1.95 mm).

the carotid bulb (bulbVWA) and total vessel wall area (totalVWA = commonVWA + bulbVWA). Maximum vessel wall thickness can reflect the degree of focal plaque formation (Figure 2), while vessel wall area provides more global information on the extent the atherosclerotic process (Figure 3).

Figure 3. Vessel wall area.



Vessel wall area provides global information on the extent of the atherosclerotic disease burden. An elevated total vessel wall area measure ($A = 5.53 \text{ cm}^2$) reflects more extensive global disease progression as seen by wall thickening and asymmetry, in comparison to lower area measures ($B = 3.01 \text{ cm}^2$).

Adipose tissue imaging

Subjects were positioned in the magnet in a supine position. The body coil was used for obtaining the images. A sagittal single shot gradient echo sequence survey scan was used for the imaging of the vertebral column in the lumbar region. Subsequently, a second single shot gradient echo sequence in the transversal plane was used for obtaining three contiguous slices of 10 mm without angulations with the following parameters: echo time 3.7 ms (TE), repetition time 7.5 ms (TR), pulse angle 45° , and 2 signal averages were performed. The slices were centred at the intervertebral disk level between the fourth and fifth lumbar vertebra. The images were obtained with three breath holds of 6 s. The field of view was 500 mm. A voxel size of $1 \text{ mm} \times 1.3$

Table 1. The clinical characteristics of the total study population and that of CRP and waist circumference strata.

	Waist circumference strata					CRP strata				
	Total Median IQR (n=439)	WCR1 Median IQR (n=143)	WCR2 Median IQR (n=158)	WCR3 Median IQR (n=86)	WCR4 Median IQR (n=52)	CRP1 Median IQR (n=132)	CRP2 Median IQR (n=103)	CRP3 Median IQR (n=97)	CRP4 Median IQR (n=109)	Δ groups p-value
Age (years)	60.5 56.4-64.2	60.4 56.9-64.3	60.9 56.7-64.7	59.3 56.3-63.8	59.1 55.1-62.5	59.9 55.8-63.5	60.5 57.1-64.2	60.52 56.4-64.3	61.2 55.8-64.7	NS
Current smoking (%)	82 (18.7)	28 (19.6)	29 (18.4)	18 (20.9)	7 (13.5)	25 (19.1)	13 (12.6)	18 (18.8)	26 (23.9)	NS
Waist circumference (cm)	105.5 100-112	98.5 96.5-100	105.8 104-107	113 111-115	124.3 120.6-128.8	104 99-108	104 99-109	106 101-114	109 102-117	†
Body weight (kg)	91.9 84.9-101.4	84.0 79.6-88.9	91.6 85.7-96.7	100.7 94.5-104.7	117.2 108.3-124.3	90.4 84.6-97.3	89.9 83.8-98	93.2 83.9-103.6	96.8 86.7-107.4	†
Height (cm)‡	178.0 (16.6)	177.8 (10.1)	178.6 (15.6)	175.4 (27.6)	181.6 (6.0)	176.8 (23.9)	177.3 (19.0)	178.9 (6.0)	179.5 (6.7)	NS
BMI (kg/m ²)	28.44 26.66-30.92	26.34 25.13-27.53	28.25 27.34-29.63	31.03 29.75-32.63	35.62 33.09-37.73	27.85 26.22-29.69	27.81 26.46-30.03	29.15 27.00-31.37	29.80 27.87-33.01	†
Systolic BP (mmHg)	145 134-159	142.0 131-151	144.0 134-157	149.5 136-163	153 138.5-167.3	144 134-154	145 135-157	144.5 133-163.75	148 136-163	NS
Diastolic BP (mmHg)	89 82-97	87 80-93	89 83-95.3	90.5 82-99.3	96 86-102	88 82-96	89 83-96	88 80-97.8	90 82-96.5	NS
Fasting blood glucose (mmol/L)	5.6 5.2-6.0	5.4 5.1-5.8	5.6 5.2-6.0	5.7 5.3-6.3	5.9 5.4-6.3	5.5 5.2-5.9	5.6 5.3-6.1	5.6 5.2-6.0	5.6 5.3-6.2	NS
Total cholesterol (mmol/L)	5.33 4.79-5.86	5.29 4.82-5.93	5.24 4.78-5.85	5.45 4.87-5.82	5.33 4.42-5.66	5.27 4.74-5.73	5.43 4.88-5.94	5.29 4.89-5.67	5.43 4.68-5.92	NS
HDL (mmol/L)	1.20 1.00-1.40	1.23 1.03-1.49	1.19 1.01-1.40	1.15 0.98-1.32	1.20 0.95-1.34	1.25 1.03-1.48	1.21 1.02-1.40	1.18 0.94-1.33	1.15 0.97-1.34	*
TG (mmol/L)	1.31 0.87-1.88	1.13 0.70-1.69	1.31 0.87-1.90	1.50 1.00-2.03	1.41 1.00-1.85	1.20 0.81-1.70	1.31 0.88-1.79	1.42 0.93-2.09	1.37 0.91-1.99	NS
CRP (mg/L)	1.64 0.93-2.99	1.18 0.82-2.57	1.48 0.91-2.63	2.07 1.06-3.32	2.84 1.69-4.44	0.77 0.55-0.89	1.34 1.10-1.52	2.23 1.97-2.63	4.33 3.39-5.74	†

* p<0.05

† p≤0.001

‡ Normal distribution. Data are demonstrated as Mean (SD).

ANOVA was used for testing the differences between the groups.

NS: Not statistically significant

BP: Blood pressure

IQR: interquartile range

mm × 10 mm was obtained. Images were assessed using the MASS software package allowing a semi-automated detection of subcutaneous (SAT) and visceral adipose tissue (VAT) area.

Statistical analysis

Continuous variables are presented as mean values ± standard error or as medians and inter-quartile ranges if the assumption of normality was not met. Categorical variables are presented as frequencies (%). As CRP levels were not normally distributed they were logarithmically transformed for bivariate correlation analysis. Comparisons between continuous variables were performed with independent samples *t*-tests or Mann–Whitney *U*-tests when not normally distributed. Testing for trends relating WCR to CRP strata in Table 2 was performed using the Chi-squared (χ^2) test. Correlations of baseline CRP levels with patient-related factors were analyzed with bivariate correlation analysis (Pearson's or Spearman's correlation depending on distribution) and stepwise multiple regression analysis. In the multiple regression analysis, the effect of CRP and covariates was assessed with logarithmically transformed MRI derived vascular endpoints as dependent variables. The covariates used were those metabolic parameters that were potentially ($p < 0.1\%$) different between the CRP+ and CRP– group.

In a post hoc exploration, in order to assess if CRP was associated with vessel wall characteristics in the low and intermediate Framingham risk groups (Framingham score ≤10%, and 11–20%, respectively) vessel wall characteristics were plotted for tertiles of CRP and analysed using ANOVA or Kruskal–Wallis as appropriate. Differences were observed only in the normally distributed variables (thus after ANOVA) and were further analysed by independent samples *t*-tests. Analyses were performed using SPSS Version 12.01 (SPSS, Chicago, IL, USA). All analyses were two-sided, with a level of significance of $\alpha = 0.05$.

Sample size calculations were difficult due to the lack of data for 3 T MRI. The sample size for this study was estimated at 40 participants (20 in each group) based on a previous report using less sensitive 1.5-T MR carotid artery imaging where MRI was calculated to be able to detect a 10% change in vessel wall volume in a study with 14 participants per group with a power of 80%, $p < 0.05$.¹⁸

RESULTS

Patient characteristics

From the 801 responding subjects, 439 were eligible for further analysis (Figure 1). Mean age of the group was 60.5 years, mean WCR 107.0 cm and CRP 2.31 mg/L. The characteristics of the subjects are summarized in Table 1. This table also provides detailed information on the characteristics of the subjects as grouped by WCR (WCR-strata) and by CRP levels (CRP-strata).

Table 2. The distribution of subjects along CRP strata according to the different waist circumference strata.

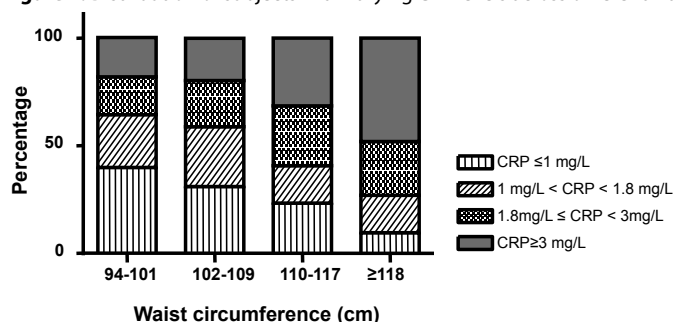
	CRP ≤ 1	1 < CRP < 1.8	1.8 < CRP < 3	3 ≤ CRP	Total
WCR 94-101 cm (count, % of total 439 subjects)	57 (13.0%)	35 (8.0%)	25 (5.7%)	26 (6.0%)	143 (32.6%)
% of the subjects in this waist group with this CRP level	39.9	24.5	17.5	18.2	100.0
% subjects in this CRP group with WCR 94-101 cm	43.5	34.0	26.0	23.9	
WCR 102-109 cm (count, % of total 439 subjects)	49 (11.2%)	44 (10.0%)	34 (7.7%)	31 (7.1%)	158 (36.0%)
% of the subjects in this waist group with this CRP level	31.0	27.8	21.5	19.6	100.0
% subjects in this CRP group with WCR 102-109 cm	37.4	42.7	35.4	28.4	
WCR 110-117 (count, % of total 439 subjects)	20 (4.6%)	15 (3.4%)	24 (5.5%)	27 (6.2%)	86 (19.6%)
% of the subjects in this waist group with this CRP level	23.3	17.4	27.9	31.4	100.0
% subjects in this CRP group with WCR 110-117 cm	15.3	14.6	25.0	24.8	
WCR ≥ 118 (count, % of total 439 subjects)	5 (1.1%)	9 (2.1%)	13 (3.0%)	25 (5.7%)	52 (11.8%)
% of the subjects in this waist group with this CRP level	9.6	17.3	25.0	48.1	100.0
% subjects in this CRP group with WCR ≥ 118 cm	3.8	8.7	13.5	22.9	
% subjects in CRP group Total (count, % total)	100.0	100.0	100.0	100.0	
	131 (29.8%)	103 (23.5%)	96 (21.9%)	109 (24.8%)	439

As expected, increasing WCR was associated with significantly increasing systolic ($p < 0.001$) and diastolic ($p < 0.001$) blood pressure, fasting blood glucose ($p < 0.001$), triglycerides ($p < 0.01$) and CRP levels ($p < 0.001$). With increasing CRP, significantly higher measures of WCR ($p < 0.001$), body weight ($p < 0.001$) and BMI ($p < 0.001$) were found. HDL-cholesterol levels were significantly lower in groups with increasing CRP levels ($p = 0.01$). Other variables known from the metabolic syndrome were not significantly different between CRP-strata.

Inflammation and visceral obesity

WCR significantly correlated with CRP levels ($r: 0.20, p < 0.001$). The distribution of subjects along WCR-strata and CRP-strata is illustrated in Table 2. The relation between WCR and CRP is further illustrated in Figure 4: 39.9% of the subjects with WCR 94–101 cm have CRP levels less than 1 mg/L, while 48.1% of subjects with WCR ≥ 118 cm were found to have CRP levels higher than 3 mg/L. Furthermore, in the two lowest WCR-strata (94–101 and 102–109 cm) most subjects (61.5%) had CRP levels below 1.8 mg/L, whereas in the two highest WCR-strata most subjects (64.5%) had CRP levels exceeding 1.8 mg/L. However, 18.2% of patients in WCR group 94–102 had increased CRP levels while 9.6% of patients in the highest waist group had low CRP levels.

Figure 4. Distribution of subjects with varying CRP levels across different waist circumference strata.



Analyzing the data from CRP-perspective, the percentage of individuals significantly decreased with increasing WCR in the 2 lowest CRP-strata. This pattern was less prominent within the third CRP stratum (1.8–3.0 mg/L) and absent in the highest CRP-stratum (≥ 3 mg/L). Thus, patients with high CRP levels were more or less randomly distributed over the WCR strata. The trends in patterns of distribution of subjects were statistically significant ($p < 0.001$). Subsequently, from each WCR-stratum subjects with low and high CRP levels were prospectively matched for further MRI evaluation as described in the materials and methods section.

CRP and the vessel wall

Vessel wall characteristics were analysed in CRP+ versus CRP-. The clinical characteristics of the two groups are summarized in Table 3. By definition, CRP levels significantly differed between the two groups. The CRP+ and CRP- groups did not differ regarding age (60.4 years vs. 60.3 years) and WCR (111.3 cm vs. 110.9 cm). Further anthropometric and metabolic variables including blood pressure were similar in both groups except for triglyceride levels ($p = 0.01$).

Table 3. The clinical characteristics of the two groups with varying CRP levels matched by WCR and age for MRI assessment

	CRP + mean (S.D.)	CRP - mean (S.D.)	p-Value
Age (years)	60.4 (5.3)	60.3 (5.2)	0.97
WCR (cm)	111.3 (9.7)	110.9 (9.8)	0.89
Body weight (kg)	100.6 (10.45)	97.8 (13.80)	0.47
BMI (kg/m²)	30.8 (3.3)	30.4 (3.5)	0.76
Systolic BP (mmHg)	149.8 (15.8)	154.2 (18.3)	0.43
Diastolic BP (mmHg)	90.7 (8.44)	93.1 (10.1)	0.42
CRP 1 (mg/L)^a	4.95 (3.44–5.75)	0.88 (0.58–1.08)	<0.001
CRP 2 (mg/L)^a	4.20 (3.25–5.45)	0.73 (0.54–1.41)	<0.001
HBA1c	4.9 (0.46)	5.02 (0.42)	0.41
FBG (mmol/L)	5.32 (0.51)	5.02 (0.68)	0.12
Cholesterol (mmol/L)	5.83 (1.14)	5.46 (0.78)	0.24
TG (mmol/L)^a	1.76 (1.27–2.16)	1.27 (0.94–1.58)	0.01
HDL (mmol/L)	1.29 (0.35)	1.48 (0.37)	0.10
LDL (mmol/L)	3.69 (0.92)	3.39 (0.69)	0.25
Insulin (mU/L)^a	12.00 (4.71–18.75)	7.00 (5.00–10.00)	0.06
HOMA_A	1.6 (0.60–2.38)	0.9 (0.61–1.30)	0.10
Framingham	13.65 (5.40)	12.60 (5.90)	0.56

WCR: waist circumference. BMI: body mass index. BP: blood pressure. FBG: fasting blood glucose. HOMA: HOMA insulin resistance index.

^a Skewed distribution, data are presented as median (inter-quartile range).

3T MRI assessments (Table 4)

Maximum vessel wall thickness was significantly higher in CRP+ compared to CRP-, both in the common carotid artery (15%) and the carotid bulb region (18%). Median and the inter-quartile range for vessel wall thickness were 1.64 mm [1.33–1.85] in CRP+ versus 1.34 mm [1.26–1.59] in CRP- ($p < 0.01$) in the common carotid artery; the respective values in the carotid bulb were 2.14 mm [1.89–2.54] versus 1.83 mm [1.63–1.99] ($p < 0.01$). Differences in vessel wall areas did not reach statistical significance, although the measurements were consistently higher in the CRP+ group for all area endpoints. No significant differences were observed in VAT and SAT between the two groups. Log CRP significantly correlated with all MRI derived measures of atherosclerosis. Further correlations between log CRP and VAT or SAT were not explored as they could have been confounded by the matching strategy (Table 4).

Table 4. MRI derived measures of atherosclerosis within the two groups and their correlation with log CRP

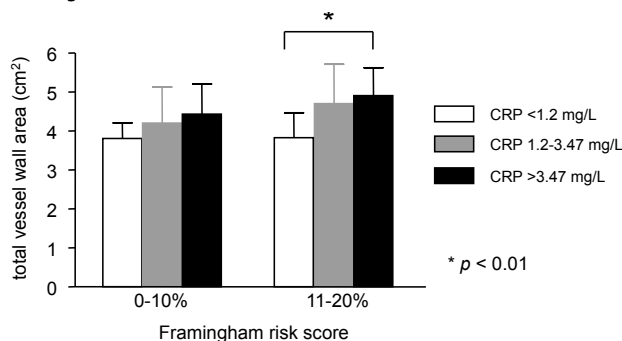
	CRP + mean (S.D.) n = 20	CRP – mean (S.D.) n = 20	p-Value	Correlation log CRP r (p-value)
CommonMVT (mm)^a	1.64 (1.33–1.85)	1.34 (1.26–1.59)	<0.01	0.47 (<0.01)
BulbMVT (mm)^a	2.14 (1.89–2.54)	1.83 (1.63–1.99)	<0.01	0.50 (<0.01)
CommonVWA (cm²)	1.79 (0.40)	1.60 (0.35)	0.12	0.45 (<0.01)
BulbVWA (cm²)	2.78 (0.49)	2.61 (0.61)	0.33	0.34 (0.03)
TotalVWA (cm²)	4.58 (0.78)	4.21 (0.91)	0.18	0.42 (<0.01)
VAT (cm²)	493.2 (143.7)	472.3 (200.4)	0.71	^b
SAT (cm²)	931.0 (317.6)	848.3 (288.7)	0.39	^b

MVT: maximum vessel thickness. **VWA:** vessel wall area. **TotalVWA:** sum of commonVWA and bulbVWA. **VAT:** visceral adipose tissue. **SAT:** subcutaneous adipose tissue.

^a Skewed distribution, data are presented as median (inter-quartile range), correlations were assessed using Spearman's correlation coefficients.

^b Not performed as it could have been confounded by the matching strategy.

Multiple regression analysis was performed with maximum vessel wall thickness as dependent variable and CRP, triglycerides, and HOMA insulin resistance index as covariates as described in the methods section. The model significantly explained 32% ($p = 0.001$) of variance for the common carotid artery maximum vessel wall thickness with CRP (β : 0.02 [0.009, 0.028]) and HOMA (β : -0.02 [-0.039, -0.003]) as significant explanatory variables. No interactions were observed between HOMA and CRP. For the carotid bulb maximum vessel wall thickness the model could explain 18% of the variance observed ($p < 0.01$) with CRP (β : 0.02 [0.006, 0.032]) as significant determinant of the model. The multiple regression analysis was repeated with CRP, HDL, and HOMA as covariates and MRI thickness measurements as dependent variables. HDL did not

Figure 5. The influence of CRP tertiles on the TVWA in subjects at an intermediate risk according to the Framingham risk score.

contribute significantly to the models. The obtained models were identical to those with CRP, triglycerides and HOMA as covariates. The models demonstrate that CRP remained a significant explanatory variable for the maximum vessel thickness both the common carotid artery and the bulb region when adjusted for HOMA, HDL and triglyceride levels.

CRP and the vessel wall in the intermediate cardiovascular risk population

In a post hoc analysis the relation between CRP and vessel wall characteristics was explored in relation to calculated cardiovascular risk according to the Framingham risk score. Within the intermediate risk group, Total VWA was significantly higher in the highest versus lowest tertile of CRP: 4.91 cm² versus 3.83 cm² ($p < 0.01$), see Figure 5. This effect was also observed for the bulb region: 3.00 cm² versus 2.35 cm² ($p < 0.01$). VAT and SAT were not significantly different between the tertiles of CRP in the intermediate risk group. Within the low cardiovascular risk group the obtained measures of vascular characteristics did not differ significantly between the tertiles of CRP.

DISCUSSION

This study demonstrates that elevated CRP levels are accompanied by significantly higher maximum vessel wall thickness both in the common carotid artery and the carotid bulb independent of VO and of MRI measured adipose tissue distribution.

Increased CRP levels have been associated with different measures of obesity.^{9-11, 19} The magnitude of this effect is typically reported to be in the range of $r = 0.50-0.60$.^{14, 20} This is in contrast to the weaker relation ($p: 0.20$) observed in our study. We studied viscerally obese subjects only while subjects with a normal waist girth were also included in the previous studies. This broader inclusion range may have contributed to higher correlation coefficients reported. Lower p values ($r = 0.37$) have recently been reported in an obese population.²¹ The relation between CRP and WCR can be appreciated using Table 2. The majority (61.5%) of the least obese subjects (VO stratum 1 and 2) have a CRP level in the range 0–1.8 mg/L while 64.5% of the subjects in the two highest VO strata have CRP levels ranging from 1.8 to 8.53 mg/L. Interestingly, high CRP levels were also observed in less obese subjects. This undoubtedly has weakened the correlation between VO and CRP. The subjects with the highest CRP levels were more or less evenly distributed across the different waist circumference strata suggesting that VO was not the only driving force behind inflammation in some of these subjects. A possible explanation for these observations could be the inter-individual differences in inflammatory repertoires and responsiveness. Timpson et al. for instance, have pointed to the potential genetic contribution to variation in CRP levels.²² To account for intra-individual variation, CRP levels were measured twice in our study. Subjects with elevated CRP levels (>15 mg/L) were excluded. In addition to intra-individual variation, CRP levels are known to vary between populations. Our cohort

consisted of white Caucasian subjects. The median CRP level within a white Caucasian population was shown to be 2.3 mg/L.²³ This CRP level was used to define the rounded-up threshold of 2.5 mg/L for CRP in our study. Changing the threshold of CRP to 2.3 mg/L neither influenced the vessel wall outcomes of the study; nor did reanalysis based on the cut-off value of 3.

We used magnetic resonance imaging at the field strength of 3 T for the assessment of atherosclerosis in this study. The precision and reproducibility of the technique in quantifying total plaque volume and disease burden has been previously reported by our group and others.^{17,24,25} The accuracy of measurements at the ultra high field strength of 3 T is due to the considerable increase in signal to noise ratio compared to 1.5 T, which in turn can be traded for a better in-plane resolution of the images. This has been demonstrated by the improved detection of complex atherosclerotic plaques as validated with histology²⁶, and improved image quality of the carotid artery at the field strength of 3 T.²⁷

Our observation that elevated CRP levels are accompanied by higher maximum vessel wall thickness independent of VO extends previous findings using other imaging modalities. An association has been observed between CRP levels and IMT as measured by ultrasonography.¹⁴⁻¹⁶ In contrast to our study, the correlation between CRP and IMT may not have been independent from obesity or metabolic dysregulation such as dyslipidemia and insulin resistance.¹⁴⁻¹⁶ In healthy children, higher CRP levels were shown to be associated with more extensive IMT thickening and disturbed endothelial function.¹⁵ The children with higher CRP levels had a significantly higher body mass index. Again the obesity-independent relation between CRP and atherosclerosis could not be fully appreciated. To overcome this we carefully matched the CRP+ and CRP- groups for age and WCR. Furthermore, the subjects were evenly selected across WCR strata to cover a broad range of VO. Metabolic profiles (Table 3) were very similar in CRP+ and CRP- except for fasting triglyceride levels. In a multiple regression analysis adjusting for potentially confounding factors such as triglycerides and HDL, CRP remained a significant independent predictor of vessel wall thickness.

It could be argued that matching by waist circumference would not automatically have resulted in successful matching for visceral and subcutaneous fat deposits. As adipose tissue distribution is causally related to metabolic disturbances²⁸, differences in the extent of adipose tissue deposits between the groups would have influenced the study observations. The importance of adipose tissue distribution is further illustrated by reports of normal risk factor profiles in patients with increased WCR due to expanded subcutaneous fat deposits.²⁹ Therefore we studied adipose tissue distribution by MRI. We did not observe differences in adipose tissue distribution between the visceral and subcutaneous depots in CRP+ versus CRP-. Thus, the observed differences in vessel wall thickness are independent of adipose tissue distribution between subcutaneous and visceral deposits.

A possible additive role of CRP in the prediction of future cardiovascular events has been demonstrated in subjects at intermediate risk according to the Framingham score.³⁰ In a post hoc analysis, we explored the relation between CRP levels and the extent of atherosclerotic disease burden in this group. Vessel wall areas (total and in the carotid bulb) significantly differed between the highest versus the lowest tertiles of CRP within the intermediate risk patients. Intriguingly, vascular wall areas in the lowest CRP tertiles were very similar independent of the Framingham risk group (Figure 5). Thus, absence of a low grade inflammation as measured by CRP was associated with limited atherosclerotic carotid vessel wall thickening as measured by MRI regardless of the calculated cardiovascular risk. These observations support reports showing that CRP levels may add to risk stratification within intermediate risk patients.³⁰

The restricted number of participants in our MRI-study may have posed a limitation on detecting other differences in atherosclerotic disease burden. In other words, only prominent effects might have been detected and less pronounced differences might have remained unobserved. This is in line with the observation that all vessel wall parameters significantly correlated with log CRP. If so, the impact of CRP on atherosclerotic burden in the setting of VO may be larger than now described. Furthermore, design of the study should be taken into account. Matching the participants by WCR was necessary to eliminate VO from the “CRP–atherosclerosis” equation. The population assessed is therefore not a random sample from a general population and does not represent it (see Table 2).

In conclusion, we demonstrated that elevated CRP levels are associated with significantly increased maximum vessel wall thickness both in the common carotid artery and the carotid bulb independent of VO and of MRI measured adipose tissue distribution.

REFERENCE LIST

1. Despres JP, Lemieux I, Prud'homme D. Treatment of obesity: need to focus on high risk abdominally obese patients. *BMJ* 2001 March 24;322(7288):716-20.
2. Van Gaal LF, Vansant GA, De L, I. Upper body adiposity and the risk for atherosclerosis. *J Am Coll Nutr* 1989 December;8(6):504-14.
3. Wong S, Janssen I, Ross R. Abdominal adipose tissue distribution and metabolic risk. *Sports Med* 2003;33(10):709-26.
4. Pascot A, Lemieux I, Prud'homme D et al. Reduced HDL particle size as an additional feature of the atherogenic dyslipidemia of abdominal obesity. *J Lipid Res* 2001 December;42(12):2007-14.
5. Lemieux I, Pascot A, Prud'homme D et al. Elevated C-reactive protein: another component of the atherothrombotic profile of abdominal obesity. *Arterioscler Thromb Vasc Biol* 2001 June;21(6):961-7.
6. Tchernof A, Lamarche B, Prud'homme D et al. The dense LDL phenotype. Association with plasma lipoprotein levels, visceral obesity, and hyperinsulinemia in men. *Diabetes Care* 1996 June;19(6):629-37.
7. Reaven GM. The metabolic syndrome: is this diagnosis necessary? *Am J Clin Nutr* 2006 June;83(6):1237-47.
8. Abbasi F, Brown BW, Jr., Lamendola C, McLaughlin T, Reaven GM. Relationship between obesity, insulin resistance, and coronary heart disease risk. *J Am Coll Cardiol* 2002 September 4;40(5):937-43.
9. Trayhurn P, Wood IS. Adipokines: inflammation and the pleiotropic role of white adipose tissue. *Br J Nutr* 2004 September;92(3):347-55.
10. Yudkin JS, Stehouwer CD, Emeis JJ, Coppack SW. C-reactive protein in healthy subjects: associations with obesity, insulin resistance, and endothelial dysfunction: a potential role for cytokines originating from adipose tissue? *Arterioscler Thromb Vasc Biol* 1999 April;19(4):972-8.
11. Couillard C, Bergeron N, Prud'homme D et al. Postprandial triglyceride response in visceral obesity in men. *Diabetes* 1998 June;47(6):953-60.
12. Ridker PM. Clinical application of C-reactive protein for cardiovascular disease detection and prevention. *Circulation* 2003 January 28;107(3):363-9.
13. Yusuf S, Hawken S, Ounpuu S et al. Obesity and the risk of myocardial infarction in 27,000 participants from 52 countries: a case-control study. *Lancet* 2005 November 5;366(9497):1640-9.
14. Hak AE, Stehouwer CD, Bots ML et al. Associations of C-reactive protein with measures of obesity, insulin resistance, and subclinical atherosclerosis in healthy, middle-aged women. *Arterioscler Thromb Vasc Biol* 1999 August;19(8):1986-91.
15. Jarvisalo MJ, Harmoinen A, Hakanen M et al. Elevated serum C-reactive protein levels and early arterial changes in healthy children. *Arterioscler Thromb Vasc Biol* 2002 August 1;22(8):1323-8.
16. Blackburn R, Giral P, Bruckert E et al. Elevated C-reactive protein constitutes an independent predictor of advanced carotid plaques in dyslipidemic subjects. *Arterioscler Thromb Vasc Biol* 2001 December;21(12):1962-8.
17. Alizadeh DR, Doornbos J, Tamsma JT et al. Assessment of the carotid artery by MRI at 3T: a study on reproducibility. *J Magn Reson Imaging* 2007 May;25(5):1035-43.
18. Saam T, Kerwin WS, Chu B et al. Sample size calculation for clinical trials using magnetic resonance imaging for the quantitative assessment of carotid atherosclerosis. *J Cardiovasc Magn Reson* 2005;7(5):799-808.
19. Fredrikson GN, Hedblad B, Nilsson JA, Alm R, Berglund G, Nilsson J. Association between diet, lifestyle, metabolic cardiovascular risk factors, and plasma C-reactive protein levels. *Metabolism* 2004 November;53(11):1436-42.
20. Couillard C, Ruel G, Archer WR et al. Circulating levels of oxidative stress markers and endothelial adhesion molecules in men with abdominal obesity. *J Clin Endocrinol Metab* 2005 December;90(12):6454-9.
21. Pou KM, Massaro JM, Hoffmann U et al. Visceral and subcutaneous adipose tissue volumes are cross-sectionally related to markers of inflammation and oxidative stress: the Framingham Heart Study. *Circulation* 2007 September 11;116(11):1234-41.

22. Timpson NJ, Lawlor DA, Harbord RM et al. C-reactive protein and its role in metabolic syndrome: mendelian randomisation study. *Lancet* 2005 December 3;366(9501):1954-9.
23. Khera A, McGuire DK, Murphy SA et al. Race and gender differences in C-reactive protein levels. *J Am Coll Cardiol* 2005 August 2;46(3):464-9.
24. Shinnar M, Fallon JT, Wehrli S et al. The diagnostic accuracy of ex vivo MRI for human atherosclerotic plaque characterization. *Arterioscler Thromb Vasc Biol* 1999 November;19(11):2756-61.
25. Varghese A, Crowe LA, Mohiaddin RH et al. Inter-study reproducibility of 3D volume selective fast spin echo sequence for quantifying carotid artery wall volume in asymptomatic subjects. *Atherosclerosis* 2005 December;183(2):361-6.
26. Cury RC, Houser SL, Furie KL et al. Vulnerable plaque detection by 3.0 tesla magnetic resonance imaging. *Invest Radiol* 2006 February;41(2):112-5.
27. Yarnykh VL, Terashima M, Hayes CE et al. Multicontrast black-blood MRI of carotid arteries: comparison between 1.5 and 3 tesla magnetic field strengths. *J Magn Reson Imaging* 2006 May;23(5):691-8.
28. Despres JP, Lemieux I. Abdominal obesity and metabolic syndrome. *Nature* 2006 December 14;444(7121):881-7.
29. Lemieux I, Drapeau V, Richard D et al. Waist girth does not predict metabolic complications in severely obese men. *Diabetes Care* 2006 June;29(6):1417-9.
30. Koenig W, Lowel H, Baumert J, Meisinger C. C-reactive protein modulates risk prediction based on the Framingham Score: implications for future risk assessment: results from a large cohort study in southern Germany. *Circulation* 2004 March 23;109(11):1349-53.

CHAPTER

6

Apolipoprotein CI levels are associated with atherosclerosis in men with the metabolic syndrome and systemic inflammation

R.L.M. van der Ham¹, R. Alizadeh Dehnavi¹, G.A. van den Berg¹, H. Putter², A. de Roos³, J.F.P. Berbée⁴, J.A. Romijn⁴, P.C.N. Rensen⁴, and J.T. Tamsma¹

¹Vascular Medicine, Department of Internal Medicine and Endocrinology, LUMC, Leiden, The Netherlands

²Department of Medical Statistics, LUMC, Leiden, The Netherlands

³Department of Radiology, LUMC, Leiden, The Netherlands

⁴Department of Internal Medicine and Endocrinology, LUMC, Leiden, Netherlands

Atherosclerosis 2009 Apr;203(2):355-7

INTRODUCTION

Apolipoprotein CI (ApoCI) is an apolipoprotein mainly present on high-density lipoprotein (HDL) and postprandial on triglyceride-rich lipoproteins (TRLs). ApoCI influences many proteins involved in the remodeling of lipoproteins in plasma.¹⁻⁶ In addition, ApoCI inhibits the ApoE-mediated binding of VLDL and chylomicrons to the LDL receptor and to the LDL receptor-related protein (LRP).⁷ Recently, an important role of ApoCI in the modulation of the inflammatory response was revealed *in vitro* and in mice.⁸ Therefore, as a possible link between lipid metabolism and inflammation, ApoCI may have the potential to contribute to the pathophysiology of atherosclerosis. Recent experimental data provided evidence that ApoCI augments the development of atherosclerosis in the setting of chronic inflammation in mice.⁹ The contribution of ApoCI to atherogenesis in humans has been examined in a few studies. The postprandial ApoCI content of TRLs was found to correlate with intima-media thickness.¹⁰ In addition, men with early asymptomatic atherosclerosis had postprandial VLDL and chylomicron particles enriched with ApoCI.⁷ Noto et al.¹¹ observed an association between the ApoCI content of VLDL and plaque size in subjects with carotid atherosclerosis.

We hypothesized that ApoCI has an adverse effect on atherosclerotic vessel wall characteristics in the presence of systemic inflammation and mild dyslipidemia observed in the metabolic syndrome (MS).

METHODS

We studied 98 male subjects, aged 50–70 years, with the MS (defined using International Diabetes Federation criteria¹²). Exclusion criteria were presence of type 2 diabetes mellitus, overt cardiovascular disease, the use of statins, fibrates or non-steroidal anti-inflammatory drugs (NSAIDs), a body mass index (BMI) above 40 kg/m², contraindications for magnetic resonance imaging (MRI), and a plasma level of high-sensitive C-reactive protein (hsCRP) exceeding 15 mg/L. The study protocol was approved by the Local Ethics Committee and all patients signed informed consent. Blood samples were collected after a 12-h overnight fast. Chemical and hematological laboratory assessments were performed in the hospital laboratory. Plasma concentrations of ApoCI and ApoCIII were determined using sandwich ELISAs specific for human ApoCI¹³ and ApoCIII.^{14, 15} MRI of the carotid artery was performed on a 3T scanner (Philips, Achieva, Best, The Netherlands) as previously described and validated.¹⁶ Images were analysed using VesselMASS software package. Ten images, covering 2 cm, were produced of the common carotid artery and bulb. Vessel wall area (VWA) for common carotid artery (common VWA) and bulb (bulbus VWA), and total VWA (common VWA + bulbus VWA) were measured. Furthermore, as a measure of focal atherosclerotic vessel wall changes, maximal

vessel wall thickness (MVT) was measured by calculating, for common carotid artery and bulb separately, the mean of the thickest of 6 equal segments per image. To address the question whether ApoCI levels are associated with increased atherosclerotic vessel wall characteristics in the presence of systemic inflammation and mild dyslipidemia, the study subjects were divided into four groups according to the absence or presence of systemic inflammation (as defined by an hsCRP level of <3 and ≥ 3 mg/L, respectively) and plasma ApoCI level (above or below the median value, 6.38 mg/dL). Plasma levels of ApoCIII, a protein with a similar distribution over lipoproteins and comparable to ApoCI in mass and structure, were measured as a negative control. Like ApoCI, ApoCIII is associated with VLDL and HDL, but it has no known interaction with inflammation.⁸ Differences in baseline characteristics, laboratory parameters and vessel wall measurements were assessed by one-way analysis of variance (ANOVA). Post hoc least significant difference (LSD) testing was performed for parameters that proved statistically significant on ANOVA. Kruskal–Wallis tests with Mann–Whitney test for pairwise comparisons (p values were multiplied by 3 to correct for multiple testing) were performed for parameters that were not normally distributed. Correlations were calculated using Spearman's rho.

RESULTS AND DISCUSSION

Clinical and laboratory parameters of the patients are given in Table 1. Between the four groups, differences were observed in BMI, total cholesterol, LDL-cholesterol, HDL-cholesterol and triglyceride levels. ApoCI did not correlate with hsCRP ($\rho = -0.042$; n.s.), and was positively correlated with total cholesterol ($\rho = 0.462$; $p < 0.001$), LDL ($\rho = 0.224$; $p < 0.05$), HDL-cholesterol ($\rho = 0.347$; $p < 0.001$) and TG levels ($\rho = 0.339$; $p < 0.001$). No significant differences in vessel wall area and MVT of the common carotid artery were observed between the groups. The maximal vessel wall thickness of the carotid bulb, however, was significantly increased in the subjects with both systemic inflammation and ApoCI above the median (Figure 1). There was no association between ApoCIII levels and vessel wall parameters in the presence or absence of systemic inflammation.

To further explore the relation between ApoCI and inflammation, univariate variance analysis was performed with maximal vessel wall thickness of the carotid bulb as the dependent variable. The variables added as covariates were the metabolic syndrome parameters (waist circumference, fasting blood glucose, systolic and diastolic blood pressure, HDL-cholesterol, triglycerides), and ApoCI and hsCRP, all as continuous variables. In this model a statistically significant interaction between ApoCI and hsCRP was observed (Model: $R^2 = 0.18$; $p = 0.035$; interaction of hsCRP with ApoCI: $p = 0.027$; $B = 0.031$; hsCRP: $p = 0.045$; $B = -0.168$, ApoCI $p = 0.06$; $B = -0.091$). When ApoCIII was added to the model instead of ApoCI, no interaction was observed between ApoCIII and hsCRP.

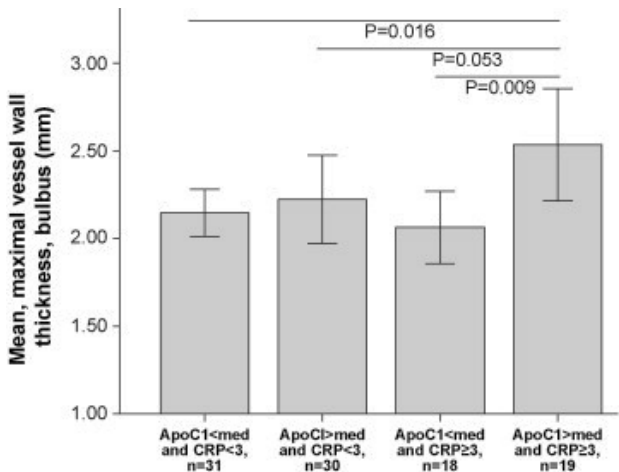
Table 1. Clinical and laboratory parameters for the four patient groups (ApoCI < median and hsCRP < 3 (1); ApoCI > median and hsCRP < 3 (2); ApoCI < median and hsCRP ≥ 3 (3); ApoCI > median and hsCRP ≥ 3 (4))

	hsCRP < 3 and ApoCI < med; n = 31 (1)	hsCRP < 3 and ApoCI > med; n = 30 (2)	hsCRP ≥ 3 and ApoCI < med; n = 18 (3)	hsCRP ≥ 3 and ApoCI > med; n = 19 (4)	p (ANOVA 4 groups)
Age (y)	59.2 (5.4)	58.5 (5.5)	58.2 (5.5)	59.9 (4.6)	Ns
BMI (kg/m²)	30.7 (3.5)	29.2 (3.3) 3*, 4 [#]	31.9 (3.5) 2*	31.4 (3.6) 2 [#]	0.041
SBP (mmHg)	154.4 (17.1)	152.8 (18.3)	150.3 (12.7)	155.2 (19.5)	Ns
DBP (mmHg)	94.0 (8.2)	89.2 (7.8)	91.8 (8.0)	91.7 (9.5)	Ns
FBG (mmol/L)	5.4 (1.0)	5.5 (0.8)	5.7 (0.5)	5.8 (1.0)	Ns
TotChol (mmol/L)	5.45 (0.9) 2*, 4*	6.23 (0.9) 1*, 3+	5.26 (0.8) 2+, 4+	6.29 (0.9) 1*, 3+	0.000
Calculated LDL (mmol/L)	3.42 (0.7) 4 [#]	3.54 (0.3)	3.16 (0.6) 4*	3.93 (0.8) 1 [#] , 3*	0.025
HDL (mmol/L)	1.08 (0.3) 2+, 3*, 4 [#]	1.37 (0.3) 1+	1.30 (0.3) 1*	1.30 (0.3) 1 [#]	0.001
Triglycerides (mmol/L)	2.07 (0.9) 2*	2.81 (1.2) 1*, 3*	1.78 (0.8) 2*	2.35 (1.0)	0.004
hsCRP (mg/L) (med)	1.74 (1.2–2.5) 3+, 4+	1.56 (1.0–2.3) 3+, 4+	4.74 (4.0–7.9) 1+, 2+	3.94 (3.4–5.1) 1+, 2+	0.000
ApoCI (mg/dL) (med)	5.06 (4.4–5.7) 2+, 4+	7.70 (7.0–9.1) 1+, 3+	4.94 (4.6–5.9) 2+, 4+	7.68 (7.0–9.6) 1+, 3+	0.000
ApoCIII (mg/dL)	8.71 (3.8) 2*, 4 [#]	12.23 (4.4) 1*, 3*	8.51 (3.6) 2*, 4 [#]	11.16 (3.3) 1 [#] , 3 [#]	0.001
Total VWA (cm²)	4.74 (1.0)	4.71 (1.4)	4.61 (1.0)	5.00 (0.8)	Ns
Common VWA (cm²)	1.81 (0.4)	1.84 (0.6)	1.83 (0.4)	1.93 (0.4)	Ns
MVT Common (mm)	1.62 (0.3)	1.64 (0.4)	1.58 (0.2)	1.68 (0.3)	Ns
Bulbus VWA (cm²)	2.93 (0.7)	2.87 (0.9)	2.78 (0.6)	3.07 (0.5)	Ns
MVT Bulbus (mm)	2.15 (0.4) 4 (p = 0.016)	2.22 (0.7)	2.06 (0.4) 4 (p = 0.009)	2.53 (0.7) 1 (p = 0.016), 3 (p = 0.009)	0.042

Mean or median with standard deviation or inter quartile range (IQR) are given, values represent means unless indicated otherwise. *p* Values for pairwise differences given below the mean values (number: group to which the value is different, [#]*p* < 0.05, **p* < 0.01, +*p* < 0.001). **SBP**: systolic blood pressure. **DBP**: diastolic blood pressure. **FBG**: fasting blood glucose. **Totchol**: total cholesterol. **VWA**: vessel wall area. **MVT**: maximal vessel wall thickness.

Thus, the observed significant interaction of ApoCI and hsCRP on atherosclerosis persisted after correction for the components of MS. In an inflammatory setting ApoCI has a different relation to the vessel wall than when inflammation is absent. This result is in line with the close association between ApoCI and inflammation-driven atherosclerosis in experimental studies.⁹ MS patients may be especially vulnerable to ApoCI-mediated atherogenesis as the MS phenotype is characterized by changes in HDL and VLDL metabolism, and is frequently associated with low grade systemic inflammation. Vessel wall area measures, and MVT of the common carotid artery, were not different between the groups in our study. This should be appreciated when interpreting the data. In our patients, many of whom were in an early phase of atherogenesis given the exclusion criteria applied, high ApoCI and systemic inflammation were associated

Figure 1. Maximal vessel wall thickness in the carotid bulb (mean with 95% confidence interval) for the four groups (ApoCI < median and hsCRP < 3; ApoCI > median and hsCRP < 3; ApoCI < median and hsCRP ≥ 3; ApoCI > median and hsCRP ≥ 3).



with increased MVT at the level of the carotid bulb. Intriguingly, this is an area where plaques typically develop. We propose the increased MVT observed in the carotid bulb reflects early focal atherosclerotic changes. Our data are in line with studies relating ApoCI content on postprandial VLDL or TRL's to ultrasonographically assessed vessel wall abnormalities.^{7, 10} This includes a recent report on plaque size.¹¹ Our data extend these observations to fasting ApoCI levels using MR as imaging modality. Performing contrast-enhanced MRI would enable studying plaque volume and plaque characteristics in addition to MVT, and could be an important extension to our 3T MRI protocol. The strong associations of ApoCI with plasma lipids hinder establishing whether ApoCI *per se* has a causal role in the pathogenesis of atherosclerosis. However, ApoCIII, the negative control, was not associated with increased vessel wall measurements. The subjects studied are representative of a primary prevention population of men aged 50–70 years, with metabolic syndrome, without diabetes or cardiovascular disease. The findings in this study cannot be extrapolated to the general population. Studying subjects with diabetes may be especially interesting because of the strong relation between diabetes and inflammation. Furthermore, studying the ApoCI concentration in fasting plasma, compared with studying the postprandial ApoCI content of VLDL, as described by Hamsten et al.¹⁰, may lead to an under estimation of the effect of ApoCI on atherosclerosis in the presence of inflammation. Although further studies are needed, our results suggest that the recent experimental findings linking ApoCI to atherosclerosis may be translated to the human setting, and that ApoCI contributes to plaque formation, provided an inflammatory environment is present.

REFERENCE LIST

1. Shachter NS. Apolipoproteins C-I and C-III as important modulators of lipoprotein metabolism. *Curr Opin Lipidol* 2001 June;12(3):297-304.
2. Conde-Knape K, Bensadoun A, Sobel JH, Cohn JS, Shachter NS. Overexpression of apoC-I in apoE-null mice: severe hypertriglyceridemia due to inhibition of hepatic lipase. *J Lipid Res* 2002 December;43(12):
3. Berbee JF, van der Hoogt CC, Sundararaman D, Havekes LM, Rensen PC. Severe hypertriglyceridemia in human APOC1 transgenic mice is caused by apoC-I-induced inhibition of LPL. *J Lipid Res* 2005 February;46(2):297-306.
4. Dumont L, Gautier T, de Barros JP et al. Molecular mechanism of the blockade of plasma cholesteryl ester transfer protein by its physiological inhibitor apolipoprotein CI. *J Biol Chem* 2005 November 11;280(45):38108-16.
5. Asztalos BF, Schaefer EJ, Horvath KV et al. Role of LCAT in HDL remodeling: investigation of LCAT deficiency states. *J Lipid Res* 2007 March;48(3):592-9.
6. Hovingh GK, Hutten BA, Holleboom AG et al. Compromised LCAT function is associated with increased atherosclerosis. *Circulation* 2005 August 9;112(6):879-84.
7. Bjorkegren J, Silveira A, Boquist S et al. Postprandial enrichment of remnant lipoproteins with apoC-I in healthy normolipidemic men with early asymptomatic atherosclerosis. *Arterioscler Thromb Vasc Biol* 2002 September 1;22(9):1470-4.
8. Berbee JF, van der Hoogt CC, Kleemann R et al. Apolipoprotein CI stimulates the response to lipopolysaccharide and reduces mortality in gram-negative sepsis. *FASEB J* 2006 October;20(12):2162-4.
9. Westerterp M, Berbee JF, Pires NM et al. Apolipoprotein C-I is crucially involved in lipopolysaccharide-induced atherosclerosis development in apolipoprotein E-knockout mice. *Circulation* 2007 November 6;116(19):2173-81.
10. Hamsten A, Silveira A, Boquist S et al. The apolipoprotein CI content of triglyceride-rich lipoproteins independently predicts early atherosclerosis in healthy middle-aged men. *J Am Coll Cardiol* 2005 April 5;45(7):1013-7.
11. Noto AT, Mathiesen EB, Brox J, Bjorkegren J, Hansen JB. The ApoC-I content of VLDL particles is associated with plaque size in persons with carotid atherosclerosis. *Lipids* 2008 July;43(7):673-9.
12. Alberti KG, Zimmet P, Shaw J. Metabolic syndrome--a new world-wide definition. A Consensus Statement from the International Diabetes Federation. *Diabet Med* 2006 May;23(5):469-80.
13. Berbee JF, Mooijaart SP, de Craen AJ et al. Plasma apolipoprotein CI protects against mortality from infection in old age. *J Gerontol A Biol Sci Med Sci* 2008 February;63(2):122-6.
14. Schaap FG, Nierman MC, Berbee JF et al. Evidence for a complex relationship between apoA-V and apoC-III in patients with severe hypertriglyceridemia. *J Lipid Res* 2006 October;47(10):2333-9.
15. Schippers EF, Berbee JF, van D, I et al. Preoperative apolipoprotein CI levels correlate positively with the proinflammatory response in patients experiencing endotoxemia following elective cardiac surgery. *Intensive Care Med* 2008 August;34(8):1492-7.
16. Alizadeh DR, Doornbos J, Tamsma JT et al. Assessment of the carotid artery by MRI at 3T: a study on reproducibility. *J Magn Reson Imaging* 2007 May;25(5):1035-43.

PART III

**Visceral Obesity and systemic
inflammation as therapeutic targets
in atherosclerosis**

CHAPTER

7

Effect of Rosiglitazone plus Lifestyle Therapy on the Prevention of Progression of Atherosclerosis in Men with Visceral Obesity and Elevated C-reactive Protein

Reza Alizadeh Dehnavi¹ MD, Albert de Roos² MD PhD, Jolein van der Kraan¹, Johannes A. Romijn¹ MD PhD, Ton J. Rabelink³ MD PhD, Hein Putter⁴ PhD, Johannes van Pelt⁵ PhD, Menno V.Huisman¹ MD PhD, Jouke T. Tamsma¹ MD PhD

¹Section of Vascular Medicine, Department of General Internal Medicine & Endocrinology, Leiden University Medical Centre, Leiden, The Netherlands

²Department of Radiology, Leiden University Medical Centre, Leiden, The Netherlands

³Department of Nephrology & Einthoven Laboratory, Leiden University Medical Centre, Leiden, The Netherlands

⁴Department of Medical Statistics and Bio-Informatics, Leiden University Medical Centre, Leiden, The Netherlands

⁵Department of Clinical Chemistry, Leiden University Medical Centre, Leiden, The Netherlands.

Submitted

ABSTRACT

Objectives

Patients with visceral obesity and elevated C-reactive protein (CRP) levels are regarded at increased cardiovascular risk even in the absence of Diabetes Mellitus. Since rosiglitazone alters fat distribution, and has anti-inflammatory effects, we hypothesized it would prevent progression of atherosclerosis in men with visceral obesity and elevated CRP when given in addition to intensive lifestyle therapy.

Design

Double blind, placebo controlled randomized clinical trial.

Setting & Subjects

Single centre primary prevention setting.

116 non-diabetic men with visceral obesity and CRP levels ≥ 1.8 mg/L.

Interventions

Daily therapy with 8mg rosiglitazone plus intensive lifestyle therapy or placebo plus intensive lifestyle therapy for 52 weeks. Patients underwent three tesla magnetic resonance imaging (MRI) to assess vessel wall characteristics of the carotid artery.

Results

The primary outcome, the median [interquartile range (IQR)] change in carotid-artery total vessel wall area, was $0.04[-0.24 \text{ to } 0.38]\text{cm}^2$ in the rosiglitazone-lifestyle group and $0.001[-0.25 \text{ to } 0.20]\text{cm}^2$ in the placebo-lifestyle group ($P=0.19$). Of the secondary endpoints, median [IQR] maximum vessel wall thickness increased $0.071[-0.06 \text{ to } 0.16]\text{mm}$ in the rosiglitazone-lifestyle group and non-significantly decreased $-0.009[-0.08 \text{ to } 0.10]\text{mm}$ in the placebo-lifestyle group ($P=0.16$). Rosiglitazone-lifestyle and placebo-lifestyle reduced median [IQR] waist circumference by $-7.5[-11 \text{ to } -3.9]\text{cm}$ and $-8.8[-13 \text{ to } -5]\text{cm}$ and median [IQR] CRP levels by $-0.87[-2.23 \text{ to } -0.26]\text{mg/L}$ and $-0.53[-1.95 \text{ to } 0.61]\text{mg/L}$, respectively. MRI assessment of fat stores showed similar decrease in visceral adipose tissue, while waist and hip subcutaneous fat stores decreased more in placebo-lifestyle treated patients.

Conclusion

Rosiglitazone did not prevent progression of atherosclerosis when given on top of intensive lifestyle therapy in men with visceral obesity and elevated C-reactive protein levels.

INTRODUCTION

Visceral obesity (VO) and elevated C-reactive protein (CRP) levels indicative of systemic inflammation are independent risk factors for myocardial infarction¹ and cardiovascular mortality.² The first step in the treatment of subjects with visceral obesity is lifestyle therapy. Intensive lifestyle therapy can prevent type 2 diabetes mellitus (DM2).⁴⁻⁶ Although, increased physical activity and a healthy diet are known to be beneficial in patients with manifest coronary heart disease^{7,8}, the effect of intensive lifestyle therapy on intermediate endpoints of atherosclerosis has not been studied in visceral obese patients with elevated CRP levels. In addition to intensive lifestyle therapy, medication that alter fat distribution and decrease systemic inflammation may have an additive potential to prevent progression of atherosclerosis. Rosiglitazone is a peroxisome-proliferator-activated receptor γ (PPAR γ) agonist that alters fat distribution and modulates metabolic and inflammatory gene repertoires.⁹⁻¹¹ More specifically, it redistributes fat from visceral to peripheral stores and decreases CRP levels.^{12,13} Given these characteristics, we hypothesized rosiglitazone would prevent progression of atherosclerosis in men with visceral obesity and elevated CRP levels, when given in addition to intensive lifestyle therapy. In line with this hypothesis, rosiglitazone reduced the progression of atherosclerosis as measured by ultrasonography yielding measures of carotid artery intima media thickness (IMT) in patients with DM2.¹⁴

In this study, we sought to determine whether the daily administration of 8mg of rosiglitazone in combination with intensive lifestyle therapy could prevent the progression of atherosclerosis in non-diabetic patients with visceral obesity and elevated CRP levels. In our study, called "A 52 week double-blind randomized controlled trial comparing the effect of Rosiglitazone versus placebo on the prevention of progression of atherosclerosis in high risk patients without diabetes (RUBENS) trial" we used three Tesla magnetic resonance imaging (MRI) of the carotid artery vessel wall as a surrogate measure to assess the progression of atherosclerosis.

MATERIALS AND METHODS

Study design

Our prospective randomized double-blind placebo controlled trial was performed at LUMC, Leiden, The Netherlands as a single centre study. Patients provided written informed consent. The study was approved by the institutional review committee and was conducted according to the principles expressed in the Declaration of Helsinki. Men of 50 years or older were eligible to participate in the study if a waist circumference ≥ 94 cm and a CRP levels of 1.8mg/L or higher was present. The cut-off value of 1.8mg/L for CRP was chosen based on the previously reported median of CRP in males in a large epidemiological study.¹⁵ Additional inclusion criteria were

the presence of either at least two other metabolic syndrome criteria according to the IDF definition¹⁶ or the presence of premature cardiovascular disease in a first degree family member. Exclusion criteria included DM2 (fasting blood glucose <7mmol/l), manifest cardiovascular disease, use of statins at baseline, use of steroids or non-steroidal anti-inflammatory drugs at baseline, heart failure (NYSE class I or higher), QTc time interval of 450ms or longer on baseline ECG, primary dyslipidemias, hypoglycaemia, presence of potential hepatic disease (i.e. subjects with ALT, total bilirubin, or alkaline phosphatase levels exceeding 2.5 times the upper limit of the normal laboratory values), risk of non compliance, alcohol abuse (>30 units/week) and MRI contraindications.

The study consisted of two periods: the screening phase and a double-blind study period with a scheduled duration of 52 weeks. After the screening phase eligible patients were randomly assigned in a 1:1 ratio to receive either daily therapy with 8mg of rosiglitazone or placebo. The treatment was titrated. During the first eight weeks of the study, the participants were treated with one tablet daily (rosiglitazone 4mg or placebo). When tolerated, the dosis was doubled after 8 weeks. Randomization was based on computer generated codes. The participants were stratified for smoking and family history of premature cardiovascular disease. The allocation sequence was generated and kept by the institutional trial pharmacist. All subjects received intensive lifestyle treatment in addition to rosiglitazone or placebo. Subjects were advised to start on a 1500kCal diet and refrain from smoking. In addition they were encouraged to increase their level of daily physical activity aiming at an extra energy-expenditure of 270kCal per day (i.e. a normal-pace walk of 30 minutes, three times daily).

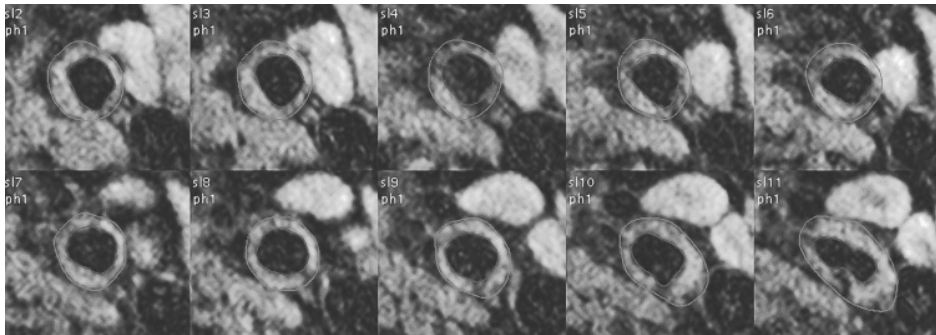
All subjects were seen at follow-up visits scheduled at 8, 22, 36 and 52 weeks after randomisation, thus at least 5 times, by the study physician and the vascular nurse. Emerging hypertension and diabetes was treated using predefined protocols. Hypertension was treated with salt restriction and step-up pharmacological therapy starting with hydrochlorothiazide 12,5mg followed by treatment with ACE inhibition. Diabetes did not emerge but would have been treated with metformin.

Magnetic Resonance Imaging Protocols

Carotid artery imaging

Magnetic resonance imaging was performed on a 3Tesla scanner (Philips, Achieva, Best, The Netherlands) using a standard Philips SENSE-flex-M surface coil as previously described.¹⁷ In brief, the left carotid artery was examined in all subjects. After localization of the vessel using fast gradient echo sequence surveys, a total of ten contiguous transverse slices were acquired from the carotid bifurcation covering 2 cm of the carotid bulb and the common carotid artery from the flow-divider in the proximal (caudal) direction (Figure 1). A dual inversion recovery

Figure 1. Contiguous transverse slices acquired by 3T MRI for the assessment of carotid vessel wall characteristics.



The top five slices cover 1 cm of the common carotid artery. The bottom five slices cover the carotid bulb.

(black-blood), spoiled segmented k-space fast gradient echo sequence with spectral selective fat suppression was used for image acquisition using the following parameters: echo time 3.6 ms, repetition time (TR) 12 ms, pulse angle 45 degrees, and 2 signal averages were performed. A reinversion slice thickness of 3 mm was used. The field of view was 140 mm. With a matrix size of 306, a voxel size of 0.46mm x 0.46mm x 2mm was obtained. Each MR study took approximately 30 minutes depending on the cardiac frequency. All images were analysed, using VesselMASS software package allowing for a semi-automated quantification of various descriptive parameters of the vessel.

Adipose tissue imaging

Adipose tissue imaging was performed as previously described.¹⁸ Subjects were positioned in a supine position. The body coil was used for obtaining the images. A sagittal single shot gradient echo sequence survey scan was used for the imaging of the vertebral column in the lumbar region. Subsequently, a second single shot gradient echo sequence in the transversal plane was used for obtaining three contiguous slices of 10mm without angulations. The slices were centred at the intervertebral disk level between the 4th and 5th lumbar vertebra. The following parameters were used for image acquisition: echo time 3.7 ms (TE), repetition time 7.5 (TR), pulse angle 45 degrees, and 2 signal averages were performed. The images were obtained with 3 breath holds of 6 seconds. The field of view was 500mm. A voxel size of 1mm x 1.3mm x 10mm was obtained. Subcutaneous (SAT) and visceral adipose tissue (VAT) areas were quantified using MASS software package.

Study outcomes

The predefined primary outcome was the change from baseline in MRI assessed total vessel wall area of the carotid artery defined as the sum of cross-sectional areas of the carotid bulb and adjacent part of the common carotid artery. The anatomical hallmark used was the most proximal separation between the internal and external carotid artery which is called "flow-divider"

in ultrasonographic literature. From this point, total vessel wall area was calculated from ten contiguous transverse slices covering 2cm of the carotid bulb and the most distal part of the common carotid artery. Secondary outcomes were other MRI measurements of the carotid bulb and common carotid artery including the change in maximum vessel wall thickness. In addition, differences in anthropometric and laboratory measures were assessed.

Statistical analysis

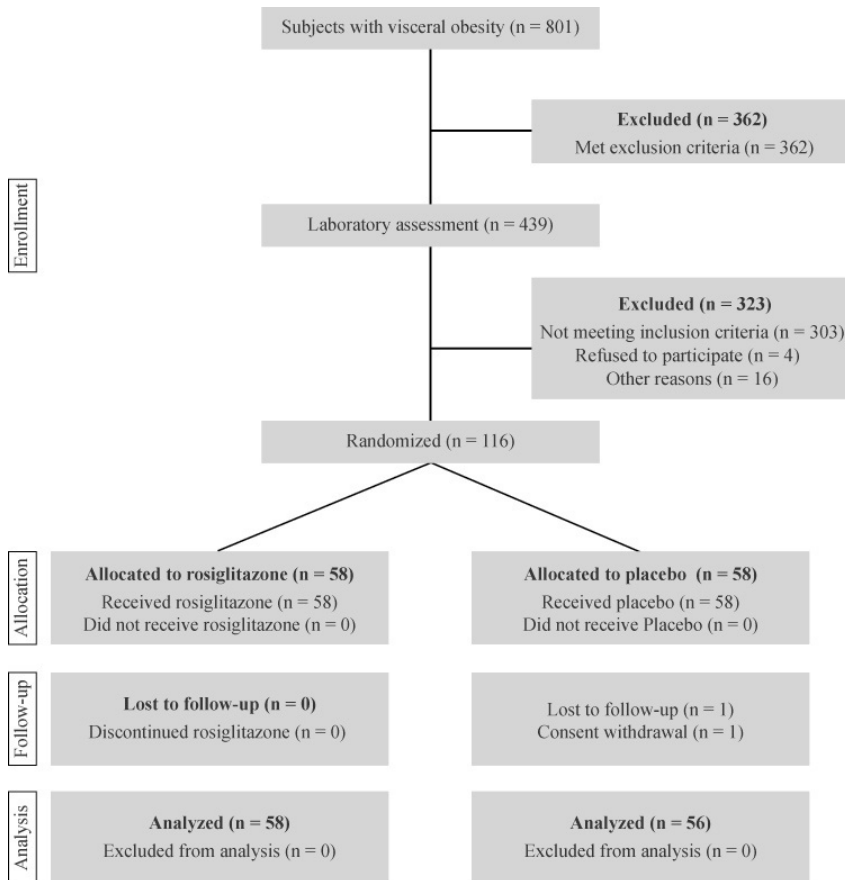
A total of 53 patients were required in each study group to provide a statistical power of 90% to detect a difference of 7mm² in change of total vessel wall area between the two groups within 52 weeks, assuming a standard deviation of 11mm² and a two sided α of 0.05. These sample size calculations were based on previously published MRI measured vessel wall data.¹⁹ In that study, a 7 mm²(SD 11) decrease from baseline was reported in vessel wall area after 12 months of treatment. Assuming a correlation of 0.5 between baseline and measurements after 12 months within individuals, the SD of change would also be 11. To allow for a dropout of 8%, the total sample size was calculated to be 116 patients.

Continuous variables are presented as mean values \pm standard deviation or as medians and interquartile ranges if the assumption of normality was not met. Categorical variables are presented as frequencies(percentages). To calculate the difference between study groups in changes from baseline we used independent samples *t* tests for continuous variables or Mann-Whitney *U* tests when data were not normally distributed. Analyses were two sided, with a *P* value of 0.05 considered to indicate statistical significance. All analyses were performed on an intention-to-treat basis. We used last observation carried forward approach for the one patient not completing the full follow-up period. Statistical analyses were performed with SPSS software, version 16.0. (SPSS, Chicago, Illinois, USA)

RESULTS

Inclusion and treatment

The study was conducted between September 2005 and August 2007. A total of 801 subjects with visceral obesity underwent screening. Of these subjects, 116 subjects underwent randomisation, with 58 patients to the rosiglitazone-lifestyle group and 58 patients to the placebo-lifestyle group (Figure 2). The intention-to-treat population consisted of these patients. Two patients did not complete the trial. One subject was lost to follow-up, and one withdrew consent during the course of the treatment. The study was prematurely ended in one participant after 46 weeks due to a planned total hip replacement operation. MRI was performed at 46 weeks in this patient. Compliance in the rosiglitazone-lifestyle (95.6%) and placebo-lifestyle (96.6%) group was high and did not significantly differ (*P*=0.27). Dose reduction of the study medication

Figure 2. Enrolment and Follow-up.

to 1 tablet daily was necessary in two patients after complaints of dizziness. The mean duration of treatment was 53.7 weeks for rosiglitazone-lifestyle vs. 53.2 weeks for the placebo-lifestyle group ($P=0.2$). Demographic and clinical characteristics of the patients are listed in table 1. No statistically significant differences were observed between the groups regarding age, waist circumference, systolic and diastolic blood pressure, and laboratory values. Non of the patients received statins. The classes of anti-hypertensive medication used did not vary significantly between the groups.

Anthropometry and laboratory results

Table 2 summarizes anthropometry and laboratory values for all patients. After 52 weeks, waist circumference decreased from 110[102 to 116.5]cm to 99,5[93.3 to 107]cm in the placebo-lifestyle group and from 107.5[101 to 116.5]cm to 99[92.8 to 106.5]cm in the rosiglitazone-lifestyle group ($P=0.18$). The reduction in body weight was significantly higher ($P=0.047$) in placebo

Table 1. Baseline characteristics

Characteristic/variable	Placebo-lifestyle (n=58)	Rosiglitazone-lifestyle (n=58)	P-value
Age (years)	59.6 ±5.0	58.4 ±5.3	0.38
Family history CVD	14 (24%)	13 (22%)	0.83
Current Smoking	14 (24%)	13 (22%)	0.83
Anthropometry			
Bodyweight (kg)*	97.0 [86.2 to 105.4]	97.2 [86.9 to 107.5]	0.66
BMI (kg/m ²)	30.5 ±3.7	30.0 ±3.5	0.46
Waist circumference (cm)*	110.0 [102.0 to 116.5]	107.5 [101.0 to 116.5]	0.50
Blood pressure			
Systolic (mmHg)	148.7 ±16.9	152.5 ±16.8	0.23
Diastolic (mmHg)	88.7 ±9.2	90.8 ±9.0	0.23
Laboratory values			
Cholesterol (mmol/l)	5.81±0.94	5.72±0.86	0.48
HDL (mmol/l)*	1.24 [1.04 to 1.47]	1.29 [1.07 to 1.50]	0.61
LDL (mmol/l)	3.70±0.78	3.56±0.73	0.33
Triglycerides (mmol/l)*	1.79 [1.38 to 2.31]	1.71 [1.12 to 2.32]	0.58
Glucose (mmol/l)*	5.15 [5.00 to 5.70]	5.20 [4.68 to 5.80]	0.30
Insulin (μU/mL)*	11.0 [7.5 to 16.0]	12.0 [7.0 to 17.0]	0.81
Insulin resistance*	1.5 [1.1 to 2.1]	1.5 [0.9 to 2.1]	0.82
C-reactive protein(mg/L)*	2.91 [1.87 to 4.20]	2.59 [1.61 to 4.17]	0.38
Medication			
Statins (%)	0 (0%)	0 (0%)	1
B-blocker (%)	10 (17%)	6 (10%)	0.28
Diuretics (%)	3 (5%)	5 (9%)	0.46
ACE-inhibitor (%)	4 (7%)	4 (7%)	1
AT2-anatgonist (%)	5 (9%)	6 (10%)	0.75
Ca-antagonist (%)	5 (9%)	2 (3%)	0.24

Plus-minus data are means±(SD). *: data presented as median (interquartile range)

WCR: Waist circumference

Insulin resistance index as calculated using HOMA-IR

treated subjects compared to the rosiglitazone group. Reductions in insulin resistance and C-reactive protein levels did not significantly differ between the groups. Total cholesterol levels decreased in placebo treated patients from 5.81±0.94mmol/L to 5.48±0.95mmol/L (P=0.003), and increased in rosiglitazone treated patients from 5.72±0.86 to 5.92±0.99mmol/L (P=0.12). HDL-cholesterol levels increased significantly more in the rosiglitazone treated group. None of the participants developed DM2 during the course of the study.

Table 2. Anthropometry, blood pressure and Levels of laboratory measurements after 52 weeks of treatment with changes from baseline

Characteristic/Variable	Placebo-lifestyle (n=56)	Rosiglitazone-lifestyle (n=58)	P-value
Level at 52 weeks			
Anthropometry			
Bodyweight (kg)*	87.7 [79.5 to 96.6]	91.1 [81.5 to 100.6]	0.20
BMI (kg/m ²)	28.0 ±3.2	28.5 ±3.5	0.43
Waist circumference(cm)*	99.5 [93.3-107.0]	99 [92.8-106.5]	0.98
Blood pressure			
Systolic (mmHg)	137.0 ±14.5	135.7 ±12.2	0.61
Diastolic (mmHg)	79.5 ±6.5	79.3 ±7.0	0.89
Laboratory values			
Cholesterol (mmol/l)	5.48 ±0.95	5.92 ±0.99	0.017
HDL (mmol/l)*	1.29 [1.09-1.52]	1.44 [1.21-1.65]	0.12
LDL (mmol/l)	3.58 ±0.82	3.73 ±0.87	0.36
Triglycerides (mmol/l)*	1.18 [0.86 to 2.04]	1.21 [0.79 to 1.81]	0.60
Glucose (mmol/l)*	4.85 [4.50 to 5.30]	4.8 [4.4 to 5.2]	0.45
Insulin (μU/mL)*	6.50 [4.00 to 10.75]	6.00 [3.00 to 8.00]	0.20
Insulin resistance*	0.80 [0.50 to 1.30]	0.70 [0.40 to 1.10]	0.35
C-reactive protein(mg/L)*	2.29 [1.55 to 3.99]	1.10 [0.65 to 2.55]	0.003
Change from baseline			
Anthropometry			
Body weight (kg)*	-7.1 [-10.6 to -3.1]	-5.3 [-8.2 to -1.2]	0.047
BMI (kg/m ²)	-2.5 ±2.0	-1.6 ±1.5	0.009
Waist circumference (cm)*	-8.8 [-13.0 to -5.0]	-7.5 [-11.0 to -3.9]	0.18
Blood pressure			
Systolic (mmHg)	-11.91 ±14.05	-16.81 ±15.62	0.08
Diastolic (mmHg)	-9.26 ±7.81	-11.43 ±9.16	0.17
Laboratory values			
Cholesterol (mmol/l)	-0.34 ±0.82	0.20 ±0.92	0.002
HDL (mmol/l)*	0.06 [-0.06 to 0.15]	0.13 [0.03 to 0.26]	0.02
LDL (mmol/l)	-0.07 ±1.05	0.17 ±0.92	0.20
Triglycerides (mmol/l)*	-0.64 [-0.93 to -0.04]	-0.38 [-0.85 to -0.01]	0.50
Glucose (mmol/l)*	-0.45 [0.95 to 0.0]	-0.40 [-0.85 to 0.0]	0.80
Insulin (μU/mL)*	-4.0 [-8.8 to -1.0]	-6.0 [-9.5 to -1.5]	0.15
Insulin resistance*	-0.70 [-0.60 to -0.20]	-0.8 [-1.4 to -0.2]	0.58
C-reactive protein(mg/L)*	-0.53 [-1.95 to 0.61]	-0.87 [-2.23 to -0.26]	0.22

Plus-minus data are means±(SD). * data presented as median (interquartile range). Insulin resistance index as calculated using HOMA-IR

Magnetic resonance imaging

At baseline, visceral adipose tissue (VAT), subcutaneous adipose tissue (SAT) at the waist and the gluteofemoral region were not different between the rosiglitazone-lifestyle and the

Table 3. Measures of Magnetic Resonance imaging of the Carotid Artery

Variable	Placebo-lifestyle	Rosiglitazone-lifestyle	P-Value
At baseline			
No. of patients	58	58	
Vessel wall area (cm ²)			
Total	4.56 [4.16 to 5.09]	4.52 [3.80 to 5.34]	0.85
Common carotid artery	1.82 [1.52 to 2.05]	1.69 [1.46 to 1.98]	0.28
Carotid Bulb	2.74 [2.35 to 3.09]	2.82 [2.34 to 3.26]	0.58
Maximal vessel wall thickness (mm)			
Common carotid artery	1.64 [1.46 to 1.83]	1.48 [1.36 to 1.75]	0.03
Carotid Bulb	2.06 [1.82 to 2.47]	2.09 [1.86 to 2.57]	0.88
At 52 weeks			
No. of patients	56	58	
Vessel wall area (cm ²)			
Total	4.53 [3.99 to 5.15]	4.63 [3.99 to 5.31]	0.39
Common carotid artery	1.78 [1.51 to 1.99]	1.69 [1.46 to 2.09]	0.85
Carotid Bulb	2.73 [2.39 to 3.01]	2.87 [2.40 to 3.35]	0.20
Maximal vessel wall thickness (mm)			
Common carotid artery	1.59 [1.48 to 1.75]	1.57 [1.44 to 1.73]	0.53
Carotid Bulb	2.09 [1.88 to 2.31]	2.11 [1.91 to 2.42]	0.61
Difference from baseline at 52 weeks			
Vessel wall area (cm ²)			
Total	0.001 [-0.25 to 0.20]	0.040 [-0.24 to 0.38]	0.19
Common carotid artery	-0.002 [-0.12 to 0.07]	0.035 [-0.06 to 0.15]	0.17
Carotid Bulb	-0.039 [-0.21 to 0.14]	0.040 [-0.17 to 0.19]	0.18
Maximal vessel wall thickness (mm)			
Common carotid artery	-0.009 [-0.08 to 0.10]	0.071 [-0.06 to 0.16]*	0.16
Carotid Bulb	-0.005 [-0.20 to 0.18]	0.036 [-0.16 to 0.17]	0.53

Data presented as median (interquartile range).

*: Significant increase within the group after one year treatment ($p < 0.05$).

placebo-lifestyle group. Median(IQR) VAT significantly decreased in the rosiglitazone-lifestyle treated patients from 460.5[348.9 to 602.1]cm² to 329.3[263.1 to 499.7]cm², and from 478.8[375 to 617.9]cm² to 346.5[283.1 to 445.4]cm² in the placebo-lifestyle group($P < 0.001$). The difference between the groups was not statistically significant($P = 0.37$). Waist SAT and gluteofemoral SAT decreased with -15.2[-91.5 to 31.7]cm² and -35.2[-100.3 to 22.35]cm² in the rosiglitazone-lifestyle group and with -82.8[-158.8 to -33.1]cm² and -84[-160.8 to -36.9]cm² in the placebo-lifestyle group. The change in waist SAT and gluteofemoral SAT after 52 weeks was significantly different between the groups($P < 0.001$).

Table 3 summarizes the results of measurements of the magnetic resonance imaging of the carotid artery. Baseline measures of carotid atherosclerosis were not different between the groups, except for a higher maximum vessel wall thickness in the common carotid artery in the placebo group ($P=0.03$).

Primary Outcome Measure. The primary outcome, the change from baseline of the median(IQR) change in carotid-artery total vessel wall area was $0.04[-0.24 \text{ to } 0.38]\text{cm}^2$ in the rosiglitazone-lifestyle group and $0.001[-0.25 \text{ to } 0.20]\text{cm}^2$ in the placebo-lifestyle group. The difference did not reach statistical significance ($P=0.19$).

Secondary Outcome Measure. The median(IQR) maximum vessel wall thickness of the common carotid artery significantly increased by $0.071[-0.06 \text{ to } 0.16]\text{mm}$ in the rosiglitazone-lifestyle group from $1.48[1.36-1.75]\text{mm}$ to $1.57[1.44-1.73]\text{mm}$ ($P=0.04$). Maximum vessel wall thickness of the common carotid artery non-significantly decreased $-0.009[-0.08 \text{ to } 0.10]\text{mm}$ in the placebo-lifestyle group from $1.64[1.46-1.83]\text{mm}$ at baseline to $1.59[1.48-1.75]\text{mm}$ ($P=0.6$). The difference between the groups did not reach statistical significance ($P=0.16$). For all other measures of carotid atherosclerosis, including common carotid artery vessel wall area and maximal vessel wall thickness, and carotid bulb vessel wall area no differences were observed between rosiglitazone-lifestyle and placebo-lifestyle treated patients.

Clinical adverse events

No cardiovascular events or interventions occurred during the treatment period. There were 4 hospital admissions in each of the groups, none of which under acute circumstances. There were 9 cases of new or increased oedema in the placebo group compared to 12 in the rosiglitazone group ($p=0.45$). Two patients were registered with complaints of dizziness in the rosiglitazone group compared to none in the placebo. In 3 patients of the placebo group ECG changes were seen at the end of study visit compared to none in the rosiglitazone group. Exercise testing was normal in all three patients. Six cases of infections were registered in the placebo group during the treatment period compared to 2 in the rosiglitazone group. There were 2 other registered clinical adverse events in the placebo group compared to 6 in the rosiglitazone treated patients.

DISCUSSION

The results of our study showed that the addition of rosiglitazone to intensive lifestyle therapy did not prevent the progression of atherosclerosis in non-diabetic patients with visceral obesity and elevated C-reactive protein levels. The primary outcome, the change in carotid artery median total vessel wall area, did not significantly differ between the two study groups, nor did the secondary outcome measures.

There are at least three possible explanations for the absence of an additional effect on MRI measured carotid-artery vessel wall measures in patients receiving rosiglitazone: a lack of vascular benefit conferred by rosiglitazone, the potential beneficial effects of lifestyle therapy on the vascular wall concealing a possible effect of rosiglitazone, and the inability of the measurement technique to accurately reflect changes in atherosclerotic burden.

The first explanation to consider is that the pharmacological effects of rosiglitazone, including improved insulin resistance and lowering of elevated CRP levels, is ineffective for slowing atherosclerosis in non-diabetic patients with visceral obesity and elevated CRP. This is in line with the observation published, while our study was ongoing, that rosiglitazone treatment did not reduce carotid-artery intima media thickness progression in insulin resistant patients without DM2.¹⁴ Although this population predominantly consisted of females, the baseline characteristics were very similar to that of our study population. This study together with our now reported data are in sharp contrast to previously published data in patients with DM2. Rosiglitazone and other PPAR- γ agonists significantly reduced carotid-artery intima media thickness progression in patients with DM2.^{14, 20-23} . Pioglitazone, a partial PPAR gamma agonist was also recently shown to lower the rate of progression of coronary atherosclerosis compared with glimepiride in diabetic patients.²⁴

However, comparing the results of our study with previous studies in insulin resistant and diabetic patients is complicated by the fact that we assigned lifestyle therapy to all patients. Intensive lifestyle therapy is the first recommended step in the treatment of patients with the metabolic syndrome. We argued it mandatory to assess the effect of rosiglitazone in addition to measures improving lifestyle. Thus, all patients were instructed to increase their level of daily exercise. In addition, all patients were advised to restrict their dietary caloric intake. Frequent counselling by a vascular nurse trained in lifestyle therapy was used to reinforce the measures taken in every patient. The lifestyle intervention was successful as measured by anthropometric and laboratory values. Bodyweight and waist circumference decreased with 7.1kg and 8.8cm respectively in placebo-lifestyle treated patients. Blood pressure improved by 11.9/9.3mmHg. In addition, insulin resistance and CRP levels improved. The beneficial effects of lifestyle were underlined by the MRI measurements of visceral and subcutaneous adipose tissue depots. In comparison with rosiglitazone-lifestyle treated patients, placebo-lifestyle treated patients lost more subcutaneous adipose fat. Intriguingly, the primary endpoint, which was the change in carotid-artery median vessel wall area, increased only by 0.001cm² in the placebo-lifestyle treated patients. Of the secondary endpoints, maximal vessel wall thickness did not change. Thus, it seemed that intensive lifestyle therapy resulted in remarkable cardiometabolic improvements that associate with stable measures of carotid-artery vessel wall characteristics during the 52 weeks follow-up. These observations suggest that intensive lifestyle treatment may prevent the progression of atherosclerosis in visceral obese patients with elevated CRP levels.

Nevertheless, the observations now reported may be the result of the inability of MR black blood carotid-artery vessel wall imaging to show differences within a 52 weeks follow-up period. This argument should receive serious attention as MRI as an intermediate endpoint to assess changes in atherosclerotic burden is not as established as for instance carotid-artery intima media thickness measurements by ultrasonography. Although MRI is known to reflect histologic differences in the carotid-artery, and we powered our study on previous published reports¹⁹, and we published the reproducibility of our test characteristics¹⁷, we cannot deny this is the first study using this technique in the setting of a randomised controlled trial for assessing atherosclerotic burden in visceral obese men with elevated CRP levels.

The present observations are of interest in the context of the ongoing debate regarding the cardiovascular safety of rosiglitazone treatment, particularly as little is known on the influence of rosiglitazone on early atherosclerosis. Recent meta-analyses related rosiglitazone treatment to an increased risk of myocardial infarction and possible cardiovascular mortality.^{25,26} An interim analysis of the RECORD study, however, showed no evidence of any increase in death from cardiovascular causes in association with rosiglitazone treatment.²⁷ Such discrepancies have also been reported with regard to the effects of rosiglitazone on the progression of atherosclerosis, suggesting varying effects in different populations. In line with these observations, European health authorities (EMA) have recommended additional caution in prescribing rosiglitazone in patients with ischemic heart disease and peripheral artery disease.

In conclusion, our study showed that the addition of rosiglitazone to lifestyle therapy did not prevent the progression of atherosclerosis in non-diabetic patients with visceral obesity and elevated C-reactive protein levels. Of the possible explanations discussed a lack of vascular benefit conferred by rosiglitazone when given in addition to the beneficial effects of lifestyle therapy could be a valid point. Although the 3T MRI measurement technique needs further validation as a surrogate measure for atherosclerotic burden its potential remains high after this study that raised data useful for the calculation of the statistical power for future trials. Finally, this study underlines the impressive impact of lifestyle therapy on many clinical features in male visceral obese patients with elevated CRP levels.

Acknowledgements:

This investigator initiated study was partially supported by an unconditional grant from Glaxo-SmithKline.

Disclosures:

No conflicts of interest

REFERENCE LIST

1. Yusuf S, Hawken S, Ounpuu S et al. Obesity and the risk of myocardial infarction in 27,000 participants from 52 countries: a case-control study. *Lancet* 2005 November 5;366(9497):1640-9.
2. Ridker PM. Clinical application of C-reactive protein for cardiovascular disease detection and prevention. *Circulation* 2003 January 28;107(3):363-9.
3. Pischon T, Boeing H, Hoffmann K et al. General and abdominal adiposity and risk of death in Europe. *N Engl J Med* 2008 November 13;359(20):2105-20.
4. Pan XR, Li GW, Hu YH et al. Effects of diet and exercise in preventing NIDDM in people with impaired glucose tolerance. The Da Qing IGT and Diabetes Study. *Diabetes Care* 1997 April;20(4):537-44.
5. Tuomilehto J, Lindstrom J, Eriksson JG et al. Prevention of type 2 diabetes mellitus by changes in lifestyle among subjects with impaired glucose tolerance. *N Engl J Med* 2001 May 3;344(18):1343-50.
6. Knowler WC, Barrett-Connor E, Fowler SE et al. Reduction in the incidence of type 2 diabetes with lifestyle intervention or metformin. *N Engl J Med* 2002 February 7;346(6):393-403.
7. Ornish D, Scherwitz LW, Billings JH et al. Intensive lifestyle changes for reversal of coronary heart disease. *JAMA* 1998 December 16;280(23):2001-7.
8. Haskell WL, Alderman EL, Fair JM et al. Effects of intensive multiple risk factor reduction on coronary atherosclerosis and clinical cardiac events in men and women with coronary artery disease. The Stanford Coronary Risk Intervention Project (SCRIP). *Circulation* 1994 March;89(3):975-90.
9. Yki-Jarvinen H. Thiazolidinediones. *N Engl J Med* 2004 September 9;351(11):1106-18.
10. Lebovitz HE, Dole JF, Patwardhan R, Rappaport EB, Freed MI. Rosiglitazone monotherapy is effective in patients with type 2 diabetes. *J Clin Endocrinol Metab* 2001 January;86(1):280-8.
11. Mohanty P, Aljada A, Ghanim H et al. Evidence for a potent antiinflammatory effect of rosiglitazone. *J Clin Endocrinol Metab* 2004 June;89(6):2728-35.
12. Kahn SE, Haffner SM, Heise MA et al. Glycemic durability of rosiglitazone, metformin, or glyburide monotherapy. *N Engl J Med* 2006 December 7;355(23):2427-43.
13. Viljanen AP, Virtanen KA, Jarvisalo MJ et al. Rosiglitazone treatment increases subcutaneous adipose tissue glucose uptake in parallel with perfusion in patients with type 2 diabetes: a double-blind, randomized study with metformin. *J Clin Endocrinol Metab* 2005 December;90(12):6523-8.
14. Hedblad B, Zambanini A, Nilsson P, Janzon L, Berglund G. Rosiglitazone and carotid IMT progression rate in a mixed cohort of patients with type 2 diabetes and the insulin resistance syndrome: main results from the Rosiglitazone Atherosclerosis Study. *J Intern Med* 2007 March;261(3):293-305.
15. Khera A, McGuire DK, Murphy SA et al. Race and gender differences in C-reactive protein levels. *J Am Coll Cardiol* 2005 August 2;46(3):464-9.
16. Alberti KG, Zimmet P, Shaw J. Metabolic syndrome—a new world-wide definition. A Consensus Statement from the International Diabetes Federation. *Diabet Med* 2006 May;23(5):469-80.
17. Alizadeh DR, Doornbos J, Tamsma JT et al. Assessment of the carotid artery by MRI at 3T: a study on reproducibility. *J Magn Reson Imaging* 2007 May;25(5):1035-43.
18. Alizadeh DR, de RA, Rabelink TJ et al. Elevated CRP levels are associated with increased carotid atherosclerosis independent of visceral obesity. *Atherosclerosis* 2008 October;200(2):417-23.
19. Corti R, Fayad ZA, Fuster V et al. Effects of lipid-lowering by simvastatin on human atherosclerotic lesions: a longitudinal study by high-resolution, noninvasive magnetic resonance imaging. *Circulation* 2001 July 17;104(3):249-52.
20. Stocker DJ, Taylor AJ, Langley RW, Jezior MR, Vigersky RA. A randomized trial of the effects of rosiglitazone and metformin on inflammation and subclinical atherosclerosis in patients with type 2 diabetes. *Am Heart J* 2007 March;153(3):445-6.
21. Minamikawa J, Tanaka S, Yamauchi M, Inoue D, Koshiyama H. Potent inhibitory effect of troglitazone on carotid arterial wall thickness in type 2 diabetes. *J Clin Endocrinol Metab* 1998 May;83(5):1818-20.
22. Mazzone T, Meyer PM, Feinstein SB et al. Effect of pioglitazone compared with glimepiride on carotid intima-media thickness in type 2 diabetes: a randomized trial. *JAMA* 2006 December 6;296(21):2572-81.

23. Nakamura T, Matsuda T, Kawagoe Y et al. Effect of pioglitazone on carotid intima-media thickness and arterial stiffness in type 2 diabetic nephropathy patients. *Metabolism* 2004 October;53(10):1382-6.
24. Nissen SE, Nicholls SJ, Wolski K et al. Comparison of pioglitazone vs glimepiride on progression of coronary atherosclerosis in patients with type 2 diabetes: the PERISCOPE randomized controlled trial. *JAMA* 2008 April 2;299(13):1561-73.
25. Nissen SE, Wolski K. Effect of rosiglitazone on the risk of myocardial infarction and death from cardiovascular causes. *N Engl J Med* 2007 June 14;356(24):2457-71.
26. Singh S, Loke YK, Furberg CD. Long-term risk of cardiovascular events with rosiglitazone: a meta-analysis. *JAMA* 2007 September 12;298(10):1189-95.
27. Home PD, Pocock SJ, Beck-Nielsen H et al. Rosiglitazone evaluated for cardiovascular outcomes--an interim analysis. *N Engl J Med* 2007 July 5;357(1):28-38.

CHAPTER

8

Rosiglitazone plus lifestyle therapy increases CD34+ cells in men with visceral obesity and elevated C-reactive protein

Reza Alizadeh Dehnavi MD¹, Hetty C. de Boer PhD², Lihui Hu MD¹, Albert de Roos MD PhD³, Hein Putter PhD⁴, Ton J. Rabelink MD PhD², Johannes A. Romijn MD PhD¹, Anton-Jan van Zonneveld PhD², Jouke T. Tamsma MD PhD¹

¹Section of Vascular Medicine, Department of Endocrinology & Internal Medicine, Leiden University Medical Centre, Leiden, The Netherlands

²Department of Nephrology & Einthoven Laboratory, Leiden University Medical Centre, Leiden, The Netherlands

³Department of Radiology, Leiden University Medical Centre, Leiden, The Netherlands

⁴Department of Statistics and Bio-Informatics, Leiden University Medical Centre, Leiden The, Netherlands

Submitted

ABSTRACT

Objective

Patients with visceral obesity and elevated C-reactive protein (CRP) levels are regarded at increased cardiovascular risk even in the absence of type 2 Diabetes Mellitus (DM2). Circulating endothelial progenitor cells are thought to reflect cardiovascular risk and their counts are reduced in association with inflammation and cardiovascular risk factors. Since rosiglitazone has anti-inflammatory potential, we hypothesized it would improve circulating progenitor cell profiles in men with visceral obesity (VO) and elevated C-reactive protein levels when given in addition to intensive lifestyle treatment.

Methods

We conducted a double blind, placebo controlled, randomized 52 weeks trial comparing the effects of daily therapy with 8 mg rosiglitazone plus intensive lifestyle therapy or placebo plus intensive lifestyle therapy in 45 non-diabetic men with visceral obesity and CRP levels of 1.8 mg/L or higher. The primary outcome measures were the difference between the groups in CD34+ and CD34+KDR+ cells as quantified by fluorescence-activated cell sorter analysis after appropriate staining and gating. MRI was used to assess adipose tissue distribution.

Results

The first outcome measure, the median change[interquartile range (IQR)] from baseline in CD34+ cells, was 0.654[0.033 to 1.083]/ μ L in the rosiglitazone-lifestyle group and 0.142[-0.470 to 0.426]/ μ L in placebo-lifestyle group. The difference between the groups was statistically significant ($P=0.03$). For CD34+KDR+ cells, the median (IQR) change was 0.001[-0.024 to 0.020]/ μ L in the rosiglitazone-lifestyle group and -0.002 [-0.025 to 0.017]/ μ L in placebo-lifestyle group ($p=0.62$). Rosiglitazone-lifestyle and placebo-lifestyle reduced median [IQR] waist circumference by -9.0[-15.0 to -4.0]cm and -10.5[-15.5 to -5.0]cm and median [IQR] CRP levels by -1.12[-2.22 to -0.16] and -0.19[-1.52 to 1.91]mg/L, respectively. MRI assessment of fat stores revealed significant higher decreases in waist and hip subcutaneous fat stores in placebo-lifestyle treated patients.

Conclusions

Rosiglitazone significantly increased circulating CD34+ cell counts when given on top of intensive lifestyle therapy in men with visceral obesity and elevated C-reactive protein levels compared to placebo. No effect of rosiglitazone was observed for CD34+KDR+ cells.

INTRODUCTION

Endothelial progenitor cells (EPC) are thought to reflect vascular damage.¹⁻⁴ They are shown to improve endothelial function, promote vascular repair, and to induce neovascularization.⁵⁻⁷ Significantly lower numbers of EPCs were reported in patients with insulin resistance and the metabolic syndrome (MS).^{8,9} Lower EPC numbers and impaired functional activity have been shown in patients with type 2 diabetes mellitus (DM2).^{2, 10, 11} Furthermore, cell counts were found to be decreased in chronic inflammatory diseases such as rheumatoid arthritis.¹² Taken together, circulating endothelial progenitor cells are interesting potential intermediate cardiovascular endpoints. They are related to metabolic derangements such as insulin resistance, and systemic inflammation^{13, 14} on the one hand, but also reflect vascular damage on the other.¹⁻⁴

Visceral obesity (VO) and elevated C-reactive protein levels, are independent risk factors for myocardial infarction¹⁵ and cardiovascular mortality.^{16, 17} The first step in the treatment of subjects with visceral obesity is lifestyle therapy. Although lifestyle interventions are known to result in significant improvements in progenitor cell profiles¹⁸⁻²⁰, these effects have not been studied in non-diabetic visceral obese patients with elevated CRP levels. In addition to intensive lifestyle therapy, medication that alters fat distribution, increases insulin sensitivity and decrease systemic inflammation may have additive potential in improving progenitor cell profiles. Rosiglitazone is a peroxisome-proliferator-activated receptor γ (PPAR γ) agonist that alters fat distribution and modulates metabolic and inflammatory gene repertoires.²¹ More specifically, it increases insulin sensitivity, redistributes fat from visceral to peripheral stores and decreases CRP levels.^{22, 23} Given these characteristics, we hypothesized that rosiglitazone would improve progenitor cell profiles in men with visceral obesity and elevated C-reactive protein levels, when given in addition to intensive lifestyle therapy.

In this study, we sought to determine whether the daily administration of 8 mg of rosiglitazone in combination with intensive lifestyle therapy would improve CD34+ and CD34+KDR+ cell counts in non-diabetic patients with visceral obesity and elevated CRP levels. We assessed these cells in a predefined sub-study of our study called "A 52 week double-blind randomized controlled trial comparing the effect of Rosiglitazone versus placebo on the prevention of progression of atherosclerosis in high risk patients without diabetes (RUBENS) trial".

MATERIALS AND METHODS

Study design

This prospective randomized double-blind placebo controlled trial was performed at LUMC, Leiden, The Netherlands as a single center study. Patients provided written informed consent.

The study was approved by the institutional review committee and conducted according to the principles expressed in the Declaration of Helsinki. Men of 50 years or older were eligible to participate in the study if a waist circumference ≥ 94 cm and a CRP levels of 1.8 mg/L or higher was present. The cut-off value of 1.8mg/L for CRP was chosen based on the previously reported median of CRP in males in a large epidemiological study.²⁴ Additional inclusion criteria were the presence of either at least two other metabolic syndrome criteria according to the IDF definition.²⁵ Exclusion criteria included DM2 (fasting blood glucose ≥ 7 mmol/l), manifest cardiovascular disease, smoking, presence of premature cardiovascular disease in a first degree family member, use of statins at baseline, use of steroids or non-steroidal anti-inflammatory drugs at baseline, heart failure (NYSE class I or higher), QTc time interval of 450ms or longer on baseline ECG, primary dyslipidemias, hypoglycaemia, presence of potential hepatic disease (i.e. subjects with ALT, total bilirubin, or alkaline phosphatase levels exceeding 2.5 times the upper limit of the normal laboratory values), risk of non compliance, alcohol abuse (>30 units/week) and MRI contraindications. The study consisted of two periods: the screening phase and a double-blind study period with a scheduled duration of 52 weeks. After the screening phase eligible patients were randomly assigned in a 1:1 ratio to receive either daily therapy with 8 mg of rosiglitazone or placebo. The treatment was titrated. During the first eight weeks of the study, the participants were treated with one tablet daily (rosiglitazone 4mg or placebo). When tolerated, the dosis was doubled after 8 weeks. Randomization was based on computer generated codes. The allocation sequence was generated and kept by the institutional trial pharmacist. All subjects received intensive lifestyle treatment in addition to rosiglitazone or placebo. Subjects were advised to start on a 1500 kCal diet and refrain from smoking. In addition they were encouraged to increase their level of daily physical activity aiming at an extra energy-expenditure of 270 kCal per day (i.e. a normal-pace walk of 30 minutes, three times daily). All subjects were seen at follow-up visits scheduled at 8, 22, 36 and 52 weeks after randomisation, thus at least 5 times, by the study physician and the vascular nurse. Emerging hypertension and diabetes was treated using predefined protocols. Hypertension was treated with salt restriction and step-up pharmacological therapy starting with hydrochlorothiazide 12,5mg followed by treatment with ACE inhibition. Diabetes did not emerge but would have been treated with metformin.

CD34+ and CD34+KDR+ cells

Enumeration of circulating CD34+ and CD34+KDR+ cells was performed as recently described.¹⁸ This method uses Trucount tubes that contain a defined number of brightly fluorescent microbeads, permitting the acquisition of absolute counts of cells, even at very low numbers. Circulating CD34+ cells were defined as cells with low-expression of CD45, positive for CD34, and located in the lympho-gate on a side- and forward-scatter plot. This gating strategy was extended by calculating the number of CD34⁺ cells that also expressed vascular endothelial growth factor receptor-2 (VEGFR-2) to define the number of CD34+KDR+ cells. This strategy

avoids inclusion of mature endothelial cells, which are also positive for CD34 and VEGFR-2, since they are located outside the lympho-gate.

MRI adipose tissue imaging

Magnetic resonance imaging was performed on a 3T scanner (Philips, Achieva, Best, The Netherlands) using the body coil as previously reported.²⁶ In short: After performing the preparatory scans, a single shot gradient echo sequence in the transversal plane was used for obtaining three contiguous slices of 10mm without angulations centered at the intervertebral disk level between the 4th and 5th lumbar vertebra. Images were assessed using the MASS software package allowing quantification of visceral adipose tissue (VAT) and subcutaneous adipose tissue (SAT).

Study outcomes

The predefined primary outcome was the change from baseline in the number of CD34+ and CD34+KDR+ cells after 52 weeks of treatment with either rosiglitazone or placebo in addition to intensive lifestyle treatment. Furthermore, differences in anthropometric and laboratory measures were assessed.

Statistical analysis

Continuous variables are presented as mean values \pm standard deviation or as medians and interquartile ranges if the assumption of normality was not met. Categorical variables are presented as frequencies (percentages). To calculate difference between study groups in changes from baseline we used independent samples *t* tests for continuous variables or Mann-Whitney *U* tests when data were not normally distributed. Comparisons within the groups were performed with paired samples *t* tests or Wilcoxon tests for related samples depending on the distribution. All analyses are two sided, with a *P* value of 0.05 considered to indicate statistical significance. Statistical analyses were performed with SPSS software, version 16.0. (SPSS, Chicago, Illinois, USA)

RESULTS

Inclusion and treatment

The study was conducted between September 2005 and August 2007. A total 45 subjects underwent randomization, with 23 patients to the rosiglitazone-lifestyle group and 22 patients to the placebo-lifestyle group. All subjects completed the study. Compliance in the rosiglitazone-lifestyle (96.8%) and placebo-lifestyle (97.7%) group was high and did not differ (*p*=0.49). Demographic and clinical characteristics of the patients are listed in table 1. No statistically significant differences were observed between the groups regarding age, waist circumference,

Table 1. Baseline characteristics

Characteristic/variable	Placebo-lifestyle (n=22)	Rosiglitazone-lifestyle (n=23)	P-value
Age (years)	58.7 (4.9)	59.9 (5.1)	0.43
Anthropometry			
Bodyweight (kg)	93.1 (86.1 to 102.5)	96.0 (87.8 to 104.0)	0.92
BMI (kg/m ²)	29.9 [28.4 to 32.5]	29.0 [27.4 to 30.8]	0.17
Waist circumference (cm)	109.0 (102.0 to 116.5)	108.0 (101.0 to 113.0)	0.55
Blood pressure			
Systolic (mmHg)	148.3 (15.7)	153.7 (17.3)	0.28
Diastolic (mmHg)	87.6 (7.6)	89.8 (8.4)	0.36
Laboratory values			
Cholesterol (mmol/l)	5.85 (0.92)	5.89 (0.84)	0.889
HDL (mmol/l)	1.28 (0.30)	1.34 (0.25)	0.477
LDL (mmol/l)	3.83 (0.72)	3.69 (0.70)	0.518
Triglycerides (mmol/l)	1.61 (1.11 to 2.00)	1.74 (1.38 to 2.19)	0.301
Glucose (mmol/l)	5.10 (4.90 to 5.83)	5.0 (4.7 to 5.5)	0.245
Insulin (μU/mL)	9.63 (6.00 to 15.25)	9.0 (4.0 to 14.0)	0.509
Insulin resistance	1.40 (1.15 to 2.23)	1.3 (0.6 to 1.9)	0.152
C-reactive protein (mg/L)	2.57 (1.64 to 3.25)	2.46 (2.10 to 3.38)	0.759
MRI adipose tissue distribution			
Waist visceral fat (cm ²)	453.1 [367.3 to 628.0]	403.9 [326.1 to 496.7]	0.19
Waist subcutaneous fat (cm ²)	750.4 [667.7 to 1105.9]	731.0 [692.4 to 923.9]	0.54
Hip subcutaneous fat (cm ²)	592.2 [506.6 to 693.6]	567.1 [512.1 to 707.9]	0.77

systolic and diastolic blood pressure, and laboratory values. None of the patients received statins. The classes of anti-hypertensive medication used did not vary significantly between the groups. None of the participants developed DM2 during the course of the study.

Anthropometry and laboratory results

Table 2 summarizes anthropometry and laboratory values for all patients including changes of the values from baseline. After 52 weeks, waist circumference decreased from 108[101 to 113]cm to 97[92 to 103]cm in the rosiglitazone-lifestyle group and from 109[102 to 116.5]cm to 98[93 to 107.3]cm in the placebo-lifestyle group($P=0.48$). Both systolic and diastolic blood pressures were significantly reduced in within both groups during follow-up ($P\leq 0.001$). For the difference between groups in systolic blood pressure, a trend toward statistical significance was seen ($P=0.06$), while the difference in diastolic blood pressure was not statistically significant ($P=0.15$). LDL-cholesterol levels increased from 3.69 ± 0.70 mmol/L to 4.11 ± 0.79 mmol/L in rosiglitazone-lifestyle treated patients and decreased from 3.83 ± 0.72 mmol/L to 3.56 ± 0.82 mmol/L

Table 2. Anthropometry, blood pressure and Levels of laboratory measurements after 52 weeks of treatment with changes from baseline

	Placebo-lifestyle (n=22)	Rosiglitazone-lifestyle (n=23)	P-value
Level at 52 weeks			
Anthropometry			
Bodyweight (kg)	86.5 (80.5 to 94.3)	90.2 (81.7 to 97.7)	0.42
BMI (kg/m ²)	27.7 [25.3 to 29.8]	27.5 [25.0 to 28.3]	0.47
Waist circumference(cm)	98.0 (93.0 to 107.3)	97.0 (92.0 to 103.0)	0.53
Blood pressure			
Systolic (mmHg)	138.6 (14.4)	135.9 (13.2)	0.52
Diastolic (mmHg)	78.2 (6.9)	78.0 (7.1)	0.56
Laboratory values			
Cholesterol (mmol/l)	5.46 (0.92)	6.24 (0.86)	0.006
HDL (mmol/l)	1.34 (0.30)	1.52 (0.24)	0.03
LDL (mmol/l)	3.56 (0.82)	4.11 (0.79)	0.03
Triglycerides (mmol/l)	1.14 [0.74 to 1.71]	1.22 [0.94 to 1.70]	0.90
Glucose (mmol/l)	4.70 (4.43 to 5.30)	4.80 (4.35 to 5.15)	0.95
Insulin (μU/mL)	4.50 (3.00 to 8.00)	4.50 (3.00 to 7.00)	0.50
Insulin resistance	0.55 (0.40 to 1.00)	0.50 (0.40 to 0.80)	0.44
C-reactive protein(mg/L)	2.42 (0.84 to 4.70)	1.05 (0.59 to 2.08)	0.04
MRI adipose tissue distribution			
Waist visceral fat (cm ²)	313.6 (268.8 to 367.7)	315.40 (228.6 to 372.4)	0.79
Waist subcutaneous fat (cm ²)	684.1 (580.7 to 887.3)	696.5 (593.0 to 876.0)	0.98
Hip subcutaneous fat (cm ²)	500.5[372.1 to 558.2]	521.4[393.6 to 598.4]	0.47
Change from baseline			
Anthropometry			
Body weight (kg)	-8.6 [-13.5 to -2.9]	-6.7 [-8.8 to -0.9]	0.06
BMI (kg/m ²)	-2.7 [-4.4 to -1.0]	-1.9 [-2.5 to -0.3]	0.08
Waist circumference (cm)	-10.5 [-15.5 to -5.0]	-9.0 [-15.0 to -4.0]	0.48
Blood pressure			
Systolic (mmHg)	-9.8 (12.2)	-17.9 (15.9)	0.06
Diastolic (mmHg)	-8.4 (7.1)	-11.9 (8.7)	0.15
Laboratory values			
Cholesterol (mmol/l)	-0.39 (0.65)	0.39 (0.96)	0.003
HDL (mmol/l)	0.05 (0.23)	0.18 (0.15)	0.04
LDL (mmol/l)	-0.27 (0.61)	0.42 (0.86)	0.003
Triglycerides (mmol/l)	-0.32 [-0.81 to 0.06]	-0.44 [-0.85 to -0.22]	0.49
Glucose (mmol/l)	-0.5 [-1.0 to -0.1]	-0.4 [-0.8 to 0.1]	0.54
Insulin (μU/mL)	-4.5 (-7.3 to -1.8)	-4.5 (-8.3 to 0.0)	0.96
Insulin resistance	-0.8 (-1.2 to -0.3)	-0.7 (-1.1 to -0.2)	0.59
C-reactive protein(mg/L)	-0.19 (-1.52 to 1.91)	-1.12 (-2.22 to -0.16)	0.049
MRI adipose tissue distribution			
Waist visceral fat (cm ²)	-147.5 [-256.4 to -50.8]	-86.4 [-173.4 to -27.0]	0.06
Waist subcutaneous fat (cm ²)	-112.0 [-231.9 to -57.5]	-55.2 [-99.4 to 15.2]	0.006
Hip subcutaneous fat (cm ²)	-126.6 [-190.4 to -75.7]	-71.8 [-123.9 to 9.8]	0.02

in placebo-lifestyle treated patients. The difference between the groups was statistically significant ($P=0.003$). HDL-cholesterol levels increased from $1.34\pm0.25\text{mmol/L}$ to $1.52\pm0.24\text{mmol/L}$ in rosiglitazone treated patients and from $1.28\pm0.30\text{mmol/L}$ to $1.34\pm0.30\text{mmol/L}$ in the placebo-lifestyle group. The difference between groups was statistically significant ($P=0.04$). Median[IQR] CRP levels decreased in the rosiglitazone-lifestyle group from $2.46[2.10 \text{ to } 3.38]\text{mg/L}$ to $1.05[0.59 \text{ to } 2.08]\text{mg/L}$ and from $2.57[1.64 \text{ to } 3.25]\text{mg/L}$ to $2.42[0.84 \text{ to } 4.70]\text{mg/L}$ in placebo-lifestyle treated patients. The change in CRP levels of $-1.12 [-2.22 \text{ to } -0.16]\text{mg/L}$ in rosiglitazone treated patients compared to $-0.19 [-1.52 \text{ to } 1.91]\text{mg/L}$ in the placebo group reached borderline statistical significance ($P=0.049$).

CD34+ and CD34+KDR+ cell counts

Table 3 summarizes the results of the cellular endpoints of the study. The cell counts of CD34+ and CD34+KDR+ are given at baseline, after 52 weeks of treatment and the median change from baseline is shown. Rosiglitazone-lifestyle treatment resulted in an increase of median[IQR] CD34+ of $0.654 [0.033 \text{ to } 1.083]/\mu\text{L}$. In placebo-lifestyle treated patients an increase of $0.142 [-0.47 \text{ to } 0.426]/\mu\text{L}$ was observed. The difference in CD34+ between the groups was statistically significant ($p=0.03$). The change in median[IQR] CD34+KDR+ counts were $0.001 [-0.024 \text{ to } 0.020]/\mu\text{L}$ in rosiglitazone-lifestyle treated patients and $-0.002 [-0.025 \text{ to } 0.017]/\mu\text{L}$ in placebo treated patients. This change in CD34+KDR+ between groups did not reach statistical significance.

Table 3. Circulating progenitor cells counts

Variable	Placebo-lifestyle	Rosiglitazone-lifestyle	P-value
At baseline			
No. of patients	22	23	
CD34+KDR+ (number/ μL)	0.028 [0.013 to 0.043]	0.013 [0 to 0.032]	0.07
CD34+ (number/ μL)	1.181 [0.786 to 2.160]	1.311 [0.476 to 1.845]	0.65
At 52 weeks			
No. of patients	22	23	
CD34+KDR+ (number/ μL)	0.016 [0 to 0.057]	0.016 [0 to 0.043]	0.81
CD34+ (number/ μL)	1.475 [0.737 to 2.103]	1.580 [1.052 to 2.707]	0.28
Difference from baseline at 52 weeks			
CD34+KDR+ (number/ μL)	-0.002 [-0.025 to 0.017]	0.001 [-0.024 to 0.020]	0.62
CD34+ (number/ μL)	0.142 [-0.470 to 0.426]	0.654 [0.033 to 1.083]*	0.03

*: Significant increase within the group after one year treatment ($p<0.01$).

MRI adipose tissue distribution

Visceral fat, waist subcutaneous fat and hip subcutaneous fat were very similar at baseline (Table 1). After 52 weeks of treatment, the visceral and subcutaneous adipose tissue did not

significantly differ between groups (Table 2). However, the median [IQR] change of waist subcutaneous adipose tissue had decreased significantly more in the placebo-lifestyle group by -112[-231.9 to -57.5]cm² compared to -55.2 [-99.4 to 15.2]cm² in the rosiglitazone-lifestyle group (P=0.006). Visceral adipose tissue decreased with -147.5 [-256.4 to -50.8]cm² in the placebo-lifestyle group and with -86.4 [-173.4 to -27.0]cm² in the rosiglitazone-lifestyle group (P=0.06).

DISCUSSION

The results of our study demonstrate that the addition of rosiglitazone therapy to intensive lifestyle treatment significantly changed circulating progenitor cell profiles in non-diabetic patients with visceral obesity and elevated C-reactive protein levels. The primary outcome, the change in the number of CD34+ cells after 52 weeks of treatment was significantly increased in rosiglitazone-lifestyle treated patients. The other outcome parameter, the change in CD34+/KDR+ cell counts, did not significantly differ between the groups.

Endothelial progenitor cells are known to correlate with cardiovascular risk factors^{1,2} and have been proposed as surrogate biological markers of vascular function and cardiovascular disease.⁷ In this regard, CD34+ cells are most closely related to cardiovascular risk.⁸ We observed significant increases in CD34+, but not in CD34+/KDR+ cells in response to rosiglitazone therapy in visceral obese male patients with elevated C-reactive protein levels. The available data on the in vivo effects of rosiglitazone on circulating endothelial progenitor cell counts are very limited. In a small, uncontrolled clinical study, 12 weeks of rosiglitazone treatment did not change CD34+ cell counts in recent onset DM2 patients.²⁷ In an experimental mouse model, rosiglitazone treatment was shown to promote the differentiation of bone marrow derived progenitor cells toward the endothelial lineage after the induction of endothelial damage.²⁸ In contrast to the results of our study, treatment with pioglitazone has been shown to increase both CD34+/KDR+, and CD34+ cell counts in patients with coronary artery disease and normal glucose tolerance and in patients with DM2.^{29, 30} Pioglitazone treatment was also shown to improve migratory response, adhesion capacity and colony formation capacity of endothelial progenitor cells.^{29, 30} These data and the results of our study show that PPAR γ agonists could increase CD34+ peripheral blood cell counts. The effects on CD34+KDR+ cells vary depending on the specific PPAR γ agonist used.

Several aspects of our study should be addressed when interpreting the results: the study population, the concomitant effects of lifestyle intervention, and, the duration of the follow-up period. First, our study population consisted of non-diabetic male patients with visceral obesity and elevated CRP levels without manifest cardiovascular disease. Endothelial progenitor cell

response after rosiglitazone treatment has not previously been studied in these patients. In this regard, the current results are additive to previous studies showing effects in non-diabetic patients without manifest cardiovascular disease. Secondly, the effect of rosiglitazone was assessed in addition to lifestyle therapy in our study. Lifestyle therapy is the first treatment step in subjects with visceral obesity. The effects of lifestyle therapy are clearly seen in the placebo-lifestyle arm of our study. Lifestyle intervention resulted in reductions in body weight, waist circumference, blood pressure and some metabolic variables. Lifestyle interventions are known to significantly improve progenitor cell profiles.¹⁸⁻²⁰ We now found that addition of rosiglitazone to effective lifestyle therapy further increased CD34+ cell counts. Finally, the presented observations of our study concern a follow-up period of 52 weeks while earlier reports of both rosiglitazone and pioglitazone concern much shorter follow-up periods. Thus, our study is clearly additive as it provides the effect of long term follow-up to the earlier reports of studies with shorter follow-up periods.

This study has limitations. First, the influence of rosiglitazone independent of lifestyle treatment could not be assessed in our study. Furthermore, all patients in our study were males. The current observations remain to be confirmed in female populations. Current smoking and the presence of premature familial CVD were exclusion criteria in our study due to their known impact on circulating progenitor cells. As a result, the observations of this study can not be extrapolated to subjects with those characteristics. Finally, we only determined CD34+ and CD34+/KDR+ cell counts and did not characterize the functional properties of these cells which may provide valuable additional information in future studies.

In summary, we observed significant increases in CD34+ cell counts in response to rosiglitazone therapy in addition to successful intensive lifestyle treatment in non-diabetic men with visceral obesity and elevated C-reactive protein levels.

Acknowledgments:

This investigator initiated study was partially supported by an unconditional grant from Glaxo-SmithKline.

REFERENCE LIST

1. Vasa M, Fichtlscherer S, Aicher A et al. Number and migratory activity of circulating endothelial progenitor cells inversely correlate with risk factors for coronary artery disease. *Circ Res* 2001 July 6;89(1):E1-E7.
2. Fadini GP, Miorin M, Faccio M et al. Circulating endothelial progenitor cells are reduced in peripheral vascular complications of type 2 diabetes mellitus. *J Am Coll Cardiol* 2005 May 3;45(9):1449-57.
3. Taguchi A, Matsuyama T, Moriwaki H et al. Circulating CD34-positive cells provide an index of cerebrovascular function. *Circulation* 2004 June 22;109(24):2972-5.
4. Werner N, Kosiol S, Schiegl T et al. Circulating endothelial progenitor cells and cardiovascular outcomes. *N Engl J Med* 2005 September 8;353(10):999-1007.
5. Kalka C, Masuda H, Takahashi T et al. Transplantation of ex vivo expanded endothelial progenitor cells for therapeutic neovascularization. *Proc Natl Acad Sci U S A* 2000 March 28;97(7):3422-7.
6. Schatteman GC, Hanlon HD, Jiao C, Dodds SG, Christy BA. Blood-derived angioblasts accelerate blood-flow restoration in diabetic mice. *J Clin Invest* 2000 August;106(4):571-8.
7. Hill JM, Zalos G, Halcox JP et al. Circulating endothelial progenitor cells, vascular function, and cardiovascular risk. *N Engl J Med* 2003 February 13;348(7):593-600.
8. Fadini GP, de Kreutzenberg SV, Coracina A et al. Circulating CD34+ cells, metabolic syndrome, and cardiovascular risk. *Eur Heart J* 2006 September;27(18):2247-55.
9. Murphy C, Kanaganayagam GS, Jiang B et al. Vascular dysfunction and reduced circulating endothelial progenitor cells in young healthy UK South Asian men. *Arterioscler Thromb Vasc Biol* 2007 April;27(4):936-42.
10. Tepper OM, Galiano RD, Capla JM et al. Human endothelial progenitor cells from type II diabetics exhibit impaired proliferation, adhesion, and incorporation into vascular structures. *Circulation* 2002 November 26;106(22):2781-6.
11. Capla JM, Grogan RH, Callaghan MJ et al. Diabetes impairs endothelial progenitor cell-mediated blood vessel formation in response to hypoxia. *Plast Reconstr Surg* 2007 January;119(1):59-70.
12. Grisar J, Aletaha D, Steiner CW et al. Depletion of endothelial progenitor cells in the peripheral blood of patients with rheumatoid arthritis. *Circulation* 2005 January 18;111(2):204-11.
13. Verma S, Kuliszewski MA, Li SH et al. C-reactive protein attenuates endothelial progenitor cell survival, differentiation, and function: further evidence of a mechanistic link between C-reactive protein and cardiovascular disease. *Circulation* 2004 May 4;109(17):2058-67.
14. Suh W, Kim KL, Choi JH et al. C-reactive protein impairs angiogenic functions and decreases the secretion of arteriogenic chemo-cytokines in human endothelial progenitor cells. *Biochem Biophys Res Commun* 2004 August 13;321(1):65-71.
15. Yusuf S, Hawken S, Ounpuu S et al. Obesity and the risk of myocardial infarction in 27,000 participants from 52 countries: a case-control study. *Lancet* 2005 November 5;366(9497):1640-9.
16. Pischon T, Boeing H, Hoffmann K et al. General and abdominal adiposity and risk of death in Europe. *N Engl J Med* 2008 November 13;359(20):2105-20.
17. Ridker PM. Clinical application of C-reactive protein for cardiovascular disease detection and prevention. *Circulation* 2003 January 28;107(3):363-9.
18. Thijssen DH, Vos JB, Verseyden C et al. Haematopoietic stem cells and endothelial progenitor cells in healthy men: effect of aging and training. *Aging Cell* 2006 December;5(6):495-503.
19. Kondo T, Hayashi M, Takeshita K et al. Smoking cessation rapidly increases circulating progenitor cells in peripheral blood in chronic smokers. *Arterioscler Thromb Vasc Biol* 2004 August;24(8):1442-7.
20. Adams V, Lenk K, Linke A et al. Increase of circulating endothelial progenitor cells in patients with coronary artery disease after exercise-induced ischemia. *Arterioscler Thromb Vasc Biol* 2004 April;24(4):684-90.
21. Yki-Jarvinen H. Thiazolidinediones. *N Engl J Med* 2004 September 9;351(11):1106-18.
22. Kahn SE, Haffner SM, Heise MA et al. Glycemic durability of rosiglitazone, metformin, or glyburide monotherapy. *N Engl J Med* 2006 December 7;355(23):2427-43.

23. Viljanen AP, Virtanen KA, Jarvisalo MJ et al. Rosiglitazone treatment increases subcutaneous adipose tissue glucose uptake in parallel with perfusion in patients with type 2 diabetes: a double-blind, randomized study with metformin. *J Clin Endocrinol Metab* 2005 December;90(12):6523-8.
24. Khera A, McGuire DK, Murphy SA et al. Race and gender differences in C-reactive protein levels. *J Am Coll Cardiol* 2005 August 2;46(3):464-9.
25. Alberti KG, Zimmet P, Shaw J. Metabolic syndrome--a new world-wide definition. A Consensus Statement from the International Diabetes Federation. *Diabet Med* 2006 May;23(5):469-80.
26. Alizadeh DR, de RA, Rabelink TJ et al. Elevated CRP levels are associated with increased carotid atherosclerosis independent of visceral obesity. *Atherosclerosis* 2008 October;200(2):417-23.
27. Pistrosch F, Herbrig K, Oelschlaegel U et al. PPARgamma-agonist rosiglitazone increases number and migratory activity of cultured endothelial progenitor cells. *Atherosclerosis* 2005 November;183(1):163-7.
28. Wang CH, Ciliberti N, Li SH et al. Rosiglitazone facilitates angiogenic progenitor cell differentiation toward endothelial lineage: a new paradigm in glitazone pleiotropy. *Circulation* 2004 March 23;109(11):1392-400.
29. Wang CH, Ting MK, Verma S et al. Pioglitazone increases the numbers and improves the functional capacity of endothelial progenitor cells in patients with diabetes mellitus. *Am Heart J* 2006 December;152(6):1051-8.
30. Werner C, Kamani CH, Gensch C, Bohm M, Laufs U. The peroxisome proliferator-activated receptor-gamma agonist pioglitazone increases number and function of endothelial progenitor cells in patients with coronary artery disease and normal glucose tolerance. *Diabetes* 2007 October;56(10):2609-15.

CHAPTER

9

Summary and Conclusions

SUMMARY AND CONCLUSIONS

The aim of this thesis was to explore the relation between visceral obesity and the accompanying metabolic disturbances, systemic inflammation and the atherosclerotic process. A newly developed magnetic resonance vessel wall imaging technique was implemented in phenotyping patients and as a therapeutic endpoint in a randomised controlled setting. A three step approach was chosen for this purpose. First, the magnetic resonance black blood vessel wall imaging technique at the magnetic field strength of 3 Tesla was developed and validated. Secondly, phenotyping of viscerally obese subjects was performed with special attention for the role of systemic inflammation and atherosclerosis. Finally, in the setting of a randomised controlled trial, the impact of reducing visceral obesity and systemic inflammation with lifestyle intervention and rosiglitazone treatment (PPAR γ agonist) on the progression of atherosclerosis was assessed.

PART I: 3T MAGNETIC RESONANCE BLACK BLOOD VESSEL WALL IMAGING

Magnetic resonance black-blood vessel wall imaging at the magnetic field strength of 3 Tesla was developed to assess the carotid artery vessel wall characteristics. A double inversion recovery fast gradient echo sequence was used on a commercial 3T system for the acquisition of images of the carotid artery. After development and optimisation of the scanning sequence, the reproducibility of the measurements was evaluated in a study using three repeated measurements as described in **Chapter 2**. A high reproducibility of the measurements was shown both for the carotid vessel wall area and the vessel wall thickness. Vessel wall area is a global measure for the atherosclerotic disease burden while increased vessel wall thickness reflects focal atherosclerotic changes of the vascular wall. Magnetic resonance vascular imaging was shown to be able to assess vessel wall characteristics of the carotid artery with high reproducibility.

Three Tesla vascular measurements of the carotid artery showed high dimensional precision with ultrasound assessments of the same vascular structure as reference as described in **chapter 3**. Ultrasound measured intima media thickness of the carotid artery is a frequently used and extensively validated imaging modality for the evaluation of carotid atherosclerosis. Significant correlations were observed between ultrasound measured intima media thickness and the MRI measured vessel wall thickness. Carotid luminal dimensional measurements evaluated by both techniques were also shown to be very similar. Furthermore, MRI successfully discriminated vessel wall characteristics in intermediate and high risk patients from young healthy control subjects.

After establishing the reproducibility of the newly developed magnetic resonance vessel wall imaging technique and its ability in discriminating vessel wall characteristics of subjects with varying cardiovascular risk profiles, the precision of the measurements were assessed using ultrasound as reference. This imaging technique could now be applied in phenotyping patients and as a therapeutic endpoint in a randomised controlled setting as described in the following chapters.

PART II: PHENOTYPING OF VISCERAL OBESITY

Both visceral obesity and the accompanying metabolic disturbances are thought to contribute to an increased risk of developing future cardiovascular disease. In **chapter 4**, vessel wall characteristics of visceral obese subjects with and without the Metabolic Syndrome were evaluated in comparison to patients who recently suffered from a ST-segment elevation myocardial infarction (STEMI). The presence of Metabolic Syndrome in visceraally obese subjects was associated with increased maximum vessel wall thickness of the carotid bulb approaching the level observed in STEMI patients. Furthermore, the imaging technique was shown to be able to discriminate groups with varying cardiovascular risk profiles using both focal and global measures for the assessment of atherosclerosis.

Visceral obesity and the accompanying metabolic disturbances and low-grade systemic inflammation, as reflected by C-Reactive Protein (CRP) levels, are interrelated and have both been shown to associate with an increased risk of cardiovascular disease. In **chapter 5** after exploring the relation between CRP and visceral obesity, we evaluated the relation between CRP and carotid atherosclerosis in male subjects without type 2 diabetes and manifest cardiovascular disease. A significant correlation was shown between visceral obesity and serum CRP levels. Furthermore, elevated CRP levels were shown to associate with significantly increased maximum vessel wall thickness independent of visceral obesity and of MRI measured adipose tissue distribution, both in the common carotid artery and the carotid bulb.

To focus on the in vivo interactions between inflammation and lipoprotein metabolism with regard to atherosclerosis, serum apolipoprotein CI (ApoCI) concentrations were evaluated in visceraally obese subjects. ApoCI influences many proteins involved in the remodelling of lipoproteins in plasma. An important role of ApoCI in the modulation of the inflammatory response has been shown both in vitro and in mice. Furthermore, recent experimental data have revealed that ApoCI augments the development of atherosclerosis in the setting of chronic inflammation in mice. In **chapter 6**, we demonstrated a significant interaction between CRP levels and ApoCI concentrations in determining carotid artery atherosclerosis in male subjects with visceral obesity. More specifically, we observed significantly increased maximum vessel wall thickness

in the carotid artery in subjects with both systemic inflammation and ApoC1 concentrations above the median. These observations confirm *in vivo*, in human subjects, previous proof of principle experiments reported in mouse models of atherosclerosis.

In this section, the presence of Metabolic Syndrome in viscerally obese subjects was shown to associate with increased focal atherosclerotic changes in the carotid artery. A close association between visceral obesity and systemic inflammation was demonstrated. Furthermore, the observations demonstrated an impact of CRP on the atherosclerotic disease burden independent of visceral obesity. CRP was also shown to affect atherosclerosis through interactions with lipoprotein metabolism. These observations support the crucial role of inflammation in the atherosclerotic process.

PART III: VISCERAL OBESITY AND SYSTEMIC INFLAMMATION AS THERAPEUTIC TARGETS IN ATHEROSCLEROSIS

In this section, the influence of rosiglitazone in addition to intensive lifestyle treatment compared to lifestyle treatment alone, on the progression of atherosclerosis and the cardiovascular risk profile was evaluated in the setting of a double blinded, placebo controlled, randomized clinical trial. Viscerally obese male subjects with the metabolic syndrome (i.e. clustering of cardiovascular risk factors) and an elevated basal inflammatory status were included in this study. The patients were without established cardiovascular disease and type2 diabetes mellitus and were treated for a period of 52 weeks. The aim of this study was to assess whether rosiglitazone therapy in addition to intensive lifestyle treatment compared to lifestyle treatment alone could prevent the progression of carotid atherosclerosis in men with visceral obesity and elevated CRP levels (**chapter 7**). Another endpoint of the study was to evaluate whether rosiglitazone therapy in addition to intensive lifestyle treatment compared to lifestyle treatment alone could improve circulating progenitor cell profiles in men with visceral obesity and elevated CRP levels (**chapter 8**). Significant improvements in cardiovascular risk factors were seen after the 52 weeks of treatment in response to effective lifestyle treatment. Both anthropometric measures and blood pressure were reduced significantly at the end of the treatment period. Increased reductions in CRP levels were seen in patients treated with rosiglitazone as hypothesized. The addition of rosiglitazone to lifestyle therapy did not prevent the progression of atherosclerosis in these patients. However, significant increases in CD34+ cell counts were seen in response to rosiglitazone therapy in addition to lifestyle treatment. CD34+ stem cells are known to be most closely related to cardiovascular risk compared with other circulating endothelial progenitor cells.

Taken together, the observations of this study underline the impressive impact of lifestyle therapy on the cardiovascular risk profile. The addition of rosiglitazone treatment to lifestyle therapy does not prevent the progression of carotid atherosclerosis, but is accompanied with a significant increase in CD34+ circulating stem cells.

FUTURE PERSPECTIVES

This thesis has explored several aspects of the relation between visceral obesity and the accompanying metabolic disturbances, systemic inflammation and the atherosclerotic process. Nonetheless, other aspects should be further evaluated in future studies. Magnetic resonance vascular imaging, although accurate and reproducible in assessing vessel wall characteristics, requires further validation with regard to ultimate cardiovascular outcome data. Furthermore, contrast enhanced plaque characterisation may provide additional valuable information in future vascular phenotyping and interventional studies.

The identification of patients at risk of developing atherosclerotic cardiovascular disease remains an essential point in the primary prevention setting. Further phenotyping of visceral obese subjects with regard to the specific inflammatory response in relation with adipose tissue distribution by evaluating the cytokine profiles may prove useful in further understanding of the inflammatory response in these individuals.

Regarding the circulating progenitor cells, assessments of the functional properties of these cells may prove useful in understanding the role of endothelial repair mechanism in the atherosclerotic process and could contribute to the early identification of subjects at risk of developing cardiovascular disease.

Finally, with regard to the treatment strategy in visceral obesity, our observations demonstrate an impressive impact of lifestyle therapy. These observations, however, concern only male patients and will have to be confirmed in female population. Furthermore, additional inhibition of the systemic inflammatory response in visceral obesity may be of importance in limiting or restoring of the endothelial function. Evaluation of endothelial functional properties in future studies may provide valuable information in this regard.

Samenvatting en Conclusies

SAMENVATTING EN CONCLUSIES

In dit proefschrift werd de invloed van viscerale obesitas en daarmee samenhangende metabole ontregelingen, en het systemische inflammatie op het atherosclerotische proces bestudeerd. Er werd gekozen voor een aanpak in drie stappen. Allereerst werd de beeldvorming van de vaatwand met behulp van de “black-blood” techniek op een 3 Tesla MRI ontwikkeld. In de tweede plaats, werd de 3T MRI techniek gebruikt in het fenotyperen van patiënten met viscerale obesitas. Tenslotte, werd de behandeling van viscerale obesitas en systemische inflammatie door middel van leefstijl begeleiding gecombineerd met rosiglitazon vergeleken met leefstijl begeleiding alleen in een gerandomiseerde klinische studie. De progressie van atherosclerose werd geëvalueerd ook in deze studie met behulp van de 3T vaatwand MRI.

DEEL I: 3 TESLA MRI VAATWAND BEELDVORMING

Op een 3 Tesla MRI systeem werd een vaatwand-imaging techniek ontwikkeld voor de beeldvorming van arteria carotis. De reproduceerbaarheid van de metingen van de vaatwand door MRI werd geëvalueerd zoals beschreven in **hoofdstuk 2**. Er werd een hoge reproduceerbaarheid gezien voor zowel de metingen van de vaatwand oppervlakte als de metingen van de vaatwanddikte. Vaatwand oppervlakte is een globale reflectie van de ernst van de aanwezige atherosclerose, terwijl vaatwanddikte een reflectie is van de locale atherosclerotische veranderingen.

Vaatwandmetingen verkregen met behulp van de MRI werden vervolgens vergeleken met echografische vaatwand metingen (intima media dikte (IMT)) van de arteria carotis. In **hoofdstuk 3** werd de goede overeenkomst tussen beide technieken in de beoordeling van vasculaire en lumenale dimensies van de arteria carotis beschreven. Verder werd in dit hoofdstuk het vermogen van de MRI techniek om vaatwandkarakteristieken te onderscheiden tussen patiënten met verschillende cardiovasculaire risicoprofielen aangetoond.

Samenvattend is de 3 Tesla vaatwand MRI techniek van de arteria carotis een reproduceerbare meting. Het kan patiënten met verschillend cardiovasculair risico profiel onderscheiden en zich meten met gevestigde echografische vaatwandmetingen.

DEEL II: HET FENOTYPEREN VAN VISCERALE OBESITAS

Viscerale obesitas en de daarmee samenhangende metabole ontregelingen worden bieden gedacht om bij te dragen aan een verhoogd risico op het ontwikkelen van cardiovasculaire

ziekten. In **hoofdstuk 4** werd de atherosclerotische gevolgen van de aanwezigheid van metabole ontregelingen in de setting van viscerale obesitas bestudeerd. De aanwezigheid van het metabool syndroom in patiënten met viscerale obesitas was geassocieerd met een grotere vaatwanddikte in de arteria carotis in vergelijking met patiënten met viscerale obesitas alleen.

Zowel viscerale obesitas als systemische inflammatie zijn geassocieerd met een verhoogd risico op het ontwikkelen van cardiovasculaire events, ook in de afwezigheid van type 2 diabetes mellitus. In **hoofdstuk 5** werd de verhouding tussen viscerale obesitas en systemische inflammatie, beoordeeld door het serum c-reactive protein (CRP) gehalte, bestudeerd in relatie tot atherosclerotische veranderingen van arteria carotis. Een significante correlatie werd geobserveerd tussen viscerale obesitas en CRP. Tevens was een verhoogd CRP gehalte geassocieerd met significant hogere maximale vaatwanddikte, onafhankelijk van de invloed van viscerale obesitas en de door MRI beoordeelde vetdistributie.

Om de in vivo interactie tussen inflammatie en het vetmetabolisme, in relatie tot atherosclerose te bestuderen, werden serum apolipoproteïne C1 (ApoC1) concentraties geëvalueerd in patiënten met viscerale obesitas. ApoC1 beïnvloedt veel eiwitten die betrokken zijn in de remodelling van plasma lipoproteïnen. Een modulerend effect van ApoC1 op de inflammatoire response is ook aangetoond zowel in vitro als in muismodellen. Recente studies hebben aangetoond dat ApoC1 bevordert de progressie van atherosclerose in de aanwezigheid van chronische inflammatie. In **hoofdstuk 6**, werd een significante interactie geobserveerd tussen CRP en ApoC1 concentraties in het bepalen van de atherosclerose van arteria carotis. Patiënten met zowel een verhoogde CRP als ApoC1 concentratie hadden een grotere vaatwanddikte in de arteria carotis.

Samenvattend werd in deel II een relatie aangetoond tussen de aanwezigheid van metabole ontregelingen en een grotere vaatwanddikte van arteria carotis. Een verhoogde serum CRP waarde bleek gepaard te gaan met een toegenomen dikte van de vaatwand onafhankelijk van viscerale obesitas. Ook werd er een interactie gevonden tussen CRP en ApoC1 als determinant van atherosclerose van de arteria carotis. Deze bevindingen bevestigen de belangrijke associatie van inflammatie met het atherosclerotische proces.

DEEL III: VISCERALE OBESITAS EN SYSTEMISCHE INFLAMMATIE ALS THERAPEUTISCHE TARGETS IN ATHEROSCLEROSE

In het laatste onderdeel van dit proefschrift lag de focus op de behandeling van viscerale obesitas en systemische inflammatie. Het doel van de behandeling was remming van de progressie van atherosclerose. In een dubbel blinde, placebo gecontroleerde, gerandomiseerde klinische studie, werd de invloed van behandeling met rosiglitazon samen met

leefstijl begeleiding vergeleken met leefstijl begeleiding alleen. De behandeling duurde 52 weken. De geïncludeerde patiënten waren mannen met viscerale obesitas en een verhoogd serum CRP gehalte. De patiënten hadden geen type 2 diabetes mellitus of klinisch manifeste cardiovasculaire ziekten. De effecten van de behandeling gemeten als de remming van de progressie van atherosclerose zijn beschreven in **hoofdstuk 7**. Een ander eindpunt van de studie was de bestudering van de invloed van de behandeling op circulerende stamcelprofielen (**hoofdstuk 8**). Effectieve leefstijlbegeleiding resulteerde in een significante verbetering van het cardiovasculaire risicoprofiel van de patiënten. Er werden significante afnames gezien van de buikomvang, lichaamsgewicht en bloeddruk na 52 weken behandeling. Bij patiënten die behandeld werden met rosiglitazon daalde het serum CRP gehalte meer dan in de placebo groep. Toevoeging van rosiglitazon aan de behandeling had geen toegevoegde waarde met betrekking tot de remming van de progressie van atherosclerose. Het endotheliale stamcelprofiel werd wel beïnvloed door rosiglitazon behandeling. Circulerende CD34+ stamcellen stegen significant meer in de met rosiglitazon behandelde groep.

Samenvattend werd gevonden dat effectieve leefstijlbegeleiding het cardiovasculaire risicoprofiel sterk verbeterde. Toevoeging van rosiglitazon aan deze behandeling had geen effect op het remmen van de progressie van atherosclerose in de arteria carotis, maar wel op circulerende CD34+ stamcellen.

TOEKOMSPERSPECTIEVEN

Met de studies beschreven in dit proefschrift, werd geprobeerd om meer inzicht te verkrijgen in de relatie tussen viscerale obesitas en de daarmee samenhangende metabole ontregelingen, systemische inflammatie en het atherosclerotische proces. De vasculaire MRI techniek toegepast in de magnetische veldsterkte van 3 Tesla dient verder geëvalueerd te worden met betrekking tot uiteindelijke cardiovasculaire klinische eindpunten. Het gebruik van contrast middelen in de 3T veldsterkte zou ook tot verdere verbetering van de beeldkwaliteit kunnen leiden bij de imaging van de vaatwand en tevens kunnen bijdragen aan vaatwand (plaque) karakterisatie.

Het identificeren van patiënten met een verhoogd risico op het ontwikkelen van atherosclerotische cardiovasculaire ziekten blijft een belangrijk aandachtspunt binnen de primaire preventie setting en de rol van imaging in dit proces verdient verdere aandacht. Met betrekking tot het stamcelprofiel bij de fenotypering van viscerale obesitas, zou de evaluatie van functionele eigenschappen van deze cellen additionele informatie kunnen verschaffen over de endotheliale reparatie en regeneratieproces.

Ten slotte, de resultaten van dit proefschrift bevestigen de grote effecten van een effectieve leefstijlbegeleiding op het cardiovasculaire risicoprofiel. Deze observaties betroffen echter alleen mannelijke patiënten en moeten ook bevestigd worden in vrouwelijke populaties. Onderdrukking van de inflammatoire response in patiënten met viscerale obesitas zou gunstige effecten kunnen hebben op endotheelfunctie en progressie van atherosclerose in patiënten met viscerale obesitas. Dit kan een aangrijpingspunt zijn voor de behandeling van atherosclerose en het voorkomen van cardiovasculaire ziekten in patiënten met viscerale obesitas.

LIST OF PUBLICATIONS

van der Ham RL, **Alizadeh Dehnavi R**, Berbée JF, Putter H, de Roos A, Romijn JA, Rensen PC, Tamsma JT. Plasma apolipoprotein CI and CIII levels are associated with increased plasma triglyceride levels and decreased fat mass in men with the metabolic syndrome. *Diabetes Care* 2009;32:184-6

van der Ham RL, **Alizadeh Dehnavi R**, van den Berg GA, Putter H, de Roos A, Berbée JF, Romijn JA, Rensen PC, Tamsma JT. Apolipoprotein CI levels are associated with atherosclerosis in men with the metabolic syndrome and systemic inflammation. *Atherosclerosis* 2009;203:355-7

Roes SD, **Alizadeh Dehnavi R**, Westenberg JJ, Lamb HJ, Mertens BJ, Tamsma JT, de Roos A. Assessment of aortic pulse wave velocity and cardiac diastolic function in subjects with and without the metabolic syndrome: HDL cholesterol is independently associated with cardiovascular function. *Diabetes Care* 2008;31:1442-4

Alizadeh Dehnavi R, de Roos A, Rabelink TJ, van Pelt J, Wensink MJ, Romijn JA, Tamsma JT. Elevated CRP levels are associated with increased carotid atherosclerosis independent of visceral obesity. *Atherosclerosis* 2008;200:417-23

Alizadeh Dehnavi R, Beishuizen ED, van de Ree MA, Le Cessie S, Huisman MV, Kluft C, Princen HM, Tamsma JT. The impact of metabolic syndrome and CRP on vascular phenotype in type 2 diabetes mellitus. *Eur J Intern Med* 2008;19:115-21

Alizadeh Dehnavi R, Doornbos J, Tamsma JT, Stuber M, Putter H, van der Geest RJ, Lamb HJ, de Roos A. Assessment of the carotid artery by MRI at 3T: a study on reproducibility. *J Magn Reson Imaging* 2007;25:1035-43

Alizadeh Dehnavi R, Tamsma JT, Edo Meinders A. The effect of prednisolone on serum sodium concentration. *Eur J Intern Med* 2006;17:201-3

Alizadeh Dehnavi R, van der Wall EE, Smits PC. Left ventricular apical ballooning. *Int J Cardiovasc Imaging* 2006;22:327-31

Alizadeh Dehnavi R, Tamsma JT. Metabolic Syndrome. *Ned Tijdschr Geneesk* 2005;149:2377

Alizadeh Dehnavi R, van der Wall EE. Transient left ventricular apical ballooning. *Ann Intern Med* 2005;142:678

ACKNOWLEDGMENTS

The realization of this thesis was made possible by the generous support and assistance of many people to whom I am very grateful.

In the first place, I would like to acknowledge the involvement of the patients and participants of the studies reported in this thesis. A special thanks to the student-assistants Maarten and Jolein for their hard work during the implementation of the studies, to Bep Ladan for her all-round logistical support, and to my colleagues Argho and Mathilde for an unforgettable time at the “bunker”.

I would like to express my profound gratitude to my sisters Mina, Sara, Elly and Mahla, and all my friends for their support and especially their understanding. Hopefully I will be able to make it up to you someday.

The degree to which I am indebted to my parents is quite impossible to express. Your sacrifices and continuous unconditional support has made it all possible. Thank you!

Reza Alizadeh Dehnavi

October 6th, 2009

CURRICULUM VITAE

Reza Alizadeh Dehnavi was born on December 31st, 1976 in Tehran, Iran. Having followed part of his secondary education in Tehran, he moved to The Netherlands where he attended the Rijnlands Lyceum in Oegstgeest and completed the International Baccalaureate programme in 1994. Following a year of Dutch studies at the University of Leiden, he began studying Medicine there in 1996. During his study, he started a research project entitled "The effect of prednisolone on the serum sodium concentration" at the Department of Internal Medicine at Leiden University Medical Centre (LUMC) under the supervision of Prof.dr. A.E. Meinders and dr. J.T.Tamsma. After receiving his medical degree in 2004, he worked for a period of six months at the Department of Cardiology in MCRZ hospital in Rotterdam. In September 2006, he started a PhD research project at the section of vascular medicine, Department of Internal Medicine and Endocrinology at LUMC under the supervision of dr. J.T.Tamsma. Initially, he was involved in developing the 3T Vascular Magnetic Resonance Imaging in collaboration with the Department of Radiology, Johns Hopkins University Medical School, Baltimore, USA. Later, he was the clinical supervisor of the RUBENS Trial, the results of which are described in this thesis. In January 2008, he started his residency in cardiology at Leiden University Medical Centre (Prof.dr.E.E.van der Wall), and is currently working at the Department of Internal Medicine (Prof.dr.J.A. Romijn) in LUMC.